

การสังเคราะห์และประยุกต์ควอเตอร์นารีแอมโมเนียมโคโชนานเป็นสารเติมแต่งในผลิตภัณฑ์บำรุงเส้นผม

นายธีระชัย เกิดชลเพชร

วิทยานิพนธ์นี้เป็นส่วนหนึ่งของการศึกษาตามหลักสูตรปริญญาวิทยาศาสตรมหาบัณฑิต
สาขาวิชาปิโตรเคมีและวิทยาศาสตร์พอลิเมอร์
คณะวิทยาศาสตร์ จุฬาลงกรณ์มหาวิทยาลัย
ปีการศึกษา 2551
ลิขสิทธิ์ของจุฬาลงกรณ์มหาวิทยาลัย


SYNTHESIS AND APPLICATIONS OF QUATERNARY AMMONIUM CHITOSAN
AS ADDITIVES IN HAIR-CARE PRODUCTS

Mr. Teerachai Kerdcholpetch

A Thesis Submitted in Partial Fulfillment of the Requirements
for the Degree of Master of Science Program in Petrochemistry and Polymer Science
Faculty of Science
Chulalongkorn University
Academic Year 2008
Copyright of Chulalongkorn University


Thesis Title SYNTHESIS AND APPLICATIONS OF QUATERNARY AMMONIUM
CHITOSAN AS ADDITIVES IN HAIR-CARE PRODUCTS
By Mr. Teerachai Kerdcholpetch
Field of Study Petrochemistry and Polymer Science
Advisor Assistant Professor Varawut Tangpasuthadol, Ph.D.
Co-Advisor Assistant Professor Voravee P. Hoven, Ph.D.

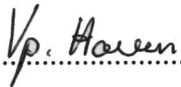
Accepted by the Faculty of Science, Chulalongkorn University in Partial Fulfillment
of the Requirements for the Master's Degree



.....Dean of the Faculty of Science
(Professor Supot Hannongbua, Dr.rer.nat.)


THESIS COMMITTEE


.....Chairman
(Associate Professor Supawan Tantayanon, Ph.D.)


.....Advisor
(Assistant Professor Varawut Tangpasuthadol, Ph.D.)


.....Co-Advisor
(Assistant Professor Voravee P. Hoven, Ph.D.)


.....Examiner
(Associate Professor Nuanphun Chantarasiri, Ph.D.)


.....External Examiner
(Assistant Professor Radchada Buntem, Ph.D.)

ธีระชัย เกิดชลเพชร: การสังเคราะห์และประยุกต์ควอเทอร์นารีแอมโมเนียมไคโตซานเป็นสารเติมแต่งในผลิตภัณฑ์บำรุงเส้นผม. (SYNTHESIS AND APPLICATIONS OF QUATERNARY AMMONIUM CHITOSAN AS ADDITIVES IN HAIR-CARE PRODUCTS) อ.ที่ปรึกษาวิทยานิพนธ์หลัก: ผู้ช่วยศาสตราจารย์ ดร.วราวุฒิ ตั้งพสุธาตล, อ.ที่ปรึกษาวิทยานิพนธ์ร่วม: ผู้ช่วยศาสตราจารย์ ดร.วรวิรุ โฮვნ, 102 หน้า.

เส้นผมของมนุษย์มีประจุลบ ณ สภาวะที่มีพีเอชสูงกว่าค่าไอโซอิเล็กทริก (~3.67) ดังนั้นส่วนผสมที่มีประจุบวกสามารถเคลือบติดเส้นผมได้ง่าย ในงานนี้ได้สังเคราะห์อนุพันธ์ไคโตซานที่มีประจุบวกสองชนิดคือ เอ็น,เอ็น,เอ็น-ไตรเมทิลแอมโมเนียมไคโตซานคลอไรด์ (TMC) และเอ็น-[(2-ไฮดรอกซิล-3-ไตรเมทิลแอมโมเนียม)โพรพิล]ไคโตซานคลอไรด์ (HTACC) ที่มีระดับควอเทอร์นารีในเซชัน (DQ) ต่างๆ กันเพื่อใช้ในน้ำยาปรับสภาพเส้นผมแบบชะโลมทิ้งไว้ ได้ยืนยันโครงสร้างทางเคมีของอนุพันธ์ที่สังเคราะห์ได้ด้วยโปรตอนเอ็นเอ็มอาร์และเอฟทีไออาร์ จากการทดสอบความเป็นพิษต่อเซลล์ในหลอดทดลองโดยวิธีเอ็มทีที พบว่า ความเป็นพิษของ HTACC ต่อเซลล์ชนิด HaCaT ขึ้นอยู่กับ %DQ ได้เลือกใช้ TMC (22%DQ) และ HTACC (24%DQ) ในสารปรับสภาพเส้นผม เพราะสารทั้งสองมีความเป็นพิษต่ำที่สุดและยังมีต้นทุนการสังเคราะห์ต่ำ น้ำยาปรับสภาพเส้นผมที่เตรียมได้นี้สามารถเคลือบติดบนเส้นผมได้ดังผลการวิเคราะห์จากกล้องจุลทรรศน์อิเล็กตรอนแบบส่องกราดและเอทีอาร์เอฟทีไออาร์ไมโครสเปกโทรสโกปี นอกจากนี้ ยังได้วิเคราะห์สมบัติการทนต่อแรงดึง, เนื้อสัมผัส และการหิวแบบเปียกของเส้นผมพบว่าน้ำยาปรับสภาพเส้นผมที่เตรียมได้นี้สามารถปรับสภาพเส้นผมที่ถูกตัดและยึดให้มีความแข็งแรงเพิ่มขึ้นและให้ความนุ่มลื่นในการสัมผัสมากกว่าผลิตภัณฑ์ที่ขายตามท้องตลาด ผลการศึกษานี้สมควรที่จะนำไปสู่การประยุกต์ใช้เชิงพาณิชย์ของสารประกอบไคโตซานที่มีประจุบวกในอุตสาหกรรมถนอมเส้นผม

สาขาวิชา ปิโตรเคมีและวิทยาศาสตร์พอลิเมอร์ลายมือชื่อนิสิต.....ธีระชัย เกิดชลเพชร
ปีการศึกษา2551.....ลายมือชื่ออาจารย์ที่ปรึกษาวิทยานิพนธ์หลัก.....
ลายมือชื่ออาจารย์ที่ปรึกษาวิทยานิพนธ์ร่วม.....

4972328723 : MAJOR PETROCHEMISTRY AND POLYMER SCIENCE

KEYWORDS: QUATERNARY AMMONIUM CHITOSAN / HAIR-CARE PRODUCT

TEERACHAI KERDCHOLPETCH: SYNTHESIS AND APPLICATIONS OF QUATERNARY AMMONIUM CHITOSAN AS ADDITIVES IN HAIR-CARE PRODUCTS. ADVISOR: ASST. PROF. VARAWUT TANGPASU-THADOL, Ph.D., CO-ADVISOR: ASST. PROF. VORAVEE P. HOVEN, Ph.D., 102 pp.

At any conditions with pH above the isoelectric point (~ 3.67), the surface of hair bears a net negative charge. Therefore, positively charged ingredients can be easily coated on it. In this work, two positively charged derivatives of chitosan, *N,N,N*-trimethylammonium chitosan chloride (TMC) and *N*-[(2-hydroxyl-3-trimethylammonium)propyl]chitosan chloride (HTACC), with varying degrees of quaternization (*DQ*) were synthesized for use in “leave-on” conditioners. The chemical structures of the charged derivatives were verified by ^1H NMR and FTIR. From *in vitro* cytotoxicity study by MTT assay, %*DQ* dependent on toxicity against HaCaT cells line was observed for HTACC. TMC (22%*DQ*) and HTACC (24%*DQ*) were used as cationic ingredients in the conditioner because of their lowest toxicity as well as synthesis costs. The prepared leave-on conditioners were able to coat on hair as evidenced by scanning electron microscopy and ATR-FTIR microspectroscopy. In addition, tests for hair’s tensile properties, texture, and wet combing were also evaluated. The prepared conditioners could increase the strength and the smooth feel of waved and straightened hairs more than did the commercial product. This study can in fact pave the way for commercial application of the positively charged chitosan compounds in hair-care industry.

Field of Study : Petrochemistry and Polymer Science Student’s Signature : teerachai
 Academic Year : 2008 Advisor’s Signature : [Signature]
 Co-Advisor’s Signature : [Signature]

ACKNOWLEDGEMENTS

I would like to express my sincere and deep gratitude to my thesis advisors, Assistant Professor Varawut Tangpasuthadol and Assistant Professor Voravee P. Hoven for invaluable suggestion, guidance, encouragement and kindness throughout the course of this work. I am sincerely grateful to the members of the thesis committee, Associate Professor Supawan Tantayanon, Associate Professor Nuanphun Chantarasiri and Assistant Professor Radchada Buntem for reviewing my thesis and making valuable suggestion and critical comments.

I gratefully acknowledge the financial support for this project provided by Life Science Cosmetics Research Center Co., Ltd. chaired by Mr. Bunyong Sombunsakdikun. My thanks also go to members of this center, Ms. Maleenart Petchsangai, Ms. Saranya Uk-karawittayapumi, and Ms. Sunida Tiamyuyen, for their encouragement. My thanks also go to Sensor Research Group (SRU), headed by Associate Professor Sanong Egkasit for ATR-FTIR facility. My special thankfulness is to Associate Professor Vijittra Leardkamolkarn and Ms. Sunida Tiamyuyen from Department of Anatomy, Faculty of Science, Mahidol University for the cytotoxicity study, and Mr. Sayun Phansomboon, Unilever Thai Trading Limited for the hair analysis.

Moreover, I wish to thank all members of VT and VH groups in Organic Synthesis Research Unit (OSRU) for their friendliness, helpful discussions, cheerful attitude and encouragements during my thesis work. Finally, I also wish to especially thank my family members for their love, kindness, encouragement and support throughout my entire study.

CONTENTS

	Page
ABSTRACT (THAI)	iv
ABSTRACT (ENGLISH)	v
ACKNOWLEDGEMENTS	vi
CONTENTS.....	vii
LIST OF TABLES.....	x
LIST OF FIGURES	xii
LIST OF SCHEMES	xvi
LIST OF ABBREVIATIONS	xvii
CHAPTER I INTRODUCTION	1
1.1 Statement of Problem	1
1.2 Objectives	2
1.3 Scope of Investigation.....	2
CHAPTER II THEORY AND LITERATURE REVIEW.....	4
2.1 Human Hair	4
2.1.1 Chemical composition of human hair	4
2.1.2 Structures of human hair	5
2.1.3 Hair damages.....	7
2.1.4 Hair product containing chitosan and its derivatives	10
2.1.5 Hair analysis.....	12
2.2 Chitosan and Charged Derivatives.....	16
2.2.1 Chitosan.....	16
2.2.2 Charged derivatives of chitosan	17
2.3 MTT Reduction Assay	21

	Page
CHAPTER III METHOD AND MATERIALS	22
3.1 Experimental Design	22
3.2 Materials	22
3.2.1 Sample and reagents	22
3.2.2 Instruments	23
3.3 Experimental Methods	24
3.3.1 Synthesis of <i>N,N,N</i> -trimethylammonium chitosan chloride (TMC)	24
3.3.2 Synthesis of <i>N</i> -[(2-hydroxyl-3-trimethylammonium)propyl]chitosan chloride (HTACC)	24
3.3.3 Characterization of chitosan and its charged derivatives.....	24
3.3.4 Solubility tests of the charged derivatives of chitosan.....	27
3.3.5 Cytotoxicity of chitosan and its charged derivatives	27
3.3.6 Preparation of leave-on conditioner	28
3.3.7 Preparation of cosmetically-treated hairs	31
3.3.8 Analysis of hair samples by attenuated total reflectance-Fourier transform infrared (ATR FT-IR)	32
3.3.9 Morphology of hair samples by scanning electron microscopy (SEM).....	34
3.3.10 Tensile testing of hair samples by miniature tensile tester (MTT).....	34
3.3.11 Hair texture analysis	35
3.3.12 Wet combing test	37
CHAPTER IV RESULTS AND DISCUSSION	38
4.1 Synthesis and Characterization of Charged Derivatives of Chitosan.....	38
4.1.1 <i>N,N,N</i> -trimethylammonium chitosan chloride (TMC)	38
4.1.2 <i>N</i> -[(2-hydroxyl-3-trimethylammonium)propyl]chitosan chloride (HTACC).....	43
4.1.3 Solubility tests of the charged derivatives of chitosan.....	47
4.1.4 <i>In vitro</i> cytotoxicity of chitosan and its charged derivatives	48
4.2 Positively-Charged Chitosan Contents in Leave-On Conditioners	51

	Page
4.2.1 Hair coating behavior.....	52
4.2.2 Homogeneity and viscosity of leave-on conditioner	59
4.3 Functional Group and Microscopic Image Analysis of Hair Samples	61
4.4 Physical and Mechanical Properties of Conditioner-Coated Hairs.....	69
4.4.1 ATR-FTIR spectra of conditioner-coated hairs	69
4.4.2 Surface morphology of conditioner-coated hairs.....	70
4.4.3 Tensile properties of hair samples	73
4.4.4 Hair texture analysis	80
4.4.5 Wet combing test	81
 CHAPTER V CONCLUSION.....	 82
5.1 Conclusions.....	82
5.2 Future Direction.....	83
 REFERENCES	 84
APPENDICES	91
APPENDIX A	92
APPENDIX B.....	98
APPENDIX C.....	101
VITAE.....	102

LIST OF TABLES

Table	Page
2-1 The amounts of amino acids ($\mu\text{mol/g}$ of dry hair) in whole unaltered human hair.....	4
2-2 Some oxidation dye precursors and oxidation dye couplers.....	8
2-3 Chemical structure and functions of ingredients in hair conditioner.....	11
2-4 Typical properties of selected optical materials used in internal reflection spectroscopy.....	14
3-1 Chemical composition of leave-on formulation without cationic polymer and leave-on formulation with 1% w/w polyquaternium-10, chitosan, TMC or HTACC.....	28
4-1 %DQ as determined by ^1H NMR of quaternary ammonium group on chitosan after reacting with iodomethane at 50°C in NMP, DMF:H ₂ O (1:1) or H ₂ O as the reaction solvent.....	42
4-2 %DQ as determined by ^1H NMR on chitosan after reacting with GTMAC at 70°C in 1% v/v acetic acid at different reaction time.....	45
4-3 %DQ of $\text{TMC}_{\text{CH}_3\text{I}_{6\text{eq}}}$ and $\text{HTACC}_{\text{GTMAC}_{4\text{eq}_{24\text{hr}}}}$, determined by ^1H NMR spectroscopy and conductivity titration method.....	46
4-4 %DQ and solubility test in water of various pHs of chitosan, TMCs, and HTACCs.....	48
4-5 IC_{50} ($\mu\text{g/ml}$) of chitosan and its charged derivatives on HaCaT cells line as determined by the MTT assay at pH 6.0.....	51
4-6 Peak assignment of virgin hair was used in this study.....	54
4-7 pH and viscosity of five leave-on conditioners.....	60
4-8 Cysteic acid contents in virgin and treated-hairs.....	63
4-9 Amide I band frequencies and assignments to secondary structure for protein.....	64

Table	Page
4-10 The number and location of individual bands obtained from second derivative of virgin and treated-hair.....	67
4-11 Tensile properties of uncoated and coated hair by five leave-on conditioner formula.....	75
A-1 Degree of quaternization (%DQ) was determined from the relative ratio between $-N^+(CH_3)_3$ and H-1.	93
A-2 Degree of quaternization (%DQ) was determined from the relative ratio between $-N^+(CH_3)_3$ and H-2.	94
A-3 Degree of quaternization (%DQ) was determined from the relative ratio between $-N^+(CH_3)_3$ and H-2',3,4,5,6,6'.....	95
A-4 Degree of quaternization (%DQ) was determined from the relative ratio between $-N^+(CH_3)_3$ and H-2,2',3,4,5,6,6'.....	96
A-5 Degree of quaternization (%DQ) was determined from the relative ratio between $-N^+(CH_3)_3$ and $-NHCOCH_3$	97
B-1 The IC ₅₀ values (<i>in vitro</i> cytotoxicity) of chitosan MW 45000, TMCs, and HTACCs on HaCaT cells line as determined by the MTT assay at pH 6.0.....	98

LIST OF FIGURES

Figure		Page
2-1	Diagram of a human hair including intermediate filament-matrix structures.....	6
2-2	Structure of α -helix proposed by Pauling and Corey.....	6
2-3	Structure of diiminium ion of <i>p</i> -phenylenediamine and quinoniminium ion of <i>p</i> -aminophenol	9
2-4	The infrared radiation tracing within the Ge μ IRE.....	15
3-1	Rayonet Photochemical Reactors model RPR-100 and the position of hairs in reactors.....	31
3-2	ATR FT-IR microscope: (A) Continuum TM infrared microscope attached to the Nicolet 6700 FT-IR spectrometer, (B) the slide-on Ge μ IRE is fixed on the position of slide-on housing on the infrared objective, and (C) homemade slide-on Ge μ IRE.	33
3-3	Industrial presses (hand toggle).....	34
3-4	Laser scanning micrometer, LSM-series 500; Miniature tensile tester, MTT.....	35
3-5	Texture Analyzer (TA.XT.Plus Stable Microsystems).....	36
4-1	¹ H NMR spectra of synthesized TMCs using (a) 4, (b) 5, (c) 6, and (d) 12 equivalents of CH ₃ I in comparison with the number of NH ₂ in chitosan (solvent: D ₂ O/TFA, 25°C).....	40
4-2	¹ H NMR spectra of synthesized HTACCs using (a) 2, (b) 4, and (c) 6 equivalents of GTMAC in comparison with the number of NH ₂ in chitosan (solvent: D ₂ O/TFA, 25°C).....	44
4-3	FTIR spectra of (a) chitosan, (b) TMC, and (c) HTACC.....	47

Figure	Page
4-4 <i>In vitro</i> cytotoxicity of (A) chitosan MW 45,000, (B) TMCs, and (C) HTACCs on HaCaT cells line as determined by the MTT assay at pH 6.0.....	50
4-5 ATR-FTIR spectrum of virgin hair.....	53
4-6 ATR FT-IR spectra of (a) virgin hair, (b) coated hair with 1% w/w chitosan solution, (c) coated hair with 2% w/w chitosan solution, and (d) coated hair with 3% w/w chitosan solution.....	55
4-7 ATR FT-IR spectra of (a) virgin hair, (b) coated hair with 1% w/w TMC (22%DQ) solution, (c) coated hair with 2% w/w TMC (22%DQ) solution, and (d) coated hair with 3% w/w TMC (22%DQ) solution.....	55
4-8 ATR FT-IR spectra of (a) virgin hair, (b) coated hair with 1% w/w HTACC (24%DQ) solution, (c) coated hair with 2% w/w HTACC (24%DQ) solution, and (d) coated hair with 3% w/w HTACC (24%DQ) solution.....	56
4-9 SEM images of virgin hair before and after treatment with (a) 1% w/w chitosan, (b) 1% w/w TMC (22%DQ) and (c) 1% w/w HTACC (24%DQ).....	57
4-10 SEM images of waved hair before and after treatment with (a) 1% w/w chitosan, (b) 1% w/w TMC (22%DQ) and (c) 1% w/w HTACC (24%DQ).....	57
4-11 SEM images of straightened hair before and after treatment with (a) 1% w/w chitosan, (b) 1% w/w TMC (22%DQ) and (c) 1% w/w HTACC (24%DQ).....	58
4-12 SEM images of dyed hair before and after treatment with (a) 1% w/w chitosan, (b) 1% w/w TMC (22%DQ) and (c) 1% w/w HTACC (24%DQ).....	58

Figure	Page
4-13 SEM images of UV-damaged hair before and after treatment with (a) 1% w/w chitosan, (b) 1% w/w TMC (22%DQ) and (c) 1% w/w HTACC (24%DQ).....	59
4-14 The appearance of the leave-on conditioner without positively charged polymer (LO), the leave-on with 1% w/w polyquaternium-10 (LO+1%quat), 1% w/w chitosan (LO+1%chitosan), 1% w/w TMC (LO+1%TMC), 1% w/w HTACC (LO+1%HTACC).....	60
4-15 Structure of cysteic acid, cystine monoxide, and cystine dioxide	61
4-16 ATR-FTIR spectra of (a) virgin hair, (b) waved hair, (c) straightened hair, (d) dyed hair, and (e) UV-damaged hair.....	62
4-17 Curve fitting of the amide I region of the cuticle spectrum (depth of 1-2 μm from the hair surface) of (A) virgin hair, (B) waved hair, (C) straightened hair, (D) dyed hair, and (E) UV-damaged hair: (a) deconvolved (solid line) spectrum and (b) original (dotted line) spectrum.....	65
4-18 SEM images of virgin, waved, straightened, dyed, and UV-damaged hairs	68
4-19 ATR-FTIR spectra of (a) virgin hair and the virgin hairs that were coated by (b) LO, (c) LO+1%quat, (d) LO+1%chitosan, (e) LO+1%TMC, and (f) LO+1%HTACC.....	70
4-20 SEM images of virgin hair after the treatment with the leave-on conditioner without positively charged polymer.....	71
4-21 SEM images of virgin hair after the treatment with the leave-on conditioner containing 1% w/w polyquaternium-10.....	71
4-22 SEM images of virgin hair after the treatment with the leave-on conditioner containing 1% w/w chitosan	72
4-23 SEM images of virgin hair after the treatment with the leave-on conditioner containing 1% w/w TMC	72

Figure	Page	
4-24	SEM images of virgin hair after the treatment with the leave-on conditioner containing 1% w/w HTACC.....	73
4-25	Stress-strain curves for five types of hair (virgin, waved, straightened hair, dyed hair, and UV-damaged hair).....	74
4-26	Break load of virgin, waved, straightened, dyed and UV-damaged hairs.....	77
4-27	Comparison of break load of (A) virgin, (B) waved, and (C) straightened hairs with and without treatment by five leave-on conditioners.....	78
4-28	SEM images of fractured cuticle scales of virgin hair caused by hair extension at 50% relative humidity: (a) original virgin hair, tensile tested samples: (b) virgin, (c) waved, (d) straightened (e) dyed, and (f) UV-damaged hairs.....	79
4-29	Comparison of the friction force of hair surface, subjected to treatment by five leave-on conditioner formula and DI water (control).....	80
4-30	Comparison of max loads of hairs tresses subjected to treatment by five leave-on conditioner formulas and DI water (control).....	81
A-1	¹ H NMR spectra of synthesized TMCs using (a) 4, (b) 5, and (c) 6 equivalents of CH ₃ I in comparison with the number of NH ₂ in chitosan (solvent: D ₂ O/TFA, 25 °C).....	92
B-1	Relationship between the log concentration (µg/ml) and the cell viability (%): (A) chitosan MW 45,000, (B) TMCs, and (C) HTACCs. Logarithmic trendline (solid line) and original trendline (dotted line)..	99
C-1	The fracture patterns for five types of hair.....	101

LIST OF SCHEMES

Scheme		Page
2-1	Mechanism of wave process	7
2-2	Mechanism of straighten process	7
2-3	Mechanisms by which different hair dyeing act: (a) temporary hair dyeing, (b) semi-permanent hair dyeing, and (c) permanent hair dyeing.....	9
2-4	Structures of chitin and chitosan	16
2-5	Soluble and insoluble form of chitosan in water.....	17
2-6	Synthesis of <i>N,N,N</i> -trimethylammonium chitosan chloride (TMC) from chitosan.....	18
2-7	Synthesis of <i>N</i> -[(2-hydroxyl-3-trimethylammonium)propyl]chitosan chloride (HTACC) from chitosan.....	19
2-8	Synthesis of NMA–HTACC.....	20
2-9	Reduction of the MTT tetrazolium salt to formazan.....	21
4-1	Mechanism of the synthesis of <i>N,N,N</i> -trimethylammonium chitosan chloride (TMC) from chitosan by reacting with CH ₃ I..	39
4-2	Mechanism of the synthesis of <i>N</i> -[(2-hydroxyl-3-trimethylammonium) propyl]chitosan chloride (HTACC).....	43
4-3	Protonation of amino groups of chitosan at pKa.....	46

LIST OF ABBREVIATIONS

Å	: Angstroms
ATR	: Attenuated total reflectance
DD	: Degree of deacetylation
DQ	: Degree of quaternization
eq	: Equivalent
FBS	: Fetal bovine serum
FTIR	: Fourier transform infrared
Ge	: Germanium
GTMAC	: Glycidyltrimethylammonium chloride
HaCaT	: Human keratinocyte cells line
IRE	: Internal reflection element
CH ₃ I	: Iodomethane
kV	: Kilovolt (10 ³ V)
LSM	: Laser scanning micrometer
LO	: Leave-on without cationic polymers
LO+1%quat	: Leave-on with 1%w/w polyquaternium-10
LO+1%chitosan	: Leave-on with 1%w/w chitosan
LO+1%TMC	: Leave-on with 1%w/w TMC
LO+1%HTACC	: Leave-on with 1%w/w HTACC
MCT	: Mercury-cadmium-telluride
MTT	: Miniature tensile tester
µm	: Micrometer (10 ⁻⁶ m)

nm	: Nanometer (10^{-9} m)
HTACC	: <i>N</i> -[(2-hydroxyl-3-trimethylammonium)propyl]chitosan chloride
HEPES	: <i>N</i> -(2-hydroxyethyl)piperazine- <i>N</i> -(2-ethanosulphonic acid)
TMC	: <i>N,N,N</i> -trimethylammonium chitosan chloride
NMR	: Nuclear magnetic resonance spectroscopy
ppm	: Part per million
SEM	: Scanning electron microscopy
w/w	: Weight per weight
ZnSe	: Zinc selenide
MTT	: 3-(4,5-dimethylthiazol-2-yl)-2,5-diphenyltetrazolium bromide

CHAPTER I

INTRODUCTION

1.1 Statement of Problem

Human hair consists of approximately 65 to 95% proteins. The remaining constituents are water, lipids, pigment, and trace elements.¹ Hair in general can be damaged by chemical reactions taking place during waving, straightening, bleaching/dyeing as well as sunlight exposure. Treating with hair conditioner is commonly known as an effective way to revitalize and improve the quality of damaged hair. In general, cationic ingredients in a hair conditioner are highly attracted to hair because of hair's low isoelectric point, which are approximately 3.67 in cosmetically unaltered hair. At any pH above the isoelectric point, the surface of hair bears a net negative charge. Therefore, positively-charged molecules are attracted to it. Over the past few decades, polymers have become increasingly important components of hair conditioners. Cationic polymers, such as quaternary ammonium polymers, are used in hair conditioners. Polyquaternium-7 (copolymer of acrylamide and diallyldimethylammonium chloride) and polyquaternium-10 (quaternized hydroxyethylcellulose) are two most important polymers used in hair conditioners.¹ Hair products containing polymers help prevent mechanical damage, and maintain the strength and integrity of hair by reducing the force required to comb through the hair.

Chitosan is a polysaccharide obtained by partial deacetylation of chitin, a natural substance found abundantly in the exoskeletons of insects, the shells of crustaceans, and fungal cell walls. Chitosan has a number of unique characteristics such as biocompatibility and low toxicity, which attract scientific and industrial interest in cosmetic fields. Due to its limited solubility (only soluble in acidic aqueous at pH < 6.5), a number of chemical routes to improve its solubility have been introduced. Among them, changing the free amino groups in the chitosan chains to positively-charged quaternary ammonium groups is recognized as an effective way to enhance chitosan solubility in water. *N,N,N*-trimethylammonium chitosan chloride (TMC)² and *N*-[(2-

hydroxyl-3-trimethylammonium)propyl]chitosan chloride (HTACC)³ are reportedly two positively charged derivatives that are water soluble and have been applied in biomaterials and textile.³

To the best of our knowledge, there are few studies discussing in detail the resulting effect of mixing chitosan or positive-charged chitosan derivatives in hair conditioners on the physical appearance and mechanical properties of human hair that was damaged by chemicals and UV. The purpose of this present study was therefore to evaluate the use of chitosan and its two positively charged derivatives, TMC and HTACC, in “leave-on” hair conditioners. Physical changes in terms of microscopic appearance, tensile strength of coated hair, as well as its chemical integrity were determined. Cytotoxicities in terms of IC_{50} or 50% inhibitory concentrations of each of the three polymers on human keratinocyte cell line (HaCaT) were also determined. Although a number of studies and patents have reported the use of chitosan in some hair-care products, this work aimed to provide a complete result of using chitosan and the two cationic derivatives as a cationic ingredient in the conditioner. The outcome of this study can definitely leads to commercial application of chitosan and its positively charged derivatives in hair-care industry.

1.2 Objectives

The objective was to evaluate the use of chitosan, TMC, and HTACC as additives in “leave-on” conditioners.

1.3 Scope of Investigation

The stepwise investigation was carried out as follows:

1. Literature survey for related research work.
2. Synthesis and characterization of two positively charged derivatives of chitosan having different degrees of quaternization.
3. *In vitro* cytotoxicity (IC_{50}) test of chitosan and its derivatives on human keratinocyte cells line or HaCaT cells line.

4. Preparation of “leave-on” conditioners containing chitosan or each of the two chitosan derivatives.
5. Preparation of cosmetically-treated and UV damaged hairs.
6. Preparation and characterization of conditioner-coated hair samples in terms of physical and mechanical properties.
7. Discussion of the results and summary.

CHAPTER II

THEORY AND LITERATURE REVIEW

2.1 Human Hair

2.1.1 Chemical composition of human hair

Human hair consists of approximately 65 to 95% proteins, mainly keratin. The remaining constituents are water, lipids, pigment, and trace elements. Twenty one amino acids was found in human hair. Because of the large number of chemical reactions that human hair is subjected to by permanent waves, alkaline straighteners, chemical bleaches, and sunlight exposure, many of these amino acids are converted to amino acid derivatives such as cystine monoxide, cystine dioxide, and cysteic acid. Table 2-1 summarizes results from several sources describing quantitative whole-fiber analyses of these 21 amino acids.

Table 2-1 The amounts of amino acids ($\mu\text{mol/g}$ of dry hair) in whole unaltered human hair.

Amino acid	Reference 1 ⁴	Reference 2 ⁵	Other references
1. aspartic acid	444–453	292–578	
2. threonine	648–673	588–714	
3. serine	1,013–1,091	705–1,090	
4. glutamic acid	995–1,036	930–970	
5. proline	646–708	374–694	
6. glycine	463–513	548–560	
7. alanine	362–384	314	
8. half-cystine	1,407–1,512	1,380–1,500	784-1,534 ⁶

Amino acid	Reference 1 ⁴	Reference 2 ⁵	Other references
9. valine	477–513	470	
10. methionine	50–56	47–67	
11. isoleucine	244–255	366	
12. leucine	502–529	489	
13. tyrosine	177–195	121–171	
14. phenylalanine	132–149	151–226	
15. cysteic acid	22–40	-	
16. lysine	206–222	130–212	
17. histidine	64–86	40–77	
18. arginine	499–550	511–620	
19. cysteine	-	41–66	17-70 ⁶
20. tryptophan	-	20–64	
21. citrulline	-	-	11 ⁷
% nitrogen as ammonia		15.5–16.9%	

2.1.2 Structures of human hair

Morphologically, human hair contains three and sometimes four different units or structures. At hair surface, hair contains a thick protective covering consisting of layers of flat overlapping scale-like structures called “cuticle”. The cuticle layers surround the “cortex”, which constitutes a major part of the fiber mass of human hair. The cortex consists of tightly packed spindle-shaped cells, called cortical cells that are aligned along the fiber axis. The cortical cells contain fibrous proteins of hair called macrofilaments that are approximately 0.1-0.4 mm in diameter. Thicker hairs often contain one or more loosely packed porous regions called “medulla”, located near the center of the fiber. The fourth unit is the cell membrane complex that glues or binds the cells together and, with other non-keratin components, forms a major pathway for diffusion into the fibers.¹ Each macrofibril consists of intermediate filaments and

matrix, a less organized structure that surrounds the intermediate filaments. These structures are illustrated schematically in Figure 2-1.

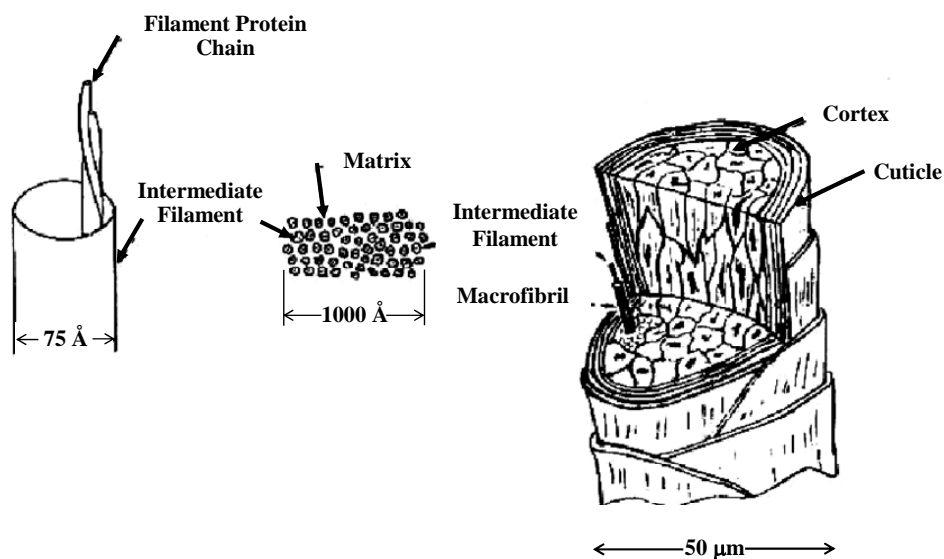


Figure 2-1 Diagram of a human hair including intermediate filament-matrix structures.¹

The subunits that constitute the intermediate filaments of hairs are polypeptide chains of proteins. Keratin polypeptides are oriented parallel to the longitudinal axis of hair shaft. The polypeptide chains can assume α -helix structure.^{8,9} Keratin fiber shows several spacings which are an equatorial spacing (perpendicular to the fiber axis) of 9.8 \AA and meridional spacings (parallel to the fiber axis) of 5.1 and 1.5 \AA (Figure 2-2).

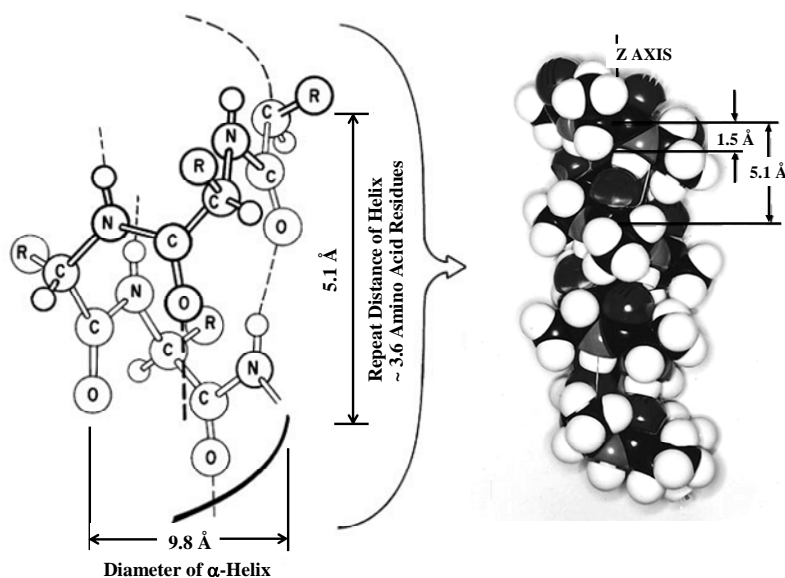


Figure 2-2 Structure of α -helix proposed by Pauling and Corey.^{8,9}

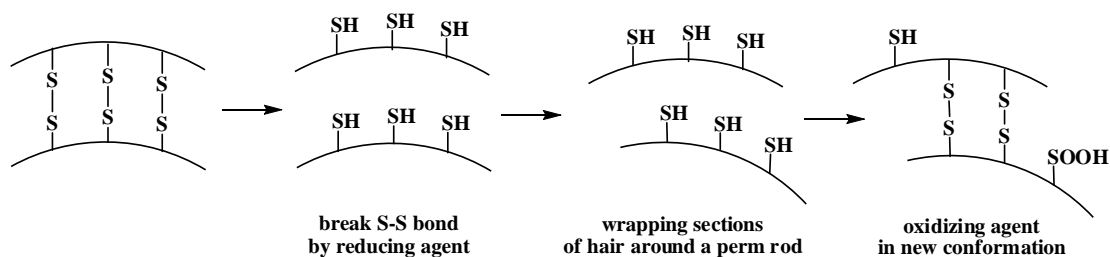
2.1.3 Hair damages

2.1.3.1 Cosmetically-treated hair

Nowadays people tend to visit beauty salon to have their hair pampered by hair stylists. Most of the time it is unavoidable for the hair to be treated with chemicals in lotion, conditioners, and waving-dyeing creams, etc. Hair therefore can be damaged by chemical ingredients from these treatments.

Permanent wave

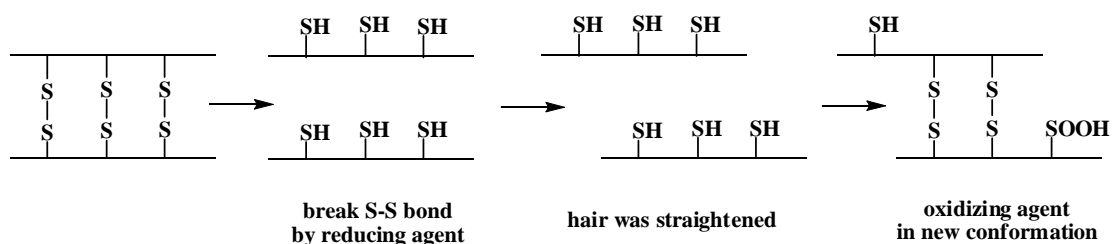
Permanent waving treatment consists of two different processes, the reducing process and the oxidizing process. The first process is intended to act chemically on the covalent disulfide bond. The hairs are wetted with thiol aqueous solution and rolled on curlers so that the imposed deformation of hair is in the shape of curls. In the second process, the curls are set by restoring the initial chemical structure to the fiber. The thiol group of keratin protein, which is produced in the first process, is re-oxidized into the disulfide bond. It is known that an incomplete re-oxidation of the thiol group in keratin protein occurs in the second process.



Scheme 2-1 Mechanism of wave process.

Straightening

Hair straightening, like permanent waving, is an operation in which a permanent deformation of hair is the objective. The same chemical process occurs during straightening as the waving.

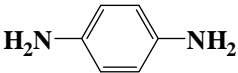
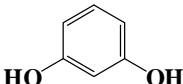
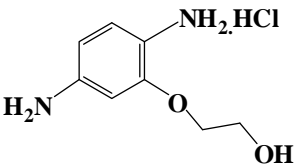
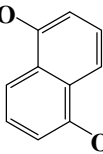
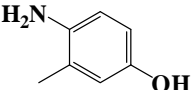
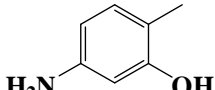
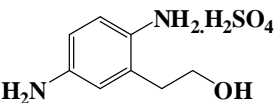
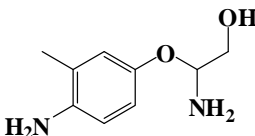


Scheme 2-2 Mechanism of straighten process.

Dyeing

The classification of human hair dyes can divide as four groups such as permanent or oxidation dyes, semi-permanent dyes, temporary dyes or color rinses, and other dyes. Oxidation dyes are often referred to permanent hair dyes and are the most important of the commercial hair dyes. Permanent hair dyes generally consist of oxidation dye precursors such as difunctional *ortho*- or *para*-diamines or aminophenols (as shown in Table 2-2) that are capable of oxidized by hydrogen peroxide to diiminium or quinoniminium ions as active intermediates (Figure 2-3) of the process. These active intermediates then reacts inside the hair with oxidation dye couplers such as substituted resorcinols or meta-phenylenediamines (Table 2-2) to color compound. Oxidation dye couplers usually produce little or no color, but in the presence of oxidation dye precursors and oxidizing agent, they modify the color formed by the precursor.¹

Table 2-2 Some oxidation dye precursors and oxidation dye couplers.

Oxidation dye precursors	Oxidation dye couplers
 p-phenylenediamine	 Resorcinol
 1,4-diaminophenoxyethanol HCl	 1,5-naphthalenediol
 4-amino-m-cresol	 4-amino-2-hydroxytoluene
 Hydroxyethyl-p-phenylenediamine sulfate	 2,4-diamino-5-methylphenoxyethanol

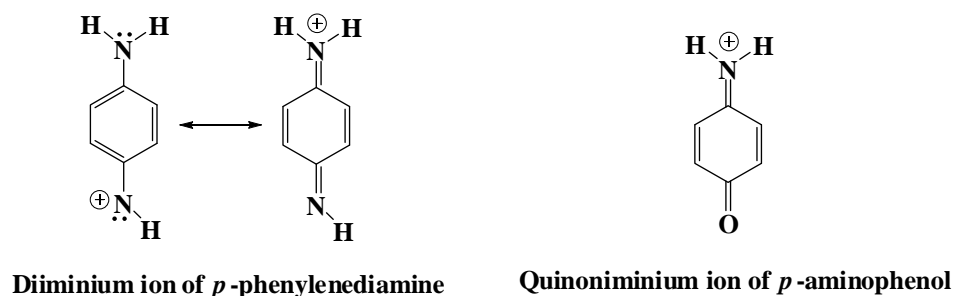
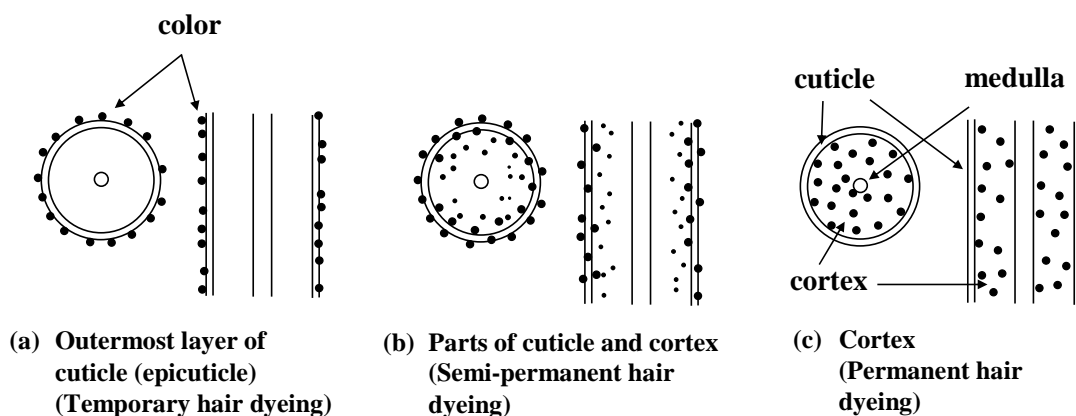


Figure 2-3 Structure of diiminium ion of *p*-phenylenediamine and quinoniminium ion of *p*-aminophenol.



Scheme 2-3 Mechanisms by which different hair dyeing act: (a) temporary hair dyeing, (b) semi-permanent hair dyeing, and (c) permanent hair dyeing.

2.1.3.2 Sunlight-exposed hair

The amino acids of the cuticle are altered to a greater extent than those of the cortex because the outer layers of the fiber receive higher intensities of radiation. Hair protein degradation by light radiation was shown to occur primarily in the wavelength region of 254 to 400 nm or UV. A recent work by Hoting and Zimmermann¹⁰ shows that the proteins of the cuticle are degraded by UV-A (320-400 nm) and UV-B (290-320 nm). This reaction is similar to the oxidative damage to proteins and mitochondrial decay associated with aging.¹¹

2.1.4 Hair product containing chitosan and its derivatives

Over the past few decades, polymers have become increasingly important component in the cosmetic industry. They are used as primary ingredients or adjuncts in hair products. They have been used to hair conditioner to improve the substantivity of other ingredients to hair, to improve emulsion stability, and to improve combing.

The types of bond between the polymer ingredient and hair fiber are valence bonds (ionic and covalent bonds), hydrogen bonds, dispersion forces (Van der Waals attractions). The primary valence bonds include ionic and covalent bonds which are the strongest binding forces. They generally have bond energies of approximately 50 to 200 kcal/mole.¹² Hydrogen bonds are the next strongest binding forces, with bond energies generally of the order of 4 to 10 kcal/mol.¹² These bonds are important to the binding of polymers containing polyalcohol or polyamide units to hair. Dispersion forces or Van der Waals attractions have bond energies generally of the order of 1 kcal/mole.¹³ These attractive forces are short range and act only between the molecule surfaces. Therefore, the total strength of Van der Waals force increases with molecular surface area i.e. increasing molecular size. In polymers, these can approach the valence bonds strength.¹ A typical conditioner consists of cationic surfactant, fatty alcohols, silicones and water. Table 2-3 displays the chemical structure and functions of the major conditioner ingredients.

Chitosan and its derivatives have been introduced in hair-care products, especially the hair conditioners for a few decades. Several studies have been revealed in patent application. In 1985, Lang *et al.*¹⁴ invented treatment cream for hair and skin containing macromolecular glyceryl-chitosan. In 1986, Maresch *et al.*¹⁵ invented film formers in hair-treatment agents. In 1990, Omura *et al.*¹⁶ invented a hair cosmetic without any stickiness, excellent in touch and brush ability, by blending a chitosan derivative which was prepared by reacting chitosan with polysaccharides. In 1996, Satou and Go¹⁷ produced a hair setting agent containing *N*-(3-carboxypropanoyl)-6-*O*-(carboxymethyl)chitosan, 6-*O*-(carboxymethyl)chitosan or 6-*O*-(carboxymethyl)chitin. In 2001, Nishimoto and Toda¹⁸ obtained the composition containing water soluble chitosan such as hydroxypropylchitosan, succinyl chitosan, succinylated carboxymethyl chitosan, and chitosan-pyrrolidone-carboxylate and a cationic polymer such as chlorinated *O*-[2-hydroxy-3-(trimethylammonio)propyl]hydroxyethyl cellulose. In

2003, Yamamoto and Taniuchi¹⁹ invented hair dyeing agents that were based on chitosan and/or chitosan derivatives mixed with oxidation dyes. The dyes showed good properties in terms of dyeing technique and hair care. In 2004, Shimogaki *et al.*²⁰ provided a gray hair-preventing/improving agent comprises a sulfated polysaccharide and/or the salts of chitin-chitosan. In 2005, Krause *et al.*²¹ invented hair treatment containing *N*-hydroxyalkyl-*O*-benzyl chitosan. In 2007, Liu²² disclosed a new detergent, prepared by mixing basic cleaning material with functional additive such as water-soluble chitosan, chitosan hydrochloride, chitosan citrate, and chitosan lactate.

Additionally, these inventors find ways of modifying chitin and chitosan by physical blending or chemical reactions in order to improve the solubility of chitin and chitosan in each type of hair-care products. This is because chitosan is difficult to manipulate because of the solubility problems in neutral water and bases which explained in section 2.2.

From all above literature reviewed, there are few studies emphasizing on the positive charge contents in TMC and HTACC and their effects on hair when used in the form of leave-on conditioner formula.

Table 2-3 Chemical structure and functions of ingredients in hair conditioner.

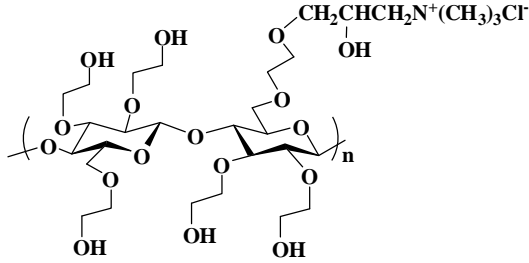
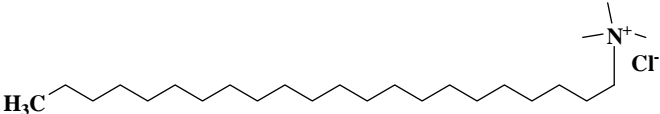
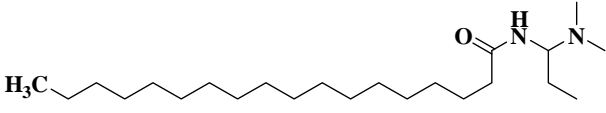
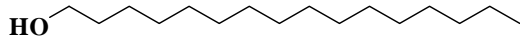
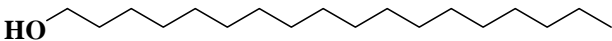
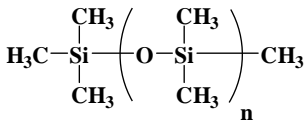
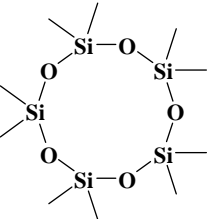
Ingredient	Chemical Structure	Functions
Cationic surfactants	 <p data-bbox="555 1563 1086 1585">Quaternized hydroxyethyl cellulose (polyquaternium-10)</p>	Lubricant and static control agent
	 <p data-bbox="639 1771 999 1798">Behentrimonium chloride (BTMAC)</p>	
	 <p data-bbox="667 1951 1007 1973">Stearamidopropyl dimethylamine</p>	

Table 2-3 *continued*

Ingredient	Chemical Structure	Functions
Fatty alcohols	 <p style="text-align: center;">Cetyl alcohol</p>  <p style="text-align: center;">Stearyl alcohol</p>	Lubricant and moisturizer
Silicones	 <p style="text-align: center;">Dimethicone</p>  <p style="text-align: center;">Cyclopentasiloxane</p>	Lubricant
Water		

2.1.5 Hair analysis

Traditionally, Analysis of human hair and/or analysis of surface hair were performed by using many techniques such as high performance liquid chromatography (HPLC),²³⁻²⁵ gas chromatography/mass spectroscopy (GC/MS),²⁶⁻³⁰ time-of-flight secondary ion mass spectroscopy (ToF-SIMS),^{31,32} Raman spectroscopy,³³⁻³⁶ and DNA analysis.³⁷ Limitations of these techniques are complicated sample preparation, large amounts of sample area for analysis, long scanning analysis times as well as sample destruction in order to obtain good spectral quality. In order to overcome these limitations, the FT-IR with a microscope attachment was developed.

2.1.5.1 ATR FT-IR for material surface analysis

Fourier transform infrared (FT-IR) spectroscopy is a technique based on the determination of absorption of infrared light due to energy resonance with vibrational motions of functional molecular groups, this technique has been applied as an analytical technique in different fields such as geology, material science, polymer science, and many others.

Recently, It was suggested that IR spectroscopy was one of the powerful technique for the forensic analysis of human hair.³⁸ This is because this method is

sensitive to the presences of chemical functional groups in a hair sample. It can provide rapid and specific chemical information at the molecular level associated with the nature of human hair and its composition.

FT-IR sampling technique is generally a transmission technique using KBr pellets.³⁹ The infrared beam is directly passed through the sample. Since the color of hair sample is usually dark, transmission technique cannot be used. Also a sample thicker than 20 μm cannot be analyzed. Reflectance sampling techniques is therefore utilized. The IR beam is bounced off the sample instead of passing through it. In the conventional attenuated total reflectance (ATR) technique, a good contact between the sample and internal reflection element (IRE) is required.⁴⁰

ATR occurs when a sample is brought into contact with an IRE that has a higher refractive index than the sample and is transparent through the mid-infrared radiation. In general, the IRE configuration includes variable-angle hemispherical crystal with single reflection and multiple reflection planar crystal. The IRE is used in internal reflection spectroscopy for establishing the conditions necessary to obtain internal reflection spectra of materials. Germanium (Ge) is a typical IRE with a refractive index of 4.0, which has significantly higher depth of penetration than that of a ZnSe IRE with a refractive index of 2.4. Table 2-4 shows optical properties of some infrared transmitting materials.⁴¹

Table 2-4 Typical properties of selected optical materials used in internal reflection spectroscopy.⁴¹

Material	Penetration depth (μm)	Mean refractive index	Property
Germanium	2.0-12	4.0	good for fine depths of penetrations
Silicon	1.1-6.5	3.5	hard, high resistivity, high-temperature applications
Cadmium telluride	1.0-23	2.64	expensive, relatively inert, can be used in aqueous studies
Zinc selenide	0.5-15	2.4	expensive, water-insoluble, toxic when used with acids
Diamond	1-3.8, 5.9-100	2.4	hard

The penetration depth is the distance from the interface of materials where the evanescent field strength decays to $1/e$ (roughly 13%) of its values at the interface. The penetration depth is given by the following equation:⁴¹

$$d_p = \frac{1}{2\pi\nu n_1 (\sin^2 \theta - (n_2/n_1)^2)^{1/2}} \quad (2.1)$$

where θ is the angle of incidence, ν is the frequency of the infrared radiation and n_1, n_2 are the refractive index of the IRE and a sample. By altering the angle of incidence while ensuring that it remains above the critical angle of the IRE, the depth of penetration can be varied and qualitative depth profiles of a sample can be obtained. In this study, ATR-FTIR was used for identifying functional groups on the surface of the films. Sampling depth of characterization was 1-2 μm .⁴²

ATR FT-IR spectroscopy is a surface sensitive technique. However, it has several limitations. One of them is an optical contact between the sample and IRE. The larger the air gap, the smaller the spectral intensity. If an air gap is large enough, the spectrum cannot be obtained. To solve this problem, high pressure is applied at the sample against the IRE. Nevertheless, it has to be handled very carefully to avoid a damage of brittle IRE by an excessive pressure.

Homemade slide-on Ge IRE accessory

The homemade slide-on Ge μ IRE was developed by Associate Professor Sanong Egkasit, from Sensor Research Unit, Department of Chemistry, Faculty of Science, Chulalongkorn University. The angle of incidence from the objective microscope is varied from 15.6° to 35.5° . To eliminate interference from the internal reflection associated with the radiation having an angle of incidence smaller than the critical angle, an opaque circular adhesive tape is placed on the center of the hemispherical dome. In such manner, ATR FT-IR spectra of a small sample or a small area can be acquired.

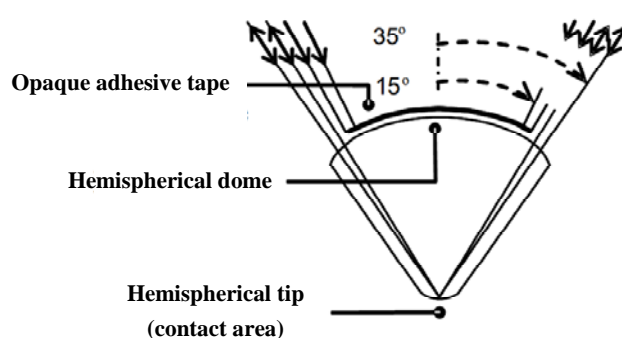


Figure 2-4 The infrared radiation tracing within the Ge μ IRE.

2.1.5.2 Tensile testing of hair samples by miniature tensile tester (MTT) and laser scanning micrometer (LSM)

In this study, hair samples were tested for their tensile properties by miniature tensile tester (MTT) and laser scanning micrometer (LSM). The parameters such as elastic modulus (N/m^2 ; Pa), plateau load ($\text{gmf/sq.}\mu\text{m}$), break extension (%strain), and break load ($\text{gmf/sq.}\mu\text{m}$) are reported.

2.1.5.3 Hair texture analysis

Hair texture in terms of smoothness or slippery feel was determined by measuring the frictional force of hair surface. The friction resistance to the relative motion of two surfaces is proportional to the force, which presses the surfaces together, as well as the roughness of the surfaces. The results can help claim about the effectiveness of hair care products. The area of friction loops (g.mm) is reported.

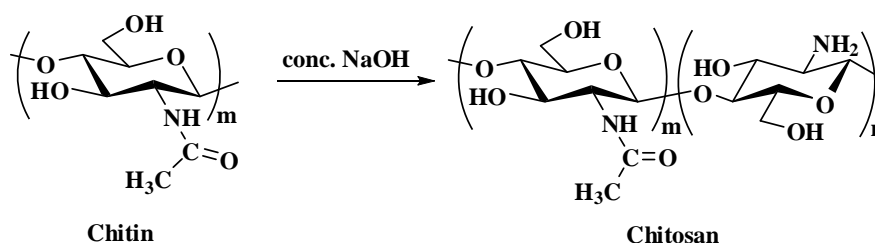
2.1.5.4 Wet combing test by Instron 5564 tensile test tester

This technique was used for measuring the frictional forces generated upon combing a hair tress with a fine toothed comb representing ease of combing and hair detangling. Instrumentally, the ease of combing can be measured by monitoring the frictional forces that result as the hair passes through the comb. These combing forces are measured as a function of the distance traveled along the hair tress. The parameters such as maximum combing force (gmf), average combing force (gmf) and combing energy (mJ) can be used to evaluate hair-care products. The distinctions of hair-care products are easier to detect during wet combing experiments.

2.2 Chitosan and Charged Derivatives

2.2.1 Chitosan

Chitosan was prepared by alkaline *N*-deacetylation of chitin, which is the second most abundant polysaccharide found on earth next to cellulose. Chitosan is a natural polysaccharide consisting primarily of the repeating unit of 2-amino-2-deoxy-D-glucose (GlcN) with a small amount of 2-acetyl-2-deoxy-D-glucose (GlcNAc) unit. Chemical structures of chitin and chitosan are shown in Scheme 2-4. The amount of GlcN unit in chitosan is generally referred to the percentage degree of deacetylation or %*DD*, which influencing its physical, chemical properties as well as biological activities. Various techniques can be used for determination of %*DD* such as IR,^{43,44} NMR,⁴⁵ colloidal titration method,⁴⁶ UV Spectrophotometry,⁴⁷ and pH-potentiometric titration.⁴⁸

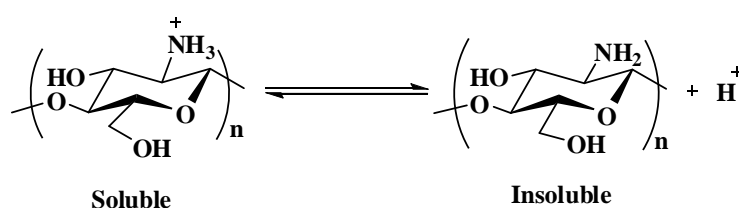


Scheme 2-4 Structures of chitin and chitosan.

As a natural renewable resource, chitosan has a number of unique properties including antimicrobial activity, non-toxicity, and biodegradability. These attract

scientific and industrial interest in such fields as cosmetics, biotechnology, pharmaceuticals, wastewater treatment, agriculture, food science, and textiles. Due to its reactive amino and hydroxyl groups, chemical modification of chitosan to achieve its derivatives is used to expand its application.

Chitosan dissolves in dilute organic acids, but is insoluble in neutral water. The pKa value of the primary amino groups in chitosan is determined to be around 6.5⁴⁹⁻⁵¹ (Scheme 2-5); it precipitates above this pH due to losing its cationic nature. The application of chitosan is thus limited owing to the insolubility in neutral or high pH region.

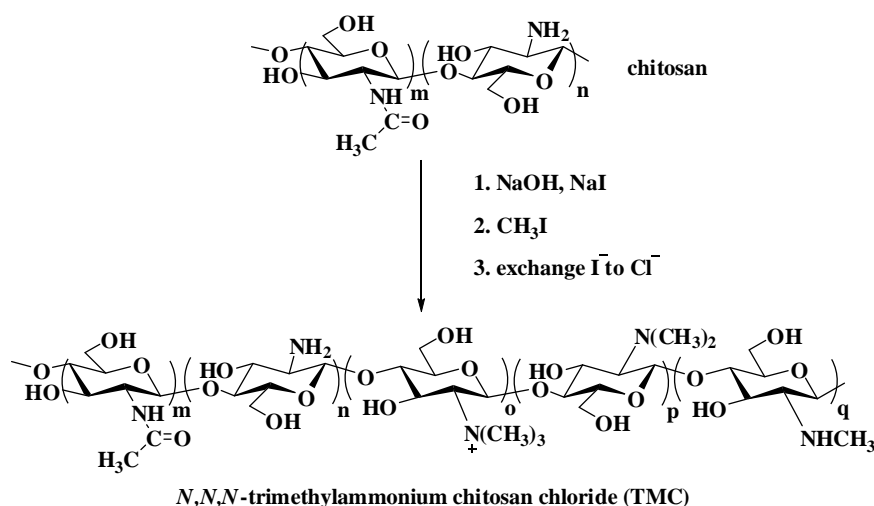


Scheme 2-5 Soluble and insoluble form of chitosan in water.

2.2.2 Charged derivatives of chitosan

An effective way to improve the solubility of chitosan is to introduce charged functional groups to the native chitosan. Chitosan has both reactive amino and hydroxyl groups, which can react as versatile functional groups for chemical modification under mild reaction conditions. This research is interested in the positively charged functional groups, i.e. TMC and HTACC, which are potentially hair-coating materials because in a normal environment human hair is negatively charged. The following related research publications have been reported on chemical modification of chitosan especially at the amino and/or hydroxyl groups to produce charged derivatives.

Methylation at the amino groups was explored by many researchers.^{2,52-54} The resulting product is *N,N,N*-trimethylammonium chitosan chloride (TMC) (Scheme 2-6). The presence of positive charges along the polymer chain helps increase its solubility in water.



Scheme 2-6 Synthesis of *N,N,N*-trimethylammonium chitosan chloride (TMC) from chitosan.

In 1998, Sieval *et al.*² synthesized TMCs and studied their solubility comparing to the native chitosan. The product yield and degree of quaternization (%*DQ*) could be controlled by means of the number of methylation steps, the duration of each reaction step and the amount of methyl iodide. %*DQ* was calculated using the following equation:

$$\%DQ = \left[\frac{\int N^+(CH_3)_3}{\int NHC\overline{O}CH_3} \times \frac{3}{9} \right] \times 100 \quad (2.2)$$

where $\int N^+(CH_3)_3$ is the integral of the 9 H's on the three methyl groups (9 H's) attached to the quaternary ammonium atom. $\int NHC\overline{O}CH_3$ is the integral of methyl protons from acetamides of GlcNAc unit. A two-step reaction gave products with high degrees of quaternization (40-80%). A three-step reaction procedure yielded products with a higher degree of quaternization > 80%, but with substantially decreased water-solubility. This was because it also resulted in methylation at the hydroxyl group (*O*-methylation), which decreased the number of -OH groups along the chitosan chain, resulting in the decrease of solubility.

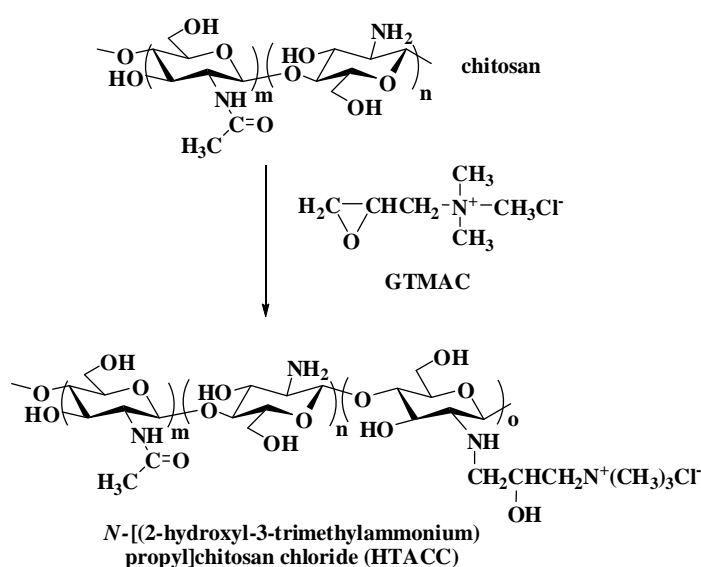
In 2008, Runarsson *et al.*⁵³ suggested a new synthesis of TMC by using DMF/H₂O mixture as a reaction solvent. The reaction was performed without the aid of a catalyst (i.e. sodium iodide). %*DQ* was calculated using the following equation:

$$\%DQ = \left[\frac{\int N^+(CH_3)_3}{\int H-2',3,4,5,6,6'} \times \frac{6}{9} \right] \times 100 \quad (2.3)$$

where $\int N^+(CH_3)_3$ is the integral of the 9 H's on the three methyl groups (9 H's) attached to the quaternary ammonium atom. $\int H-2',3,4,5,6,6'$ is the integral corresponding to the H-2',3,4,5,6 and 6' protons. This reaction condition significantly reduced *O*-methylation. They obtained TMCs with degree of quaternization between 81 and 88% without any *O*-methylation.

Additionally, positively charged chitosan was prepared by grafting glycidyltrimethyl ammonium chloride (GTMAC), a molecule carrying an ammonium group, on the chitosan chain via epoxide ring opening by the amino groups of chitosan.

In 2000, Seong *et al.*³ synthesized *N*-(2-hydroxy)propyl-3-trimethyl ammonium chitosan chloride (HTACC), using a reaction of GTMAC (Scheme 2-7) and chitosan. The complete substitution of NH_2 in chitosan with GTMAC was achieved when the reaction was performed at 80°C for 18 h with a 4:1 mole ratio of GTMAC to $-NH_2$ in the presence of acetic acid. HTACC showed superior antimicrobial activity to chitosan due to the quaternary ammonium group from the substitution of NH_2 in chitosan with GTMAC. They were applied to the cotton fabrics.



Scheme 2-7 Synthesis of *N*-(2-hydroxy)propyl-3-trimethylammonium chitosan chloride (HTACC) from chitosan.

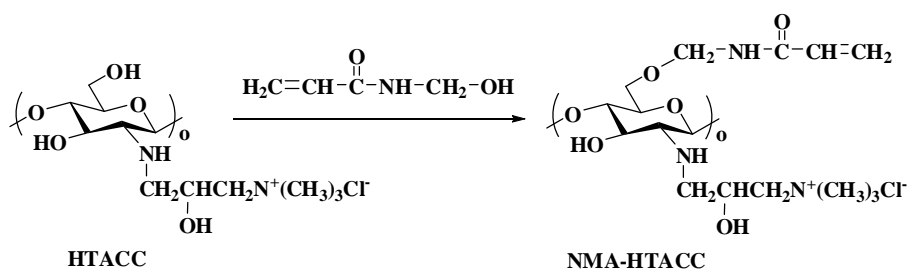
In 2006, Cho *et al.*⁵⁵ synthesized HTACC in order to facilitate its use as a novel material for biomedical applications. Varying the molar ratio of GTMAC to chitosan

from 3:1 to 6:1 produced HTACCs with %*DQ* that ranged from 56% to 74%. %*DQ* was determined based on the conductivity and calculated using the following equation:

$$\%DQ = \frac{1.7 \times 10^{-5} \times V_{AgNO_3}}{\left(\frac{W_w - (1.7 \times 10^{-5} \times V_{AgNO_3} \times m_{GTMAC})}{(m_G \times DD) + m_{AG}(1 - DD)} \right)} \times 100 \quad (2.4)$$

where 1.7×10^{-5} corresponds to the number of moles of $AgNO_3$ in 1 mL of solution. W_w is the weight of HTACC in 100 mL (0.1 g). m_{GTMAC} is the molecular weight of GTMAC (151 g/mol). m_G is the molecular weight of glucosamine (161 g/mol). m_{AG} is the molecular weight of *N*-acetyl-glucosamine (203 g/mol). The *DD* of chitosan is 0.92. The HTACC with the highest %*DQ* was soluble in water up to concentrations of 25 g/dL at room temperature.

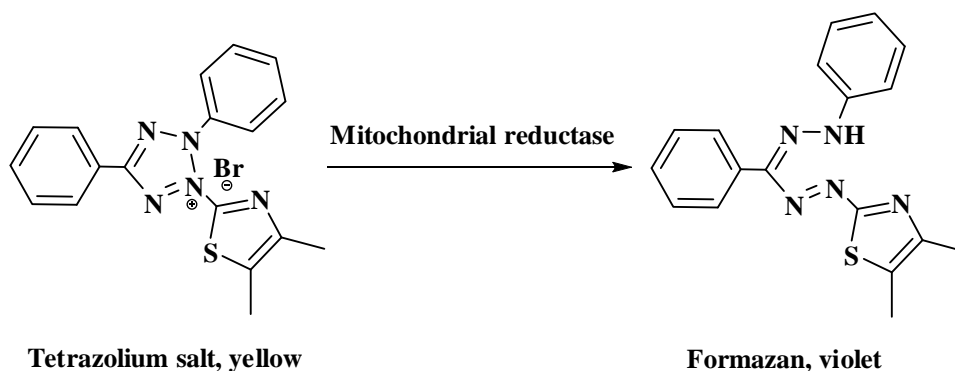
In 2004, Lim *et al.*⁵⁶ synthesized a fiber-reactive chitosan derivative in two steps from low molecular weight chitosan and low degree of acetylation. First, HTACC was prepared as presented in Scheme 2-7. Second, this derivative was further modified by reacting with *N*-methylolacrylamide (NMA), which can be covalently bonded to cellulose textile fibers having nucleophilic groups under alkaline conditions. The prepared fiber-reactive chitosan derivative, *O*-acrylamidomethyl-HTACC (NMA-HTACC) is shown in Scheme 2-8. The NMA-HTACC showed complete bacterial reduction within 20 min at the concentration of 10 ppm, when contacted with *Staphylococcus aureus* and *Escherichia coli* [$1.5\text{--}2.5 \times 10^5$ colony forming units per milliliter (CFU/mL)].



Scheme 2-8 Synthesis of NMA-HTACC.

2.3 MTT Reduction Assay

An alternative method that was originally developed as a rapid assay for growth and survival of mammalian lymphoma cells is based on the transformation and colorimetric quantification of MTT [3-(4,5-dimethylthiazol-2-yl)-2,5-diphenyl tetrazolium bromide] assay that described by Mosmann in 1983.⁵⁷ MTT assay is based on the ability of a mitochondrial dehydrogenase enzyme from viable cells to cleave the tetrazolium rings of the pale yellow MTT and thereby form non-water-soluble violet formazan crystals within the cell (Scheme 2-5) which is largely impermeable to cell membranes, thus resulting in its accumulation within healthy cells. Solubilization of the cells by the addition of a detergent results in the liberation of the crystals that are solubilized. The number of surviving cells is directly proportional to the level of the formazan product created. The color can then be quantified using a simple colorimetric assay, such as a UV spectrophotometer.



Scheme 2-9 Reduction of the MTT tetrazolium salt to formazan.⁵⁷

The MTT assay is used in many studies to evaluate the viability of different cells because this test is fast. Many samples can be examined at the same time and many replications of each sample can be performed simultaneously.

CHAPTER III

METHODS AND MATERIALS

3.1 Experimental Design

This work was divided into three parts. The first part was to synthesize the two-chitosan derivatives, TMC and HTACC, by varying equivalent of reacting agent and reaction times. In addition, the cytotoxicity of chitosan and its derivatives were examined. IC_{50} or 50% inhibitory concentrations values were determined with human keratinocyte cell line (HaCaT) by using the 3-(4,5-dimethylthiazol-2-yl)-2,5-diphenyl tetrazolium bromide (MTT) assay. The second part was to prepare five “leave-on” formulations i.e. leave-on formulation without cationic polymers (LO), leave-on formulation with polyquaternium-10 (LO+quat), leave-on with chitosan (LO+chitosan), leave-on with TMC (LO+TMC), and leave-on with HTACC (LO+HTACC). Moreover, four types of damaged hairs i.e. waved, straightened, dyed, and UV damaged were used as test substrates. The last part, the roles of leave-on were studied in terms of physical and mechanical properties of leave-on coated hairs. The presence of the compounds coated on hair was determined by scanning electron microscopy (SEM) and microscope-attached attenuated total reflection-Fourier transform infrared (ATR FT-IR) microspectroscopy with a slide-on germanium internal reflection element (IRE).

3.2 Materials

3.2.1 Sample and reagents

Black hairs from an Asian thirty two-year old female used in this study were supplied by Life Science Cosmetics Research Center Co., Ltd. All reagents and materials are analytical grade. Chitosan with a weight-average molecular weight of 45,000 Da was purchased from Seafresh Chitosan (Lab) Co., Ltd., Thailand. The degree of deacetylation (DD) was 85% as determined by 1H NMR. A dialysis tubing cellulose membrane (Sigma) with molecular weight cut-off of 12,400 g/mol (avg. diameter. 49 mm; avg. flat width 76 mm) was used to purify all modified chitosans. Iodomethane,

CH₃I (Riedel-deHaen); glycidyltrimethylammonium chloride, GTMAC (Fluka); *N*-Methyl-2-pyrrolidone, NMP (Merck); acetic acid, glacial (Merck); acetone, analytical grade (Merck); silver nitrate, AgNO₃ (Merck); sodium chloride, NaCl (Merck); sodium hydroxide, NaOH (Merck); sodium iodide, NaI (Aldrich); sodium sulfide, Na₂S (Merck); sulfuric acid, conc. (Merck) were used as received.

3.2.2 Instruments

1. Labconco Corporation freeze dryer model 7753501
2. Mercury Varian 400 MHz nuclear magnetic resonance (NMR) spectrometer
3. Perkin Elmer Fourier transform infrared (FT-IR) spectrometer model system 2000
4. Rayonet Photochemical Reactors model RPR-100 and UV lamps with 313 nm (UVB)
5. Nicolet 6700 FT-IR spectrometer equipped with a mercury-cadmium-telluride (MCT) detector (Thermo Electron Corporation, Madison, WI, USA)
6. Contiuµm™ infrared microscope with 15X Cassegrain infrared objective and 10X glass objective
7. Homemade slide-on germanium (Ge) µIRE
8. Scanning electron microscope (SEM) model JEOL, JSM-6480LV
9. Industrial presses (Hand Toggle) (HMC-Brauer Ltd, Milton Keynes, England)
10. Miniature tensile tester (MTT)
11. Laser scanning micrometer (LSM-series 500)
12. TA.XT.Plus Stable Microsystems Texture Analyzer
13. Instron 5564 tensile test tester equipped with Bluehill software version 2.0
14. Brookfield digital viscometer model DV-I+ (Brookfield Engineering Laboratories, Inc., Middleboro, USA)

3.3 Experimental Methods

3.3.1 Synthesis of *N,N,N*-trimethylammonium chitosan chloride (TMC)

TMCs were synthesized by methylation of chitosan with iodomethane in the presence of NaOH as described by Sieval *et al.*² Chitosan (~5 g) was dispersed in NMP at 50°C for 18 h. NaI (3.8 g, 1 equiv) and 15% w/v aqueous NaOH were added and stirred at 50°C for 15 min. Subsequently, iodomethane (9.52 mL, 6 equiv) was added in two equal portions (4.76 mL each) at 6 h intervals at 50°C. Finally, the mixture was stirred at 50°C for 18 h. After methylation, the product was precipitated in acetone. The precipitate was then isolated by centrifuge. The solid product was dispersed in 15% w/v NaCl solution in order to exchange the I⁻ counter-ions of the TMC for Cl⁻. The final suspension was dialyzed with deionized water for three days, followed by freeze-drying to obtain a cotton-like material. The amounts of iodomethane were varied to 4.76 mL (4 equiv) or 7.93 mL (5 equiv) or 14.28 mL (12 equiv) in order to synthesize TMC having different *DQs*.

Moreover, NMP solvent was replaced by DMF:H₂O (1:1) or H₂O in order to increase methylating efficiency of iodomethane on chitosan.

3.3.2 Synthesis of *N*-[(2-hydroxyl-3-trimethylammonium)propyl] chitosan chloride (HTACC)

HTACCs were synthesized by reacting chitosan with GTMAC as described by Seong *et al.*³ Chitosan (~5 g) was dissolved in 1% v/v acetic acid at room temperature. Then GTMAC (7.7 g, 2 equiv) was added into the chitosan solution. The reaction was performed at 70°C for 24 h. After the reaction, products were dialyzed with deionized water for three days, followed by freeze-drying to obtain a cotton-like material. HTACCs with different *DQs* were synthesized by starting with 5 g of chitosan but using 15.3 g (4 equiv) or 23.0 g (6 equiv) of GTMAC and varying the reaction times (2, 4, 8, 12, and 24).

3.3.3 Characterization of chitosan and its charged derivatives

Chemical structures of chitosan and its charged derivatives were determined by ¹H NMR spectroscopy. Chemical shifts (δ) were reported in part per million (ppm) relative to tetramethylsilane (TMS) or using the residual protonated solvent signal as a

reference. All measurements were performed at 300K, using pulse accumulations of 128 scans. D₂O/CF₃COOD was the solvents for 10 mg chitosan and its derivatives. According to the literature, the hydrogen atom bonded to carbon 2-6 of the glucopyranose ring is responsible for the set of signals ranging from 3.25 to 4.25 ppm (for TMC) and from 3.40 to 3.80 ppm (for HTACC) while those signals observed at 3.10 ppm are attributed to the hydrogen atoms of the three methyl groups (9 H's). From the ratio between the area under a reference signal and that under the signals of the quaternary ammonium group, it is possible to determine the degree of quaternization (%DQ) of the TMCs and HTACCs by using expression:

$$\text{Degree of quaternization} = \%DQ = \left[\frac{\int N^+(CH_3)_3/9}{\left(\int H-2',3,4,5,6,6'/6\right) \times DD} \right] \times 100 \quad (3.1)$$

where, %DQ is the degree of quaternization; $\int N^+(CH_3)_3$ is the integral of the 9 H's on the three methyl groups (9 H's) attached to the quaternary ammonium atom. $\int H-2',3,4,5,6,6'$ is the integral corresponding to the H-2',3,4,5,6 and 6' protons from 3.25 and 4.25 ppm (for TMC) and from 3.40 to 3.80 ppm (for HTACC). The DD of chitosan determined by ¹H NMR was 0.85.

In addition, the signals observed at 2.85 and 2.65 ppm are attributed to the hydrogen atoms of the methyl groups pertaining to di- and monomethylated amino groups, respectively in TMC. The average degree of dimethylation (%DS_{N(CH₃)₂}) and degree of monomethylation (%DS_{NHCH₃}) of the methylated product were analyzed by using expression:

$$\text{Degree of monomethylation} \quad \%DS_{NHCH_3} = \left[\frac{\int NHCH_3/3}{\left(\int H-2',3,4,5,6,6'/6\right) \times DD} \right] \times 100 \quad (3.2)$$

$$\text{Degree of dimethylation} = \%DS_{N(CH_3)_2} = \left[\frac{\int N(CH_3)_2/6}{\left(\int H-2',3,4,5,6,6'/6\right) \times DD} \right] \times 100 \quad (3.3)$$

where, $\int N(CH_3)_2$ is the integral of the dimethyl peak (6 H's). $\int NHCH_3$ is the integral of the monomethyl peak (3 H's). $\int H-2',3,4,5,6,6'$ is the integral corresponding to the H-2',3,4,5,6 and 6' protons from 3.25 and 4.25 ppm.

In addition, undesired methylation at the hydroxy groups on chitosan (3.20 and 3.15 ppm) was also found in TMC. The degrees of methylation at 3-O and 6-O (*DOM-3* and *DOM-6*) of the TMCs were calculated by using the following equation:

$$\%DOM - 3 = \left[\frac{\int 3 - OCH_3 / 3}{(\int H - 2', 3, 4, 5, 6, 6' / 6) \times DD} \right] \times 100 \quad (3.4)$$

$$\%DOM - 6 = \left[\frac{\int 6 - OCH_3 / 3}{(\int H - 2', 3, 4, 5, 6, 6' / 6) \times DD} \right] \times 100 \quad (3.5)$$

In addition, the %*DQ* of TMCs and HTACCs were determined by titration method. The Cl⁻ counter ions of TMC and HTACC were titrated with aqueous silver nitrate (AgNO₃) as described by Lim *et al.*⁵⁶ Briefly, 0.1 g of TMC or HTACC was dissolved in 100 mL deionized water. The conductivity of the TMC or HTACC solution was measured as a function of the volume of 0.017 M AgNO₃ added using a conductivity meter. The volume of 0.017 M AgNO₃, V_{AgNO_3} , that resulted in the lowest conductivity for TMC or HTACC solution was employed to calculate the %*DQ* using the following equation:

$$\%DQ_{(TMC)} = \frac{1.7 \times 10^{-5} \times V_{AgNO_3}}{\left(\frac{W_w - (1.7 \times 10^{-5} \times V_{AgNO_3} \times m_{CH_3Cl})}{(m_G \times DD) + m_{AG}(1 - DD)} \right) \times DD} \times 100 \quad (3.6)$$

$$\%DQ_{(HTACC)} = \frac{1.7 \times 10^{-5} \times V_{AgNO_3}}{\left(\frac{W_w - (1.7 \times 10^{-5} \times V_{AgNO_3} \times m_{GTMAC})}{(m_G \times DD) + m_{AG}(1 - DD)} \right) \times DD} \times 100 \quad (3.7)$$

Specifically, 1.7×10^{-5} corresponds to the number of moles of AgNO₃ in 1 mL of solution. W_w is the weight of TMC or HTACC in 100 mL (0.1 g). m_{CH_3Cl} is the molecular weight of CH₃Cl (50 g/mol). m_{GTMAC} is the molecular weight of GTMAC (151 g/mol). m_G is the molecular weight of glucosamine (161 g/mol). m_{AG} is the molecular weight of *N*-acetyl-glucosamine (203 g/mol). The *DD* of chitosan is 0.85.

The FT-IR spectra of chitosan and its derivatives were recorded with a Perkin Elmer model system 2000 Fourier Transform Infrared (FT-IR) spectrometer, with 32 scans at resolution 4 cm^{-1} . A frequency of $4000\text{-}400\text{ cm}^{-1}$ was collected by using TGS detector. All samples were prepared as potassium bromide pellets.

3.3.4 Solubility tests of the charged derivatives of chitosan

Solubility was monitored visually. Solid samples of TMCs or HTACCs (100 mg) were dispersed in H_2O (20 mL) according to a method of Sashiwa *et al.*⁵⁸ The pH of the solution was adjusted with 0.5% w/v aqueous HCl and NaOH.

3.3.5 Cytotoxicity of chitosan and its charged derivatives

Cytotoxicity in terms of IC_{50} of chitosan, TMCs, and HTACCs were examined on human keratinocyte cells line or HaCaT using MTT assay at pH 6.0. Dulbecco's Modified Eagle's Medium (DMEM, Hyclone, pH=7.4) solution containing *N*-(2-hydroxyethyl)piperazine-*N*-(2-ethanosulphonic acid) (HEPES), NaHCO_3 , 1% v/v penicillin/streptomycin, 10% v/v fetal bovine serum in sterilized H_2O , was used as culture medium. HaCaT cell cultures of passage numbers 5-13 were used for all of the experiments. The cells were seeded in 96-well plates (Costar) at a seeding density of 1×10^5 cells/mL. The test sample was dissolved in the above-mentioned solution at concentrations ranging from 0.5-5000 $\mu\text{g/mL}$. HaCaT cells were treated with varying concentrations of the test sample for 24 h in humidified atmosphere with 5% CO_2 at 37°C .

Statistical analysis of IC_{50} comparison between concentrations of the test sample was performed using Statistical Package for the Social Science (SPSS) version 14.0 software. Statistical comparisons made by the One-Way Analysis of Variance (ANOVA) with the Fisher's Least Square Difference (Fisher's LSD) tests. Each experiment was performed at least twelve times. All data were presented as a mean value with its standard deviation indicated. Differences were considered to be statistically significant when the *p* values were less than 0.05.

3.3.6 Preparation of leave-on conditioner

Five formula of leave-on conditioners were prepared; leave-on without cationic polymers (LO), leave-on with polyquaternium-10 (LO+1%quat), with chitosan (LO+1%chitosan), with TMC (LO+1%TMC), and with HTACC (LO+1%HTACC).

Table 3-1 Chemical composition of leave-on formulation without cationic polymer and leave-on formulation with 1%w/w polyquaternium-10, chitosan, TMC or HTACC

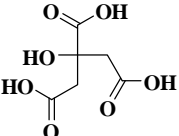
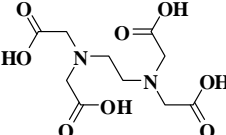
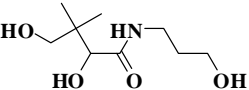
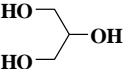
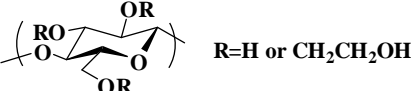
Composition of leave-on formula		Amount (%w/w)	
		LO	LO+cationic polymers
PART A: Water phase			
Citric acid	 <p style="text-align: center;">Citric acid</p>	q.s.	q.s.
Disodium EDTA	 <p style="text-align: center;">EDTA</p>	0.100	0.100
DI water		84.630	83.630
DL-panthenol	 <p style="text-align: center;">DL-panthenol</p>	0.150	0.150
Glycerine	 <p style="text-align: center;">Glycerine</p>	5.000	5.000
Hydroxyethyl-cellulose	 <p style="text-align: center;">Hydroxyethylcellulose</p>	0.020	0.020

Table 3-1 *continued*

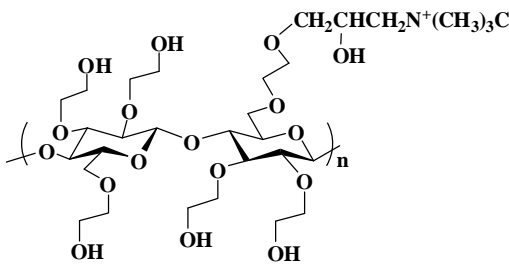
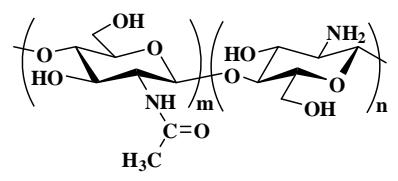
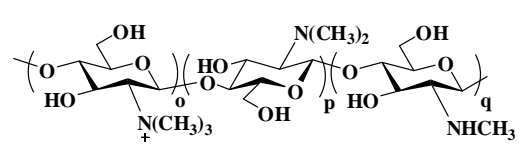
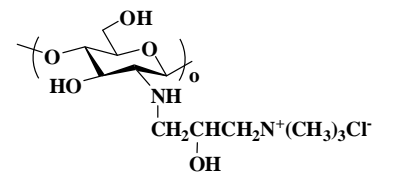
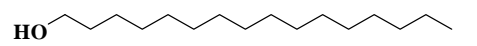
Composition of leave-on formula		Amount (%w/w)	
		LO	LO+cationic polymers
Polyquarternium-10, Chitosan, TMC, or HTACC	 <p>Quaternized hydroxyethyl cellulose (polyquarternium-10)</p>  <p>Chitosan</p>  <p><i>N,N,N</i>-trimethylammonium chitosan chloride (TMC)</p>  <p><i>N</i>-[(2-hydroxyethyl)-3-trimethylammonium]propylchitosan chloride (HTACC)</p>	-	1.000
PART B: Oil phase			
Cetareth-6	a polyoxyethylene ethers of a mixture of cetyl alcohol and stearyl alcohol	2.000	2.000
Cetyl alcohol	 <p>Cetyl alcohol</p>	2.000	2.000

Table 3-1 *continued*

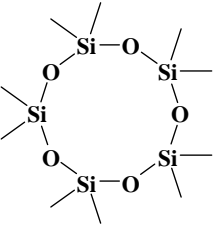
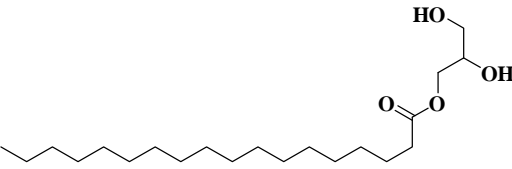
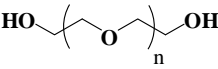
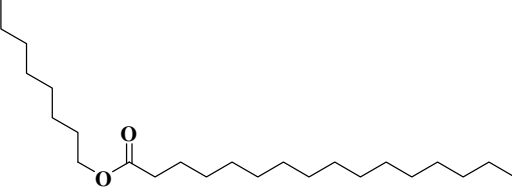
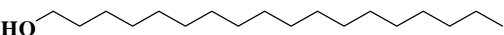
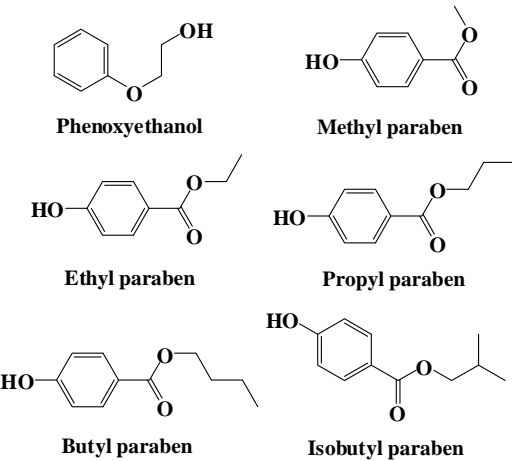
Composition of leave-on formula		Amount (%w/w)	
		LO	LO+cationic polymers
Cyclomethicone	 <p>Cyclomethicone</p>	2.000	2.000
Glyceryl stearate and PEG-100	 <p>Glyceryl stearate</p>  <p>Polyethylene glycol</p>	1.000	1.000
Octyl palmitate	 <p>Octyl palmitate</p>	1.000	1.000
Stearyl alcohol	 <p>Stearyl alcohol</p>	1.000	1.000
PART C: Additive			
Euxyl K300	 <p>Phenoxyethanol Methyl paraben</p> <p>Ethyl paraben Propyl paraben</p> <p>Butyl paraben Isobutyl paraben</p>	0.500	0.500

Table 3-1 *continued*

Composition of leave-on formula	Amount (%w/w)	
	LO	LO+cationic polymers
Hydrolyzed wheat protein	0.100	0.100
Hydrolyzed silk protein	0.100	0.100
Quaternium-79 a cationic conditioning agent from virgin hydrolyzed collagen palm oil combine with collagen	0.100	0.100
Sunshine	0.300	0.300
Total	100.00	100.00

3.3.7 Preparation of cosmetically-treated hairs

Waved, straightened, and dyed hairs were prepared by treating hair strands with Angela™ Cold wave lotion (Just Modern), Caring® Hair straightener cream, and Caring® Beauty hair colour cream, respectively. A UV lamp with 313 nm (UVB, RPR-3000A° lamp) was used as an irradiation source to prepare UV-damaged hairs. Hair strands were clamped vertically at a distance of 1.5 inches from the UV lamp (as shown in Figure 3-1).

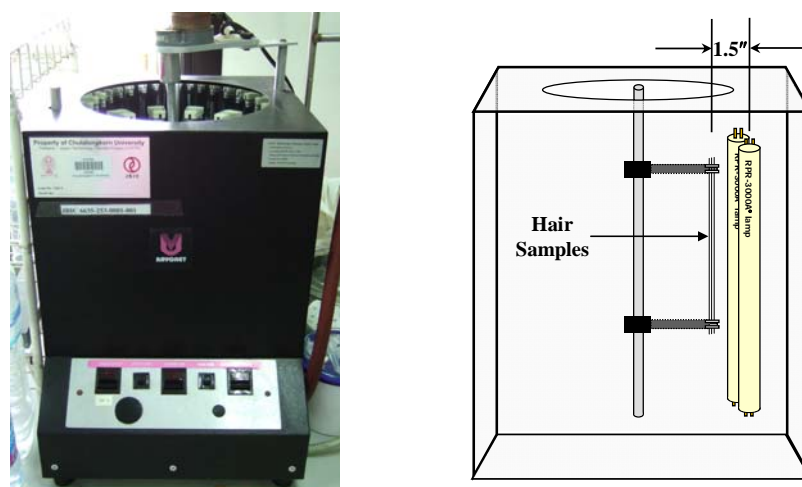


Figure 3-1 Rayonet Photochemical Reactors model RPR-100 and the position of hairs in reactors.

3.3.8 Analysis of hair samples by attenuated total reflectance-Fourier transform infrared (ATR FT-IR)

All human hair samples were air-dried prior to analyses. All ATR spectra of hair surface were collected with a ContinuumTM infrared microscope equipped with a liquid N₂ cooled mercury-cadmium-telluride (MCT) detector. The microscope was connected to a Nicolet 6700 FT-IR spectrometer (Thermo Electron Corporation, Madison, WI, USA). Spectra in the mid-infrared region (4000-650 cm⁻¹) at a spectral resolution of 4 cm⁻¹ were collected with 128 co-addition scans. A homemade ATR accessory with a slide-on miniature germanium (Ge) IRE was lightly pressed on the hair sample during spectral acquisitions.

Cysteic acid content of hair surface

Normalization of IR spectra of virgin and treated hairs was carried out based on amide I band at 1657 cm⁻¹, in which the peak area was large and not influenced by the chemical and photochemical treatment on the hair. The cysteic acid content of the hair surface was determined from the area ratio of the S=O band (calculated from the peak to a baseline, which was drawn between 1020 and 1070 cm⁻¹), and the amide I peak. (calculated from the peak to a baseline, which was drawn between 1580 and 1730 cm⁻¹).

Secondary structure of chemical constituents on hair surface

The information of secondary structure of keratin proteins were acquired by curve fitting analysis. The amide I region between 1580 and 1730 cm⁻¹ was deconvoluted by fitting with Gaussian and Lorentzian functions. The peak position and peak area of the fitted peak were identified and used to elucidate the secondary structure information.

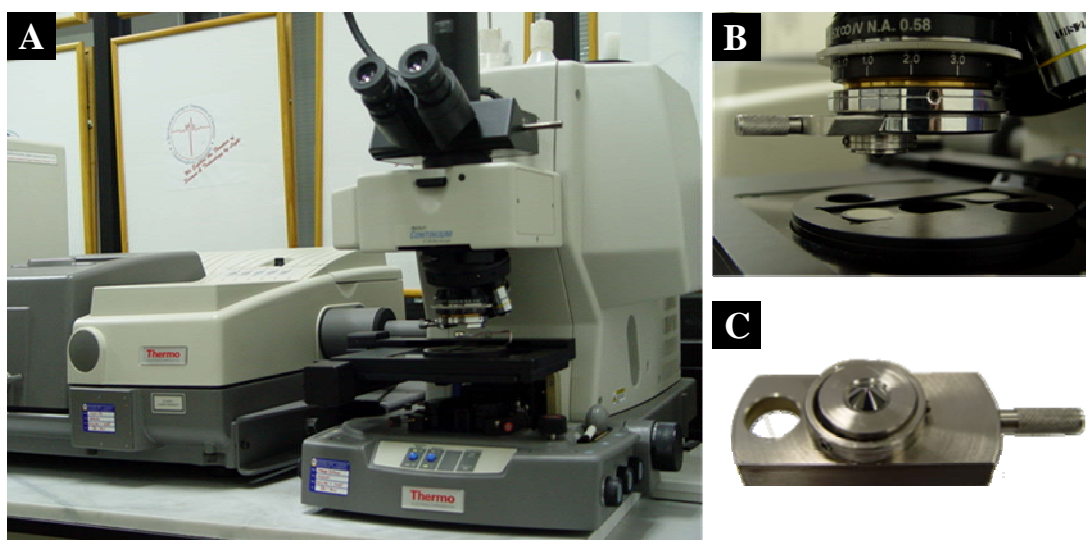


Figure 3-2 ATR FT-IR microspectroscopy: (A) Continuum™ infrared microscope attached to the Nicolet 6700 FT-IR spectrometer, (B) the slide-on Ge μ IRE is fixed on the position of slide-on housing on the infrared objective, and (C) homemade slide-on Ge μ IRE.

Default Spectral Acquisition Parameter

Nicolet 6700 FT-IR Spectrometer

Instrumental Setup

Source	Standard Globar™ Infrared Light Source
Detector	MCT
Beam splitter	Ge-coated KBr

Acquisition Parameters

Spectral resolution	4 cm^{-1}
Number of scans	128 scans
Spectral format	Absorbance
Mid-infrared range	4000-650 cm^{-1}

Advanced Parameters

Zero filing	none
Apodization	Happ-Genzel

Phase correction Mertz

Continuum™ Infrared Microscope

Instrumental Setup

Detector MCT

Objective 15X Schwarzschild-Cassegrain

Aperture size 150 μm \times 150 μm

3.3.9 Morphology of hair samples by scanning electron microscopy (SEM)

All human hair samples were air-dried on a glass slide. The samples were sputter-coated by gold films, and moved to specimen chamber. The morphology of hairs was then analyzed. The operating accelerating voltage was 15 kV for capturing the image of samples.

3.3.10 Tensile testing of hair samples by miniature tensile tester (MTT)

Hair samples were randomly selected. The single hair was threaded onto ferrules. Then, the hair was laid on the sample-mounting block as shown in Figure 3-3. One side of hair was clung and the remaining of hair was also clung while gently pulling the hair straight. After the hair block was placed under press, the hair was released from the sample-mounting block and uses a sharp tool to remove the crushed ferrules from the block.

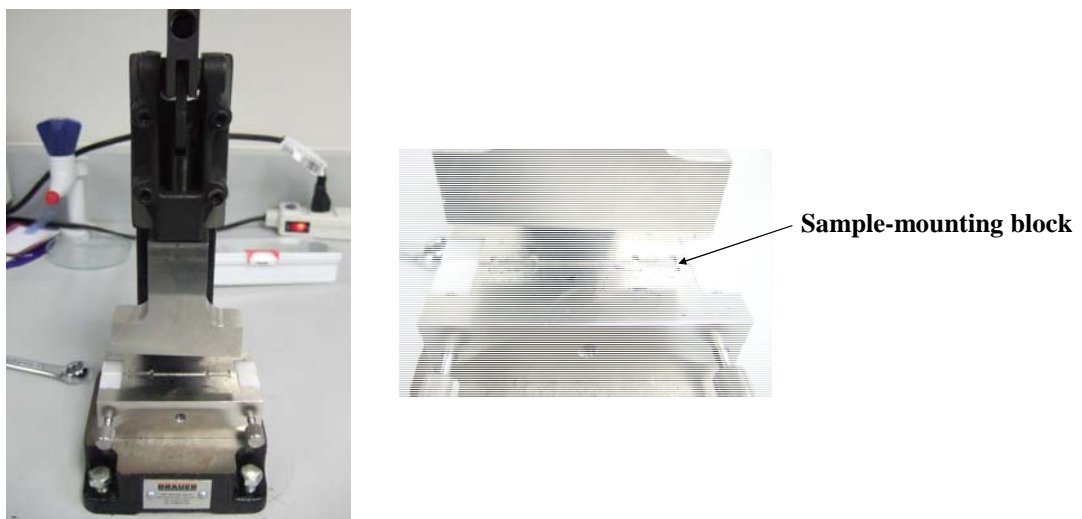


Figure 3-3 Industrial presses (Hand Toggle).

The hair sample was extended to break on miniature tensile tester (MTT) as shown in Figure 3-4. The rate of extension was 20 mm/min. All the single hair was initially conditioned at temperature and humidity control room (22°C, 50%RH). Ten specimens were tested for each sample type. The cross-sectional area (sq.µm) of the hair sample was determined by laser scanning micrometer (LSM).

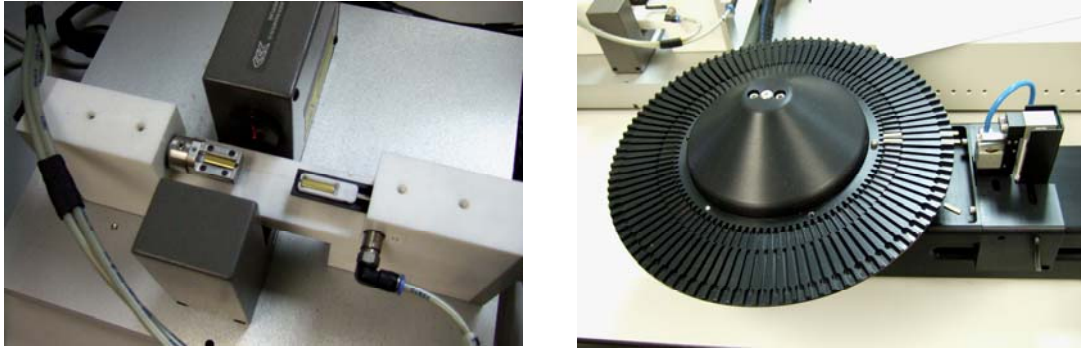


Figure 3-4 Laser scanning micrometer, LSM-series 500 (left); Miniature tensile tester, MTT (right).

Elastic modulus (N/m^2 ; Pa), plateau load (gmf/sq.µm), break extension (%strain), and break load (gmf/sq.µm) that are associated with hair strength were determined. The mean and standard deviation values of each parameter were recorded for each sample. Data is analyzed by Fisher's Least Square Difference (Fisher's LSD) at 95% confidence level.

3.3.11 Hair texture analysis

3.0 g of virgin hairs with 7 inches and 1.5 inches wide dimension were aligned in parallel. Then hairs were secured at the root end by aluminium clip and glue. The remaining hair tip was trimmed out, to obtain 2.5 g of hair tress with 6 inches long for the test. Five tresses were wetted together under tap water at a flow rate 4 L/min, at 37°C for 5 sec. The tresses were washed with 1.25 g of 14% sodium lauryl ether sulfate (SLES).2eo, twice before treatment. Then the tresses were combed through until the tresses were aligned. An amount of 2.15 g of leave-on conditioner was applied for 1 min. Each sample was tested wet by rolling neoprene probe. Five specimens were tested for each sample type by Texture Analyzer as shown in Figure 3-5. All tested tresses were left overnight in a temperature and humidity control room (22°C, 50%RH) before measuring by the same procedure but at dry state.

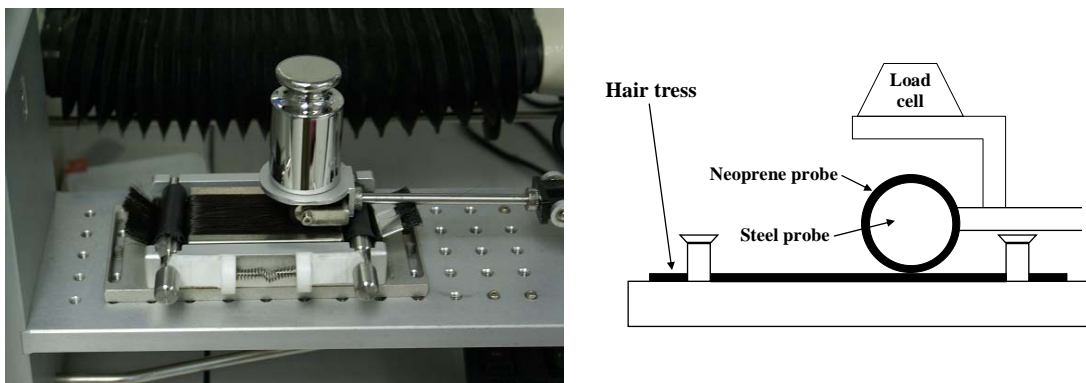


Figure 3-5 Texture Analyzer (TA.XT.Plus Stable Microsystems)

Texture Analyzer Settings

Test mode	: Compression
Pre-test speed	: 1.0 mm/sec
Test speed	: 10.0 mm/sec
Post-test speed	: 10.0 mm/sec
Target mode	: Distance
Distance	: 40.0 mm
Trigger type	: Auto (force)
Trigger force	: 0.1 g
Break mode	: Off
Stop point at	: Start position
Tare mode	: Auto
Advanced option	: On

The area of each friction loops was calculated as the measure of the hair friction and was typically reported in the unit of g.mm. Five replications of hair tresses were collected for each treatment. Mean and standard deviation values of each parameter were recorded for each sample. Data is analyzed by Fisher's Least Square Difference (Fisher's LSD) at 95% confidence level.

3.3.12 Wet combing test

3.0 g of virgin hairs with 7 inches and 1.5 inches wide dimension were aligned in parallel. Then hairs were secured at the root end by aluminium clip and glue. The remaining hair tip was trimmed out, to obtain 2.5 g of hair tress with 6 inches long for the test. Five tresses were wetted together under tap water at a flow rate 4 L/min, at 37°C for 5 sec. The tresses were washed with 1.25 g of 14% sodium lauryl ether sulfate (SLES).2eo, twice before treatment. An amount of 2.15 g of leave-on conditioner was applied for 1 min. The treated tress was suspended on the load cell and inserted into the middle of the fine toothed comb. The treated tress was passed through a comb at a speed of 40 inch/min and the friction force was measured as a function of distance. All the tresses were tested by Instron 5564 tensile tester equipped with Bluehill software version 2.0. Five combing were measured per tress and five tresses were measured in each treatment.

After analysis, the graph showed the force measured by the load cell as a function of the distance traveled by the crosshead. The calculated parameters such as the maximum combing force (gmf), the average combing force (gmf), and the combing energy (mJ) were obtained automatically. The maximum combing force was the highest load recorded during the experimental. The average energy was an averaged value between two pre-determined points, while the combing energy was the energy under the curve. The mean and standard deviation values of each parameter were recorded for each sample. Data was analyzed by Fisher's Least Square Difference (Fisher's LSD) at 95% confidence level.

CHAPTER IV

RESULTS AND DISCUSSION

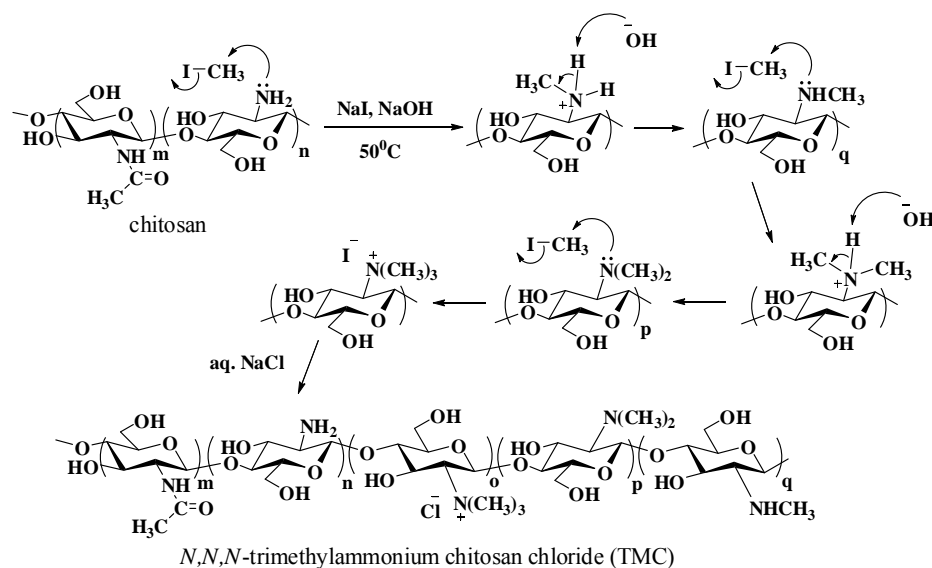
This chapter was divided into four parts. The first part covered the synthesis and characterization of *N,N,N*-trimethylammonium chitosan chloride (TMC) and *N*-[(2-hydroxyl-3-trimethylammonium)propyl]chitosan chloride (HTACC). The preparations of five types of “leave-on” conditioners and four types of damaged hairs were reported in the second and third parts, respectively. The last part was dedicated to the evaluation of coated hairs with each of the prepared leave-on conditioners in terms of physical and mechanical properties.

4.1 Synthesis and Characterization of Charged Derivatives of Chitosan

4.1.1 *N,N,N*-trimethylammonium chitosan chloride (TMC)

TMC was synthesized by a method based on the methylation of chitosan with iodomethane (CH₃I) in the presence of sodium hydroxide and sodium iodide (Scheme 4-1).

Traditionally, an ion exchange resin, amberlite[®] IRA402 (Cl⁻ form), was used to exchange the I⁻ counter-ion with Cl⁻. It was however found that the I⁻ ion remained in the product, as observed from the precipitation of AgI when the dissolved products were titrated with AgNO₃. The amberlite[®] IRA402 was replaced by NaCl aqueous solution in order to completely replace the I⁻ by Cl⁻ in TMC.



Scheme 4-1 Mechanism of the synthesis of *N,N,N*-trimethylammonium chitosan chloride (TMC) from chitosan by reacting with CH_3I .

Over the past decades, researchers have taken an interest to determine degree of quaternization (%*DQ*) of TMC by various methods. Sieval *et al.*² and Sajomsang *et al.*⁵⁴ determine %*DQ* from the relative ratio between the signal of $-\text{N}^+(\text{CH}_3)_3$ and H-1 of the glucosamine ring. Thanou *et al.*⁵⁹ determine %*DQ* by the ratio between $-\text{N}^+(\text{CH}_3)_3$ and $-\text{COCH}_3$. The signal of H-2 and H-2',3,4,5,6,6' of chitosan could not be used after the methylation process. This is because the signals relates to H-2 as observed at δ 2.95 ppm and H-2',3,4,5,6,6' at δ 3.25-4.30 ppm in the chitosan spectrum (Figure 4-1) shift or are overlapped by other signals when TMC is formed. The localization of that peak remains uncertain. However, in this research, the sum of integral signal relates to H-2',3,4,5,6,6' at δ 3.25-4.30 ppm in the TMC spectrum was used to determine the %*DQ* instead of H-1 signal to compare with $-\text{N}^+(\text{CH}_3)_3$ signals. It was found that H-1 shifted and was overlapped by solvent signal, H-2 was overlapped by the signal of $-\text{N}^+(\text{CH}_3)_3$, and the signal of $-\text{COCH}_3$ was interfered by trace acetic acid solvent. Nevertheless, the relative ratio between the signal of H-1, H-2, H-2',3,4,5,6,6', H-2,2',3,4,5,6,6' or $-\text{COCH}_3$ and the signal of $-\text{N}^+(\text{CH}_3)_3$ were determined as shown in Appendix A. The standard derivative of the relative ratio between the signal of H-2',3,4,5,6,6' and $-\text{N}^+(\text{CH}_3)_3$ is the smallest value and %*DS* (*total*) is closed to 100.

The ^1H NMR spectra of the synthesized TMCs is depicted in Figure 4-1. It is similar to the spectrum reported by Sieval *et al.*² The %*DQ* of TMCs were determined from the relative ratios between the signal at 3.10 ppm assigned to three methyl groups of quaternary ammonium group and the sum of integral signal of H-2',3,4,5,6,6' of chitosan (δ 3.25-4.30 ppm) analyzed by ^1H NMR (Figure 4-1). Moreover, %*DS*_{*N(CH*₃)₂}, %*DS*_{*NHCH*₃}, %*DS* (total), %*DOM*-3, and %*DOM*-6 are *N,N*-dimethylation, *N*-methylation, a total degree of *N*-methylation, *O*-methylation at 3-hydroxyl, and *O*-methylation at 6-hydroxyl positions of GlcN of chitosan were determined from ^1H NMR. The positions of those signals in the TMC spectra are shown in Figure 4-1.

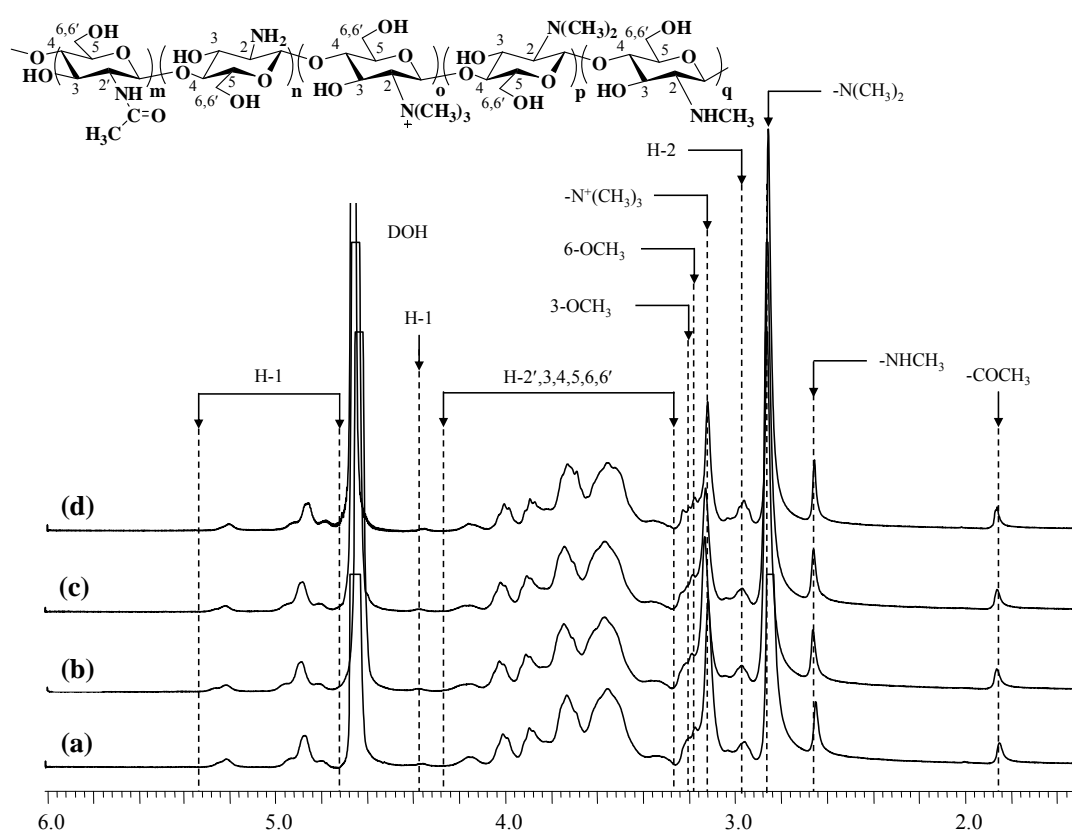


Figure 4-1 ^1H NMR spectra of synthesized TMCs using (a) 4, (b) 5, (c) 6, and (d) 12 equivalents of CH_3I in comparison with the number of NH_2 in chitosan (solvent: $\text{D}_2\text{O}/\text{TFA}$, 25°C).

In this study, the resulting %*DQ*'s of TMC or the composition of trimethylated amino groups of chitosan after methylation with iodomethane (4, 5, 6, and 12 eq) are ranged from 17 to 22%, which are almost independent of the iodomethane equivalent. Moreover, replacing NMP solvent by $\text{DMF}:\text{H}_2\text{O}$ (1:1) or H_2O could increase

methylating efficiency of iodomethane on the chitosan for upto 15%*DQ*. Based on the lowest chemical costs and toxicity, TMC synthesis by using 4 eq of CH₃I was therefore suggested as an optimal preparation method of TMC for this study.

Table 4-1 %DQ as determined by ¹H NMR of quaternary ammonium group on chitosan after reacting with iodomethane at 50°C in NMP, DMF:H₂O (1:1) or H₂O as the reaction solvent.

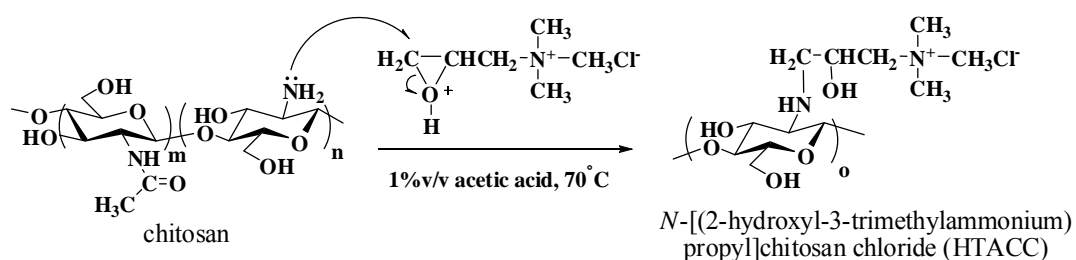
Equivalent of CH ₃ I	Solvent	%DQ (1)	%DS _{N(CH₃)₂} (2)	%DS _{NHCH₃} (3)	%DS (total) (1)+(2)+(3)	%DOM-3	%DOM-6	%Recovery
4	NMP	21.7 ± 0.1	71.6 ± 5.7	10.2 ± 3.4	103.5 ± 9.2	8.7 ± 2.3	24.1 ± 3.6	82.0
5	NMP	21.1 ± 0.4	70.3 ± 3.1	24.6 ± 1.4	116.0 ± 2.4	13.5 ± 1.3	19.3 ± 1.1	95.4
6	NMP	17.8 ± 0.1	70.1 ± 0.2	14.0 ± 8.7	101.9 ± 8.6	9.1 ± 5.5	24.4 ± 4.9	80.3
12	NMP	17.1 ± 0.4	62.8 ± 0.7	15.4 ± 5.3	95.3 ± 6.0	8.4 ± 3.3	22.2 ± 1.8	64.7
4 ^a +12 ^b	NMP, DMF:H ₂ O (1:1)	30.8 ± 1.1	90.2 ± 0.8	8.5 ± 5.5	129.6 ± 3.7	7.8 ± 1.4	26.7 ± 5.0	83.4
4 ^a +12 ^c	NMP, H ₂ O	34.5 ± 1.8	88.7 ± 2.6	4.7 ± 0.6	128.0 ± 3.9	14.5 ± 1.0	40.4 ± 1.4	69.7

%DQ is degree of quaternization; %DS_{N(CH₃)₂} is *N,N*-dimethylation; %DS_{NHCH₃} is *N*-methylation; %DS (total) is total degree of *N*-methylation; %DOM is degree of *O*-methylation at 3-*O* and 6-*O* at 3-hydroxyl and 6-hydroxyl positions of GlcN of chitosan, respectively; %Recovery is weight of product (g)/weight of starting reactants (g)×100

^aMethylating with 4 eq of iodomethane in NMP, ^bMethylating with 12 eq of iodomethane in DMF:H₂O (1:1), ^cMethylating with 12 eq of iodomethane in H₂O

4.1.2 *N*-[(2-hydroxyl-3-trimethylammonium)propyl]chitosan chloride (HTACC)

HTACCs were synthesized by epoxide ring opening of glycidyltrimethyl ammonium chloride (GTMAC) (Scheme 4-2) by the amino groups of chitosan under acidic condition. GTMAC mainly reacts with amino groups of chitosan under acidic condition but preferably reacts with hydroxyl groups under neutral and alkaline conditions. The acidic condition causes protonation at the oxygen atom and makes the epoxy ring of GTMAC more reactive towards the NH_2 groups of chitosan.



Scheme 4-2 Mechanism of the synthesis of *N*-[(2-hydroxyl-3-trimethylammonium)propyl]chitosan chloride (HTACC).

Figure 4-2 illustrates ^1H NMR spectra of the synthesized HTACCs. All signals found in this work match the result reported by Cho *et al.*⁵⁵ and Lim *et al.*⁵⁶ Signals corresponding to the protons of (a) $-\text{NHCH}_2-$, (b) $-\text{CH}(\text{OH})-$, and (c) $-\text{CH}_2-$ appeared at δ 2.88, 4.44 and 3.32 ppm, respectively. A strong peak at δ 3.05 ppm indicates the presence quaternary ammonium group $-\text{N}^+(\text{CH}_3)_3$ in the obtained product, and is used in %DQ calculation (equation 3.1).

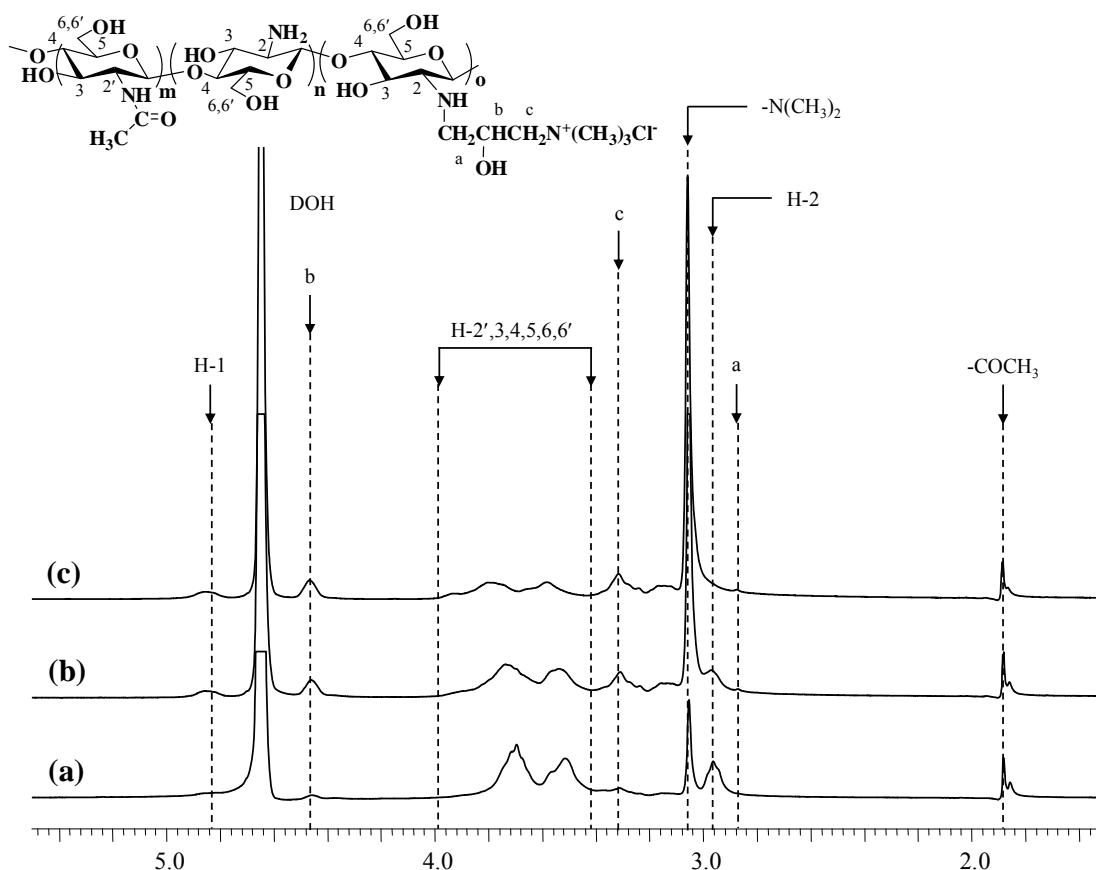


Figure 4-2 ^1H NMR spectra of synthesized HTACCs using (a) 2, (b) 4, and (c) 6 equivalents of GTMAC in comparison with the number of NH_2 in chitosan (solvent: $\text{D}_2\text{O}/\text{TFA}$, 25°C).

In this study, $\%DQ$ of HTACC was determined from the relative ratio between the area of H signal from the trimethyl ammonium group of grafted GTMAC at δ 3.05 ppm and the sum of integral signal of H-2',3,4,5,6,6' (δ 3.40-4.00 ppm) from all pyranose repeat units. From Table 4-2, the $\%DQ$ on chitosan was increased from 24 to 139 when the GTMAC equivalent used in the synthesis and the reaction time were increased from 2 to 6 and from 2 to 24 h, respectively. It was however found that increase of mole equivalent resulted in more drastic increase of $\%DQ$ than an increase of reaction time. Moreover, the $\%DQ$ of HTACC was more than 100% when 6 eq of GTMAC was used. It was possibly because of an error from peak integration caused by signal overlapping between the signal of $-\text{N}^+(\text{CH}_3)_3$ and H-2 [Figure 4-2(c)].

Based on chemical costs and toxicity, the synthesis scheme that required the lowest amount of GTMAC but yielded a soluble derivative was preferred. Therefore,

the amount of GTMAC was set at be 2 eq for preparing HTACC for use in leave-on conditioner.

Table 4-2 %DQ as determined by ^1H NMR on chitosan after reacting with GTMAC at 70°C in 1%v/v acetic acid at different reaction time.

Equivalent of GTMAC	Time (h)	%DQ	%Recovery
2	24	23.8 ± 0.3	53.9
4	2	37.8 ± 0.1	62.5
4	4	62.2 ± 0.4	83.7
4	8	77.1 ± 0.7	93.6
4	12	84.6 ± 1.5	71.5
4	24	84.4 ± 0.6	121.3
6	24	139.4 ± 2.7	126.9

%DQ is degree of quaternization.; %Recovery is weight of product (g)/weight of starting reactants (g) $\times 100$

Besides ^1H NMR, the %DQ of TMCs and HTACCs were also determined by conductivity titration method. This method was used to analyze the amount of chloride ion at the lowest conductivity found in the TMC or HTACC solution. The %DQ was calculated as follows:

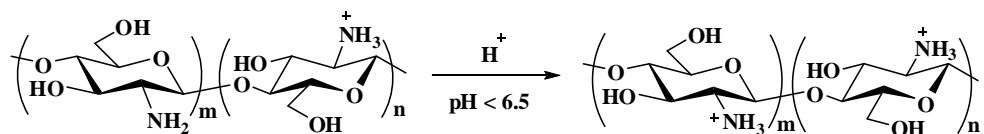
$$\%DQ_{(TMC)} = \frac{1.7 \times 10^{-5} \times V_{AgNO_3}}{\left(\frac{W_w - (1.7 \times 10^{-5} \times V_{AgNO_3} \times m_{CH_3Cl})}{(m_G \times DD) + m_{AG} (1 - DD)} \right) \times DD} \times 100 \quad (4.1)$$

$$\%DQ_{(HTACC)} = \frac{1.7 \times 10^{-5} \times V_{AgNO_3}}{\left(\frac{W_w - (1.7 \times 10^{-5} \times V_{AgNO_3} \times m_{GTMAC})}{(m_G \times DD) + m_{AG} (1 - DD)} \right) \times DD} \times 100 \quad (4.2)$$

Table 4-3 %DQ of TMC_{CH₃I 6eq} and HTACC_{GTMAC 4eq_24hr}, determined by ¹H NMR spectroscopy and conductivity titration method.

Sample	%DQ		
	¹ H NMR	Conductivity titration	
		pH = 5.0	pH = 7.0
TMC _{CH₃I 6eq}	17.8 ± 0.1	101.7	69.4
HTACC _{GTMAC 4eq_24hr}	84.4 ± 0.6	113.9	54.1

As a result, the %DQ's of TMC and HTACC at pH 5.0 are more than the %DQ at pH 7.0. This is because at pH 5 the $-NH_2$ group is protonated, resulting in more Cl⁻ than expected. From the results, %DQ obtained from the conductivity titration method was not used as the tool to determine %DQ because it was too sensitive to acidic pH, and had a high tendency to produce unreliable results.



Scheme 4-3 Protonation of amino groups of chitosan at pKa.

According to FTIR spectra, the IR spectrum was consistent with the reported spectra.^{3,52} The formation of TMC and HTACC was verified by the decrement of the N-H bending peak signal at 1597 cm⁻¹ of the amino groups of chitosan and the appearance of the C-N stretching peak of the methyl groups in quaternary ammonium groups at 1480 cm⁻¹ (Figure 4-3). Besides, the characteristic peaks of C-O stretching of primary and second alcohol at 1040 and 1080 cm⁻¹ are also present in chitosan, TMC, and HTACC.

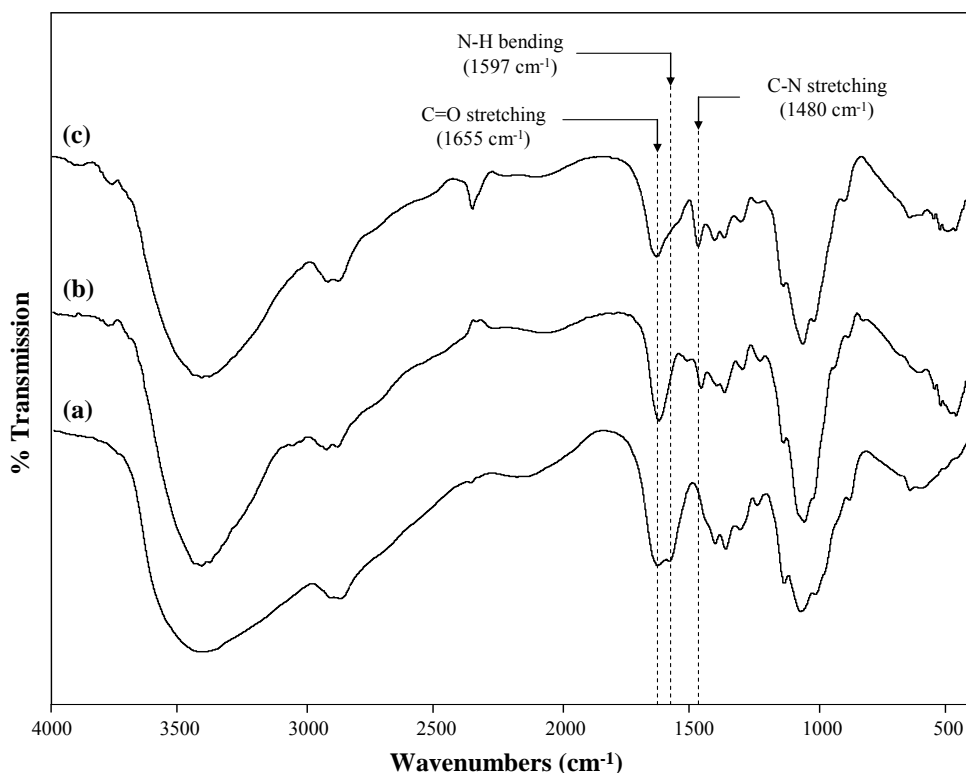


Figure 4-3 FTIR spectra of (a) chitosan, (b) TMC, and (c) HTACC.

4.1.3 Solubility tests of the charged derivatives of chitosan

The solubility test was performed according to a method of Sashiwa *et al.*⁵⁸ A solid sample of charged derivatives of chitosan (100 mg) was mixed in water (20 mL). The pH of the solution was adjusted with 0.5%w/v aqueous HCl and NaOH. As illustrated in Table 4-4, chitosan dissolves in acidic region pH below 6.5. The solubility of chitosan in the acidic region is ascribed to the protonation of amino group (from $-NH_2$ to $-NH_3^+$). The synthesized TMC with 17-22%DQ is unexpectedly insoluble in basic solution at pH above 6.5. It was possible that %DQ of TMC was too low to dissolve in neutral and basic aqueous media. In addition, the methylation at $-OH$ group, as evidenced by the NMR result (Figure 4-1), can reduce H-bonding site on the polymer structure. On the contrary, HTACC with 24-139 %DQ is soluble over the entire pH range. However, 2 eq of GTMAC cannot be soluble at pH above 13 due to low DQ (24%).

Table 4-4 %DQ and solubility test in water of various pHs^a of chitosan, TMCs, and HTACCs.

Sample	%DQ	Solubility ^b													
		pH: 1	2	3	4	5	6	7	8	9	10	11	12	13	14
chitosan	-	6.50													
TMC _{CH₃I 4eq}	22	6.62													
TMC _{CH₃I 5eq}	21	6.73													
TMC _{CH₃I 6eq}	18	6.55													
TMC _{CH₃I 12eq}	17	7.03													
HTACC _{GTMAC 2eq}	24													12.93	
HTACC _{GTMAC 4eq}	84														
HTACC _{GTMAC 6eq}	139														

^aSolid sample (100 mg) was dispersed in H₂O (20 mL). The pH of the solution was adjusted with 0.5%w/v aqueous HCl and NaOH.

^bWhite bar = soluble, black bar = insoluble.

4.1.4 *In vitro* cytotoxicity of chitosan and its charged derivatives

To the best of our knowledge, there are few reports^{60,61} explaining in detail the biological response of human keratinocyte cells line and the HaCaT cells line against chitosan and positively charged derivatives. Therefore, the cytotoxicity of chitosan and positive-charged chitosan on the HaCaT cells was investigated. This test is in fact crucial since the polymers are to be used in a product that directly contacts human skin. All tests were performed in pH 6.0 medium, the same pH as in the leave-on conditioner.

The result of MTT test was displayed in Figure 4-4. Cell viabilities of chitosan, TMCs and HTACCs having different DQ_s were investigated as a function of concentration. The IC_{50} values or the half-maximum inhibitory concentrations, which represented concentration of the polymers resulting in 50% inhibition of cell growth, were calculated from a logarithmic regression which obtained from plotted graph of the concentration (x axis) and the cell viability (y axis) as shown in Appendix B. Log_{10} scale is frequently used when concentration values are a serial dilution.

As a result, chitosan in acidic media inhibited cell viability due to the fact that its amino group ($-NH_2$) was converted to an ammonium ion ($-NH_3^+$) that electrostatically interacted with the negatively charged cell membrane. All derivatized polymers exhibited dose-dependent cytotoxicity response, that increased with the % DQ . Both chitosan derivatives in acidic media also inhibited cell viability due to the ammonium ion ($-NH_3^+$) and the quaternized group. IC_{50} of TMC with 18-22% DQ indicated dose-dependent cytotoxicity in the concentration range of 14.1, 38.6, 1725.9 $\mu\text{g/mL}$ as shown in Table 4-5. The reason for the high toxicity of TMC having 21 and 18% DQ is unclear but it may happen from the remaining of the material which was used in the synthesis. HTACC with 24-139% DQ also indicated dose-dependent cytotoxicity in the concentration range of 174.2, 181.9, >1000 $\mu\text{g/mL}$ as shown in Table 4-5. Increasing the equivalent of GTMAC resulted in the HTACC with increased toxicity to the HaCaT cells line. The cytotoxicity was not much increased when using 4 to 6 equivalents of GTMAC. According to the cytotoxicity results, HTACC is less toxic than TMC when compared between samples with similar $DQ's$ as shown in Figure 4-4(B) and (C). The mechanism by which chitosan and its derivative interacts with HaCaT cells line is unclear. It may interact with growth factors in the serum or metal ions (e.g. calcium), reducing the availability of these to the cells.⁶⁰ Nevertheless, there are currently very few detailed reports on the effect of chitosan and its derivatives on HaCaT cells line or primary human keratinocytes.

From the cytotoxicity results obtained, it can be concluded that 4 eq of iodomethane per amino groups of chitosan ($TMC_{CH_3I\ 4eq}$) and 2 eq of GTMAC per amino groups of chitosan ($HTACC_{GTMAC\ 2eq}$) are the materials of choice in preparing the conditioners, since they both showed the least toxic effect against the HaCaT cells line.

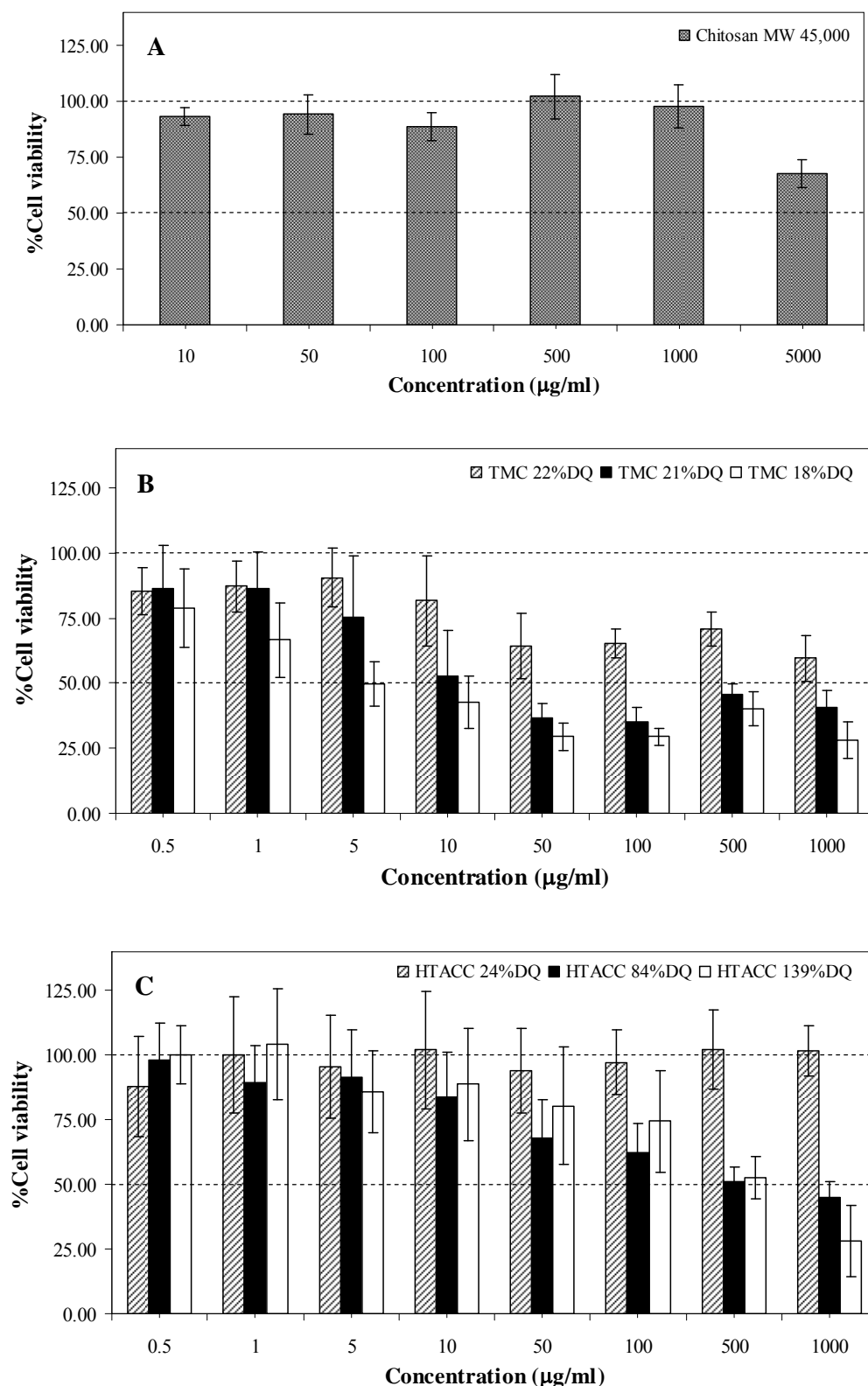


Figure 4-4 *In vitro* cytotoxicity of (A) chitosan MW 45,000, (B) TMCs, and (C) HTACCs on HaCaT cells line as determined by the MTT assay at pH 6.0. The cell viability compared with cell culture medium without polymer. The data shown were averaged from 5 data sets for chitosan and 12 data sets for the chitosan derivatives.

Table 4-5 IC₅₀ (μg/mL) of chitosan and its charged derivatives on HaCaT cells line as determined by the MTT assay at pH 6.0.

Sample treatment	%DD	%DQ	IC ₅₀ (μg/mL)
Chitosan	85	–	>5000 ^a
TMC _{CH₃I 4eq}	–	22	1725.9
TMC _{CH₃I 5eq}	–	21	38.6
TMC _{CH₃I 6eq}	–	18	14.1
HTACC _{GTMAC 2eq}	–	24	>1000 ^a
HTACC _{GTMAC 4eq}	–	84	181.9
HTACC _{GTMAC 6eq}	–	139	174.2

^aThe IC₅₀ value could not certainly calculated due to the log (x) value is negative.

Additionally, *in vitro* cytotoxicity tests will be more convincing when performed with cells that are homologous with the cell in hair skin. In accordance, cell lines for use in cytotoxicity concerning the skin would be human dermal fibroblasts and human epidermal keratinocytes, as they take an active part in the immune response, inflammatory processes, and wound healing.⁶² The evaluation of the cytotoxicity of chitosan and charged derivatives is based on several factors such as passage numbers of cell cultures, growth behavior of cell culture after direct or indirect contact with the materials, growth factors in the serum, and the different environment of *in vitro* and *in vivo*. Another suggestion is the cytotoxicity test should be also performed using the whole leave-on conditioner in order to closely simulate real usage.

4.2 Positively-Charged Chitosan Contents in Leave-On Conditioners

In general, the amount of positively charged macromolecules mixed in the leave-on conditioner is varied upon the type of macromolecules. These positively charged molecules have been used to help control viscosity and attraction to negatively charged hair surface. In this study, chitosan, TMC, or HTACC was used to replace a polyquaternium-10 (commercial ingredient) in the conditioner. The amount and %DQ of the chitosan and its charged derivatives must be at optimum level in order to achieve

good homogeneity and viscosity of the prepared conditioner. The investigation therefore focused on five important factors i.e. chemical costs, solubility, cytotoxicity on HaCaT cells line, the ability to attach to human hair, and homogeneity and viscosity of the prepared leave-on conditioners.

As discussed in section 4.1, TMC (22%DQ) and HTACC (24%DQ) were chosen for the conditioner, because these had the lowest cost and toxicity. Solubility of TMCs and HTACCs did not influence on the selection due to the fact that the pH value of the leave-on conditioner was between 4.5 to 5.5, in which TMCs and HTACCs were in the soluble forms.

4.2.1 Hair coating behavior

Black virgin hairs from an Asian thirty two-year old female used in this study were supported by Life Science Cosmetics Research Center Co., Ltd. Prior to the coating experiment, the hair samples were shampoo-washed and rinsed with DI water three times. Afterward, they were blown dry with cold air and left at room temperature overnight.

Surface characterization of virgin hair was done by ATR FT-IR microspectroscopy with a slide-on Ge μ IRE. This novel method was nondestructive. The small contact area of μ IRE was less than $100 \times 100 \mu\text{m}^2$ which was suitable for the hair samples. The analysis time was rather short but the results were accurate and reliable.

The ATR FT-IR spectrum acquired by Ge μ IRE of the virgin hair was shown in Figure 4-5. The observed spectrum shows a broad band at 3277 cm^{-1} attributed to O–H stretching of water together with N–H stretching vibration. The predominant absorption bands at 1641 , 1532 and 1234 cm^{-1} are related to amide I, amide II and amide III vibrations, respectively. The absorption bands at 2957 - 2851 cm^{-1} and 1454 , 1406 cm^{-1} are the C–H stretching and C–H deformation vibration, respectively. The IR peak assignments are summarized in Table 4-6.

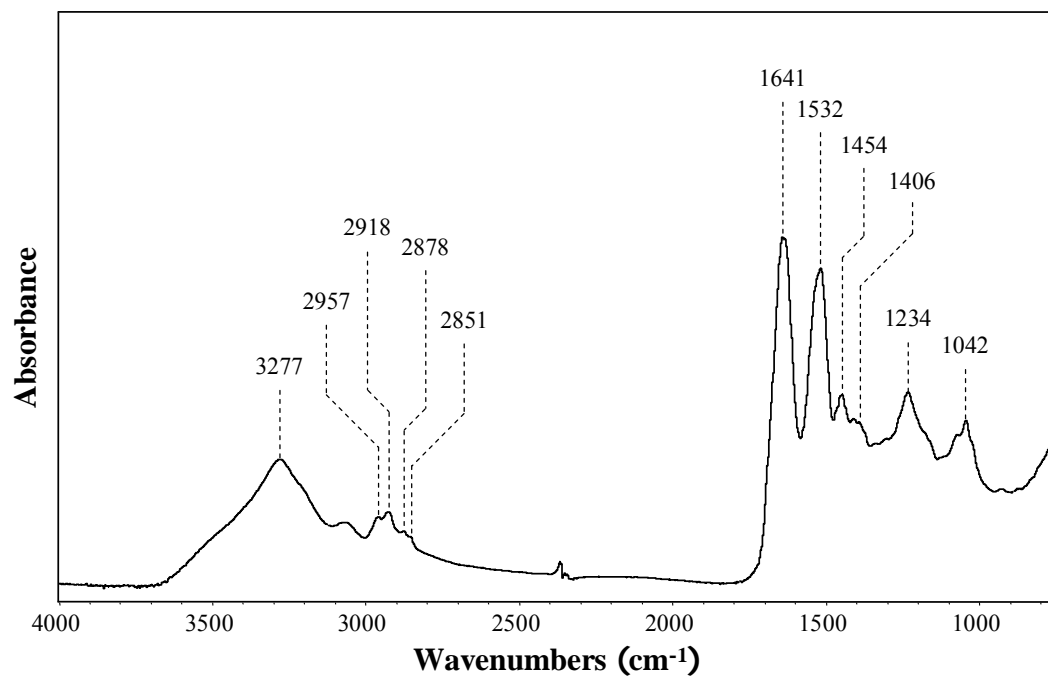


Figure 4-5 ATR FT-IR spectrum of virgin hair.

Table 4-6 Peak assignment of virgin hair used in this study.

Wavenumbers (cm ⁻¹)		Assignments
Literature ³⁸	Current work	
3295	3277	asymmetric N–H stretching
2960	2957	asymmetric C–H stretching of CH ₃
2926	2918	asymmetric C–H stretching of CH ₂
2875	2878	symmetric C–H stretching of CH ₃
2851	2851	symmetric C–H stretching of CH ₂
1670-1643	1641	Amide I C=O stretching and a small contribution from N–H bending (scissoring)
1548-1517	1532	Amide II C–N stretching plus N–H bending (wagging)
1453	1454	C–H bending (scissoring) of CH ₂
1397	1406	C–H bending (wagging) of CH ₃
1311-1239	1234	Amide III N–H bending (twisting) plus C–N stretching and contribution from O=C–N bending
1040	1042	S=O

The ATR-FTIR spectra of coated hair sample are shown in Figures 4-6 to 4-8. Apparently, chitosan, TMC (22%DQ), and HTACC (24%DQ) were detected on the coated unaltered hair samples as demonstrated by the presence of C–O stretching signals of primary and secondary alcohol at 1040 and 1080 cm⁻¹ of chitosan structure. For TMC and HTACC, these signals remarkably increased when the concentration (1-3%w/w) of coating solution increased [Figures 4-7(b-d) and 4-8(b-d)]. Interestingly, the intensity increase of C–O signal of chitosan-coated hair was not as high as those of TMC-, HTACC-coated hairs. This probably suggests that the amount of chitosan coated on the hair strand is less than that of the two derivatives.

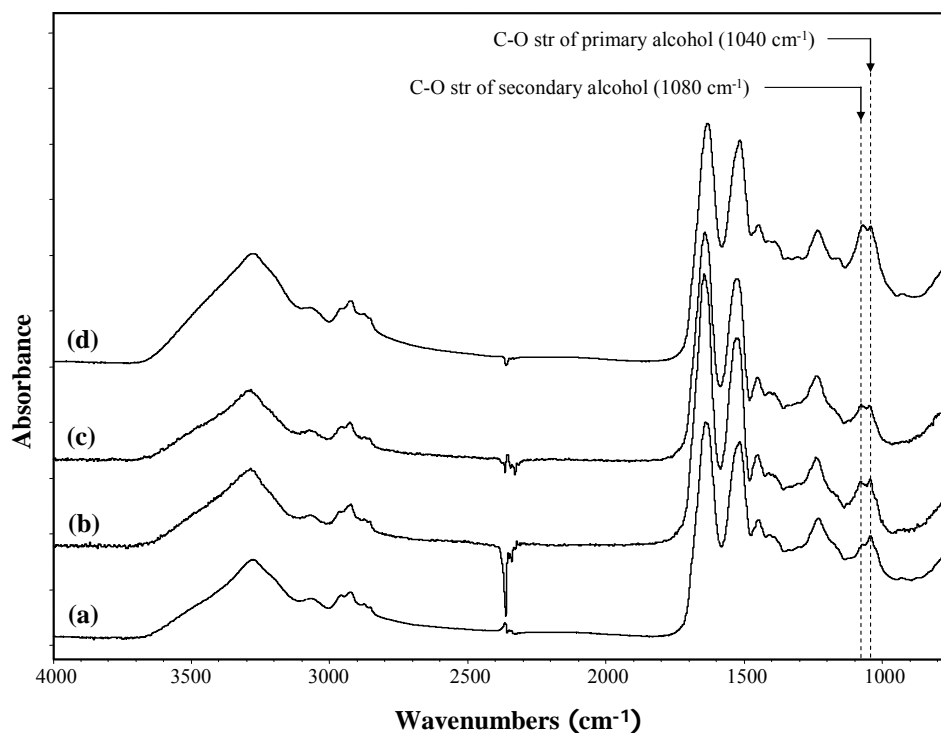


Figure 4-6 ATR FT-IR spectra of (a) virgin hair, (b) coated hair with 1%w/w chitosan solution, (c) coated hair with 2%w/w chitosan solution, and (d) coated hair with 3%w/w chitosan solution.

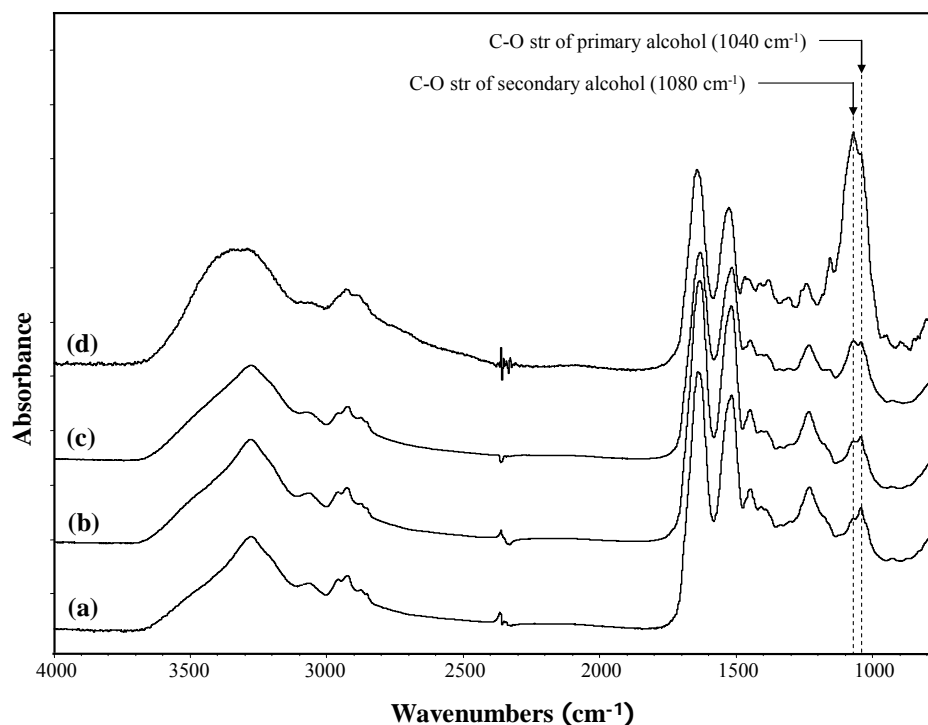


Figure 4-7 ATR FT-IR spectra of (a) virgin hair, (b) coated hair with 1%w/w TMC (22%DQ) solution, (c) coated hair with 2%w/w TMC (22%DQ) solution, and (d) coated hair with 3%w/w TMC (22%DQ) solution.

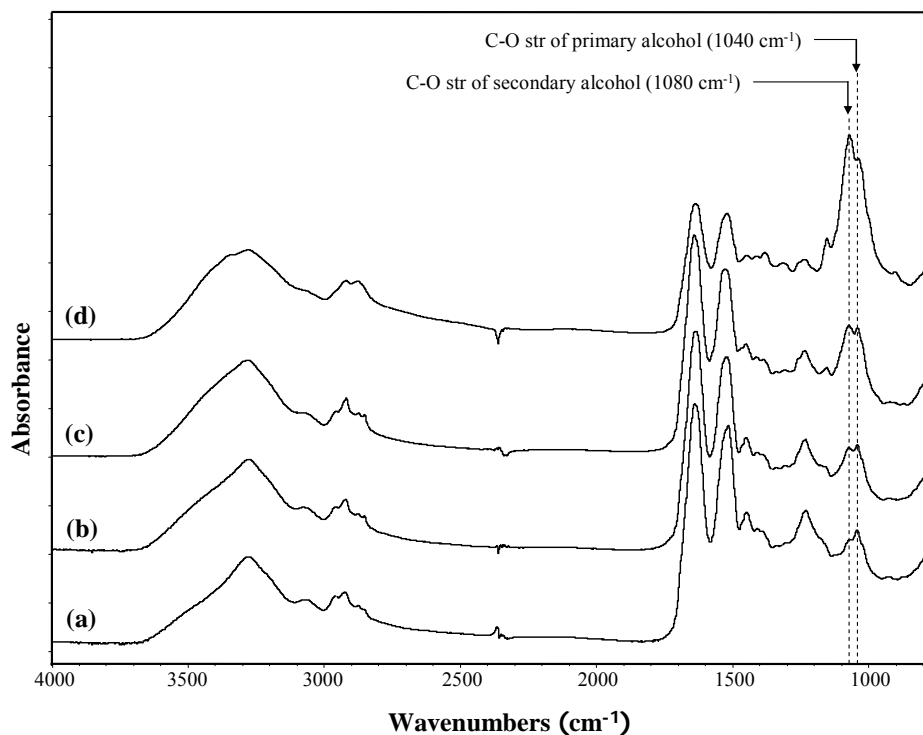


Figure 4-8 ATR FT-IR spectra of (a) virgin hair, (b) coated hair with 1%w/w HTACC (24%DQ) solution, (c) coated hair with 2%w/w HTACC (24%DQ) solution, and (d) coated hair with 3%w/w HTACC (24%DQ) solution.

Microscopic surface of virgin and treated-hair before and after the treatment with 1%w/w chitosan, TMC (22%DQ) or HTACC (24%DQ) solution were analyzed by SEM as shown in Figures 4-9 to 4-13. The negative charge on the surface hair is attracted to the $-NH_3^+$ group of chitosan and positively charged chitosan. Coating these treated-hairs, especially the waved and straightened hairs, by the polymer solution can flatten the lifted cuticle scales, occurred after the cosmetically treatments or UV irradiation. It is thus believed that the treated-hair can be physically “repaired” by the treatment with the chitosan and derivative solutions.

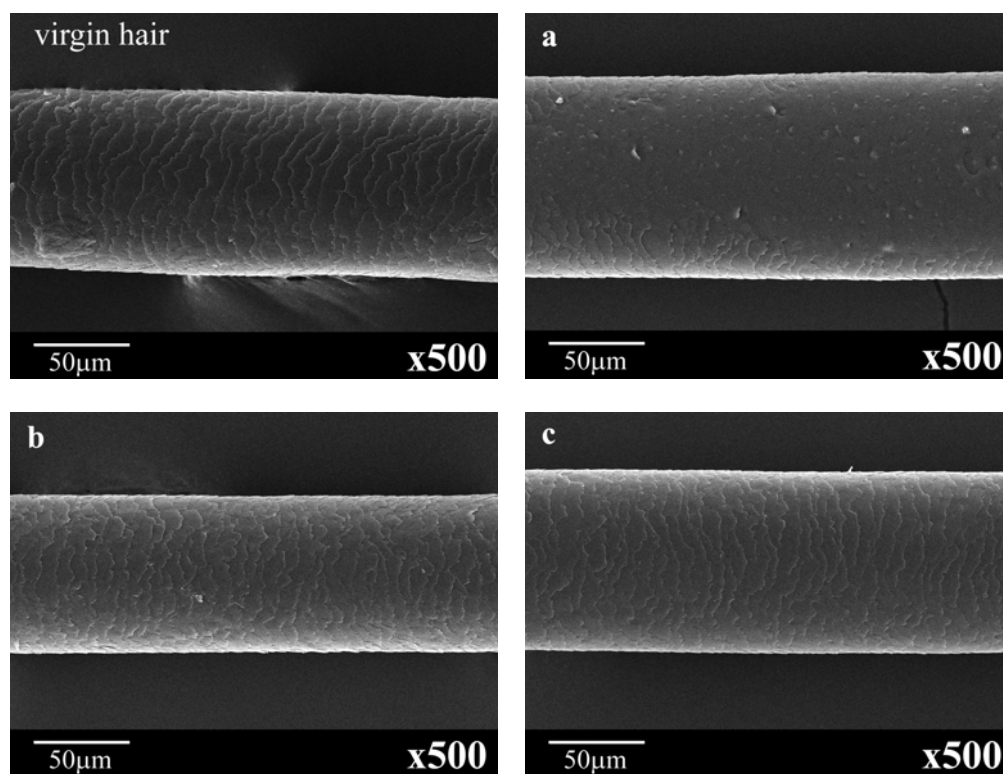


Figure 4-9 SEM images of virgin hair before and after treatment with (a) 1%w/w chitosan, (b) 1%w/w TMC (22%DQ) and (c) 1%w/w HTACC (24%DQ).

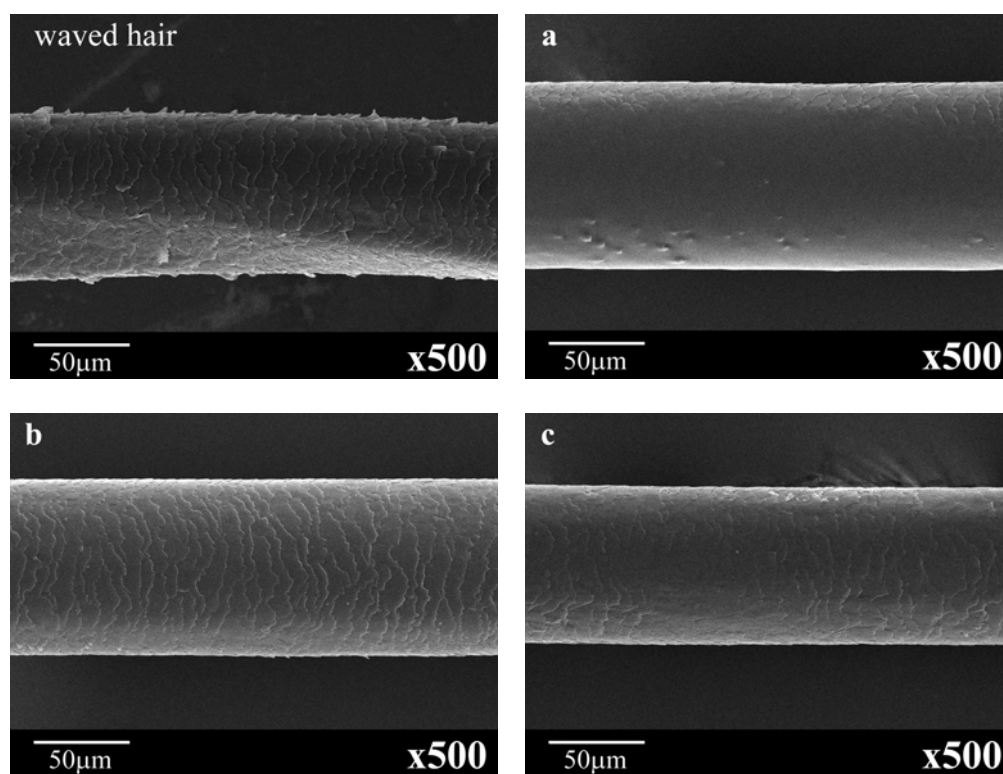


Figure 4-10 SEM images of waved hair before and after treatment with (a) 1%w/w chitosan, (b) 1%w/w TMC (22%DQ) and (c) 1%w/w HTACC (24%DQ).

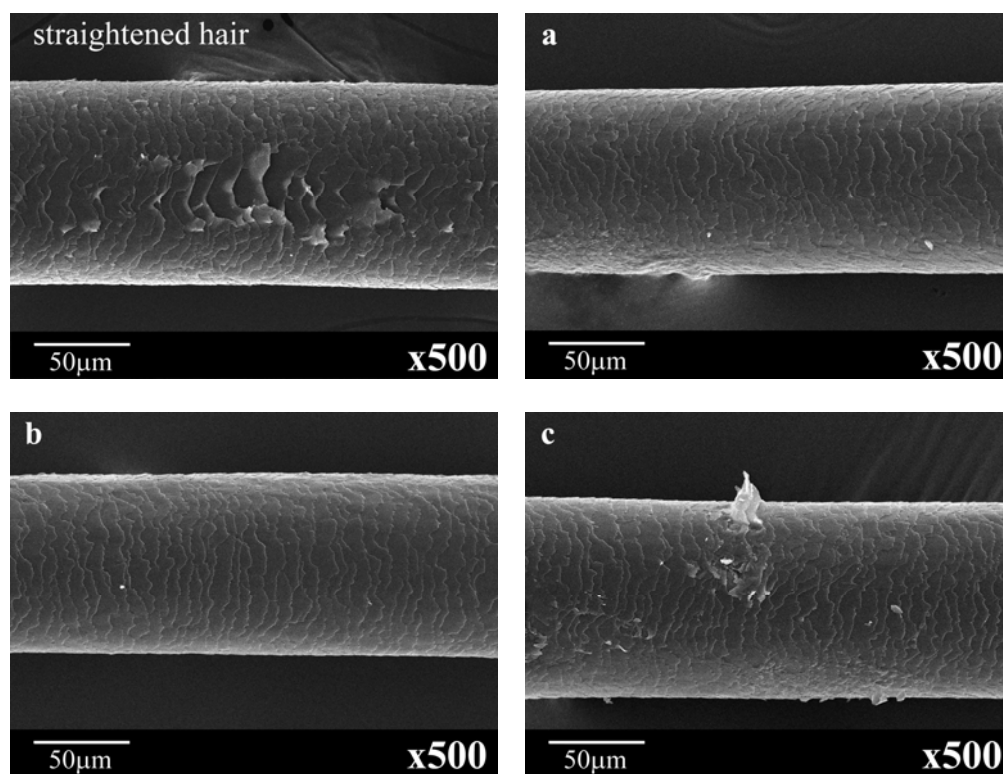


Figure 4-11 SEM images of straightened hair before and after treatment with (a) 1%w/w chitosan, (b) 1%w/w TMC (22%DQ) and (c) 1%w/w HTACC (24%DQ).

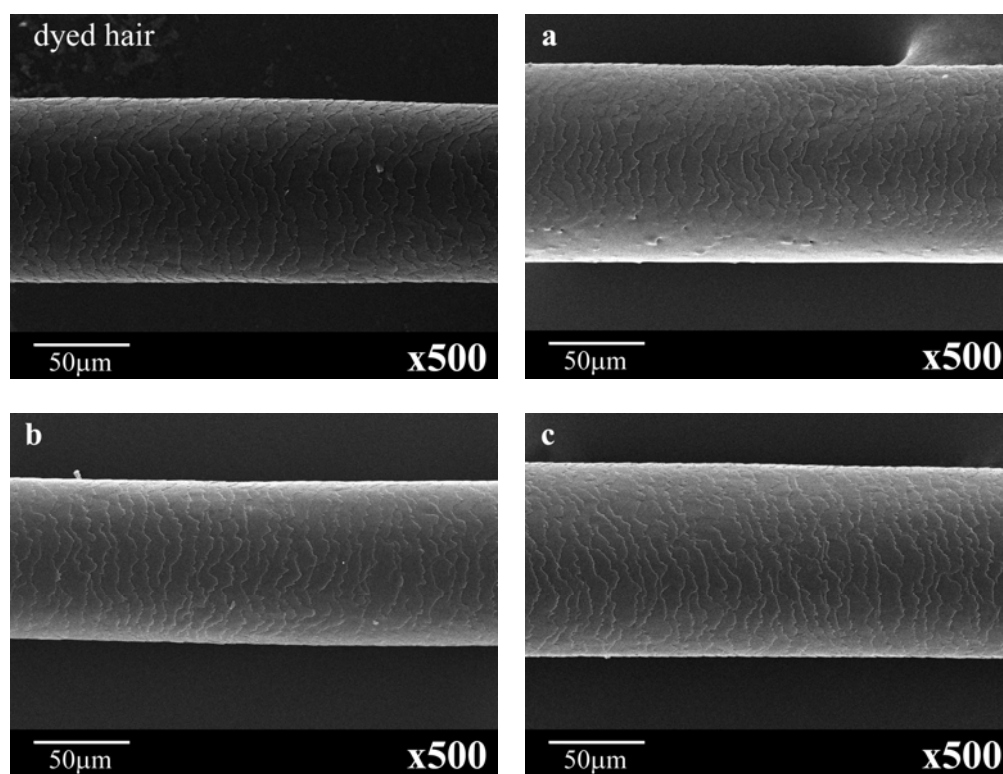


Figure 4-12 SEM images of dyed hair before and after treatment with (a) 1%w/w chitosan, (b) 1%w/w TMC (22%DQ) and (c) 1%w/w HTACC (24%DQ).

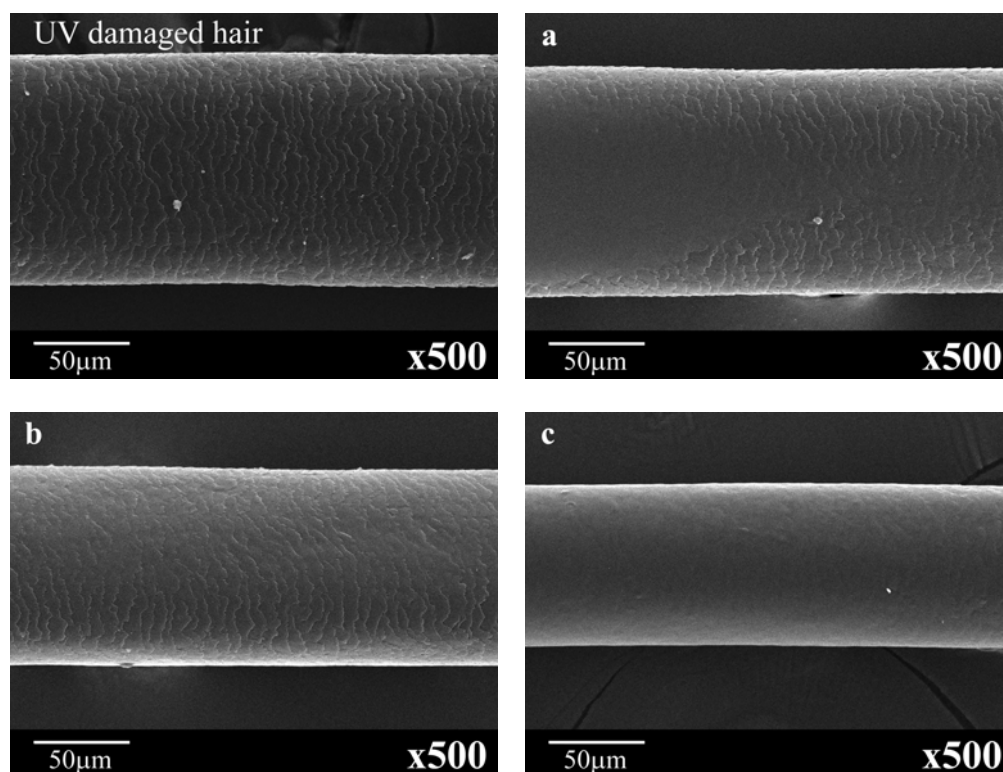


Figure 4-13 SEM images of UV-damaged hair before and after treatment with (a) 1%w/w chitosan, (b) 1%w/w TMC (22%DQ) and (c) 1%w/w HTACC (24%DQ).

From the results in section 4.2.1, 1-3%w/w chitosan and its derivatives can coat on the virgin and treated hairs surfaces as confirmed by ATR FT-IR and SEM analyses. Consequently, 1-3%w/w chitosan, TMC, and HTACC were used in preparing the leave-on conditioners.

4.2.2 Homogeneity and viscosity of leave-on conditioner

From the three concentrations 1-3%w/w, only the 1%w/w solution of chitosan, TMC or HTACC could be mixed into the conditioner to obtain good homogeneity. The conditioner creams tended to aggregate and form lumps when the concentration of polymer solution was 2 and 3%w/w. For comparison purpose, the conditioner without positively charged polymer (LO) and the one with 1%w/w polyquaternium-10 (LO+1%quat), as in a commercial product, were also investigated. Figure 4-14 shows the texture of five conditioner formulas. The natural color of chitosan is rather yellow therefore affecting the color of the prepared leave-on conditioners.

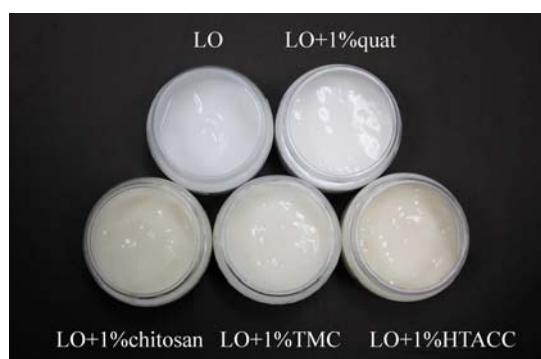


Figure 4-14 The appearance of the leave-on conditioner without positively charged polymer (LO), the leave-on with 1%w/w polyquaternium-10 (LO+1%quat), 1%w/w chitosan (LO+1%chitosan), 1%w/w TMC (LO+1%TMC), and 1%w/w HTACC (LO+1%HTACC).

The viscosity of the prepared five leave-on conditioners was analyzed by Brookfield Digital Viscometer model DV-I+. The condition of parameters as follows: spindle, speed, time, and temperature are S5, 60 rpm, 120 s, 25°C, respectively. The results are shown in Table 4-7. LO+1%TMC (3646 mPa.s) and LO+1%HTACC (3305 mPa.s) have low viscosity values because the solubilities of the two chitosan derivatives are higher than that of chitosan. Furthermore, the conditioners containing TMC or HTACC have lower viscosity values than does the conditioner containing polyquaternium-10. This characteristic should make the hair coated with LO+1%TMC and LO+1%HTACC feel more smooth than that coated with LO+1%quat as can be evidenced from the result of wet combing test shown in section 4.4.5.

Table 4-7 pH and viscosity of five leave-on conditioners.

Types of leave-on conditioner	pH	average \pm SD (mPa.s)
LO	4.85	3611 \pm 68
LO+1%quat	4.89	4526 \pm 122
LO+1%Chitosan (85%DD)	4.51	4709 \pm 81
LO+1%TMC (22%DQ)	4.81	3646 \pm 40
LO+1%HTACC (24%DQ)	4.80	3305 \pm 150

4.3 Functional Group and Microscopic Image Analysis of Hair Samples

Angela™ Cold wave lotion (Just Modern), Caring® Hair straightener cream, and Caring® Beauty hair colour cream were used in preparation of waved, straightened, and dyed hairs, respectively. A UV lamp (313 nm) was used as a UVB source for irradiation to prepare the UV-damaged hair. Human hair undergoes oxidation by both chemical treatment (permanent waves, straightener cream, or permanent dyes) and photochemical (exposure to UV radiation). Oxidation usually affects the decreased tensile strength of hair due to disulfide (–SS–) scission and the color changes, caused by melanin degradation and abraded cuticle.

The usual products from –SS– oxidation of cystine are the sulfonic acid of cystine or cysteic acid (R-SO₂-OH), cystine monoxide (R-SOS-R) and cystine dioxide (R-SO₂S-R), with IR absorption bands at 1040, 1075 and 1125 cm⁻¹, respectively (see structure in Figure 4-15).

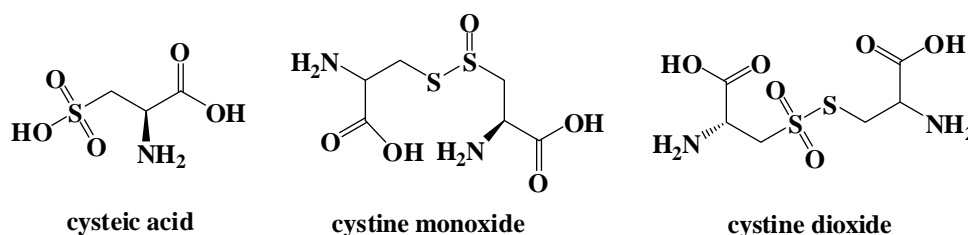


Figure 4-15 Structure of cysteic acid, cystine monoxide, and cystine dioxide.

An oxidizing agent in permanent wave, hair straightener cream, and hair coloring caused an increase in cysteic acid contents. In addition, weathering (exposure to sunlight or wind), could also increase the content of the cysteic acid as can be evidenced from the band intensity at 1040 cm⁻¹.⁶³

However, reports by other researchers on the changing of virgin and damaged hairs are still different in comprehensiveness. In this work, cysteic acid contents and secondary structure of protein in hair samples were explored in detail using ATR FT-IR technique.

As a result, the spectra of different treated hairs in the 1070-1020 cm⁻¹ region are somewhat different, indicating the difference in cysteic acid content of the keratin protein samples. This suggests that the partial –SS– groups on the surface of virgin hair has changed to cysteic acid through oxidation. The results from the ATR FT-IR analysis

(as shown in Figure 4-16) demonstrate that the oxidation has proceeded to a depth of at least 1-2 μm (estimated depth of ATR-FTIR sensitivity). The depth of 1-2 μm from surface corresponds to the cuticle region.

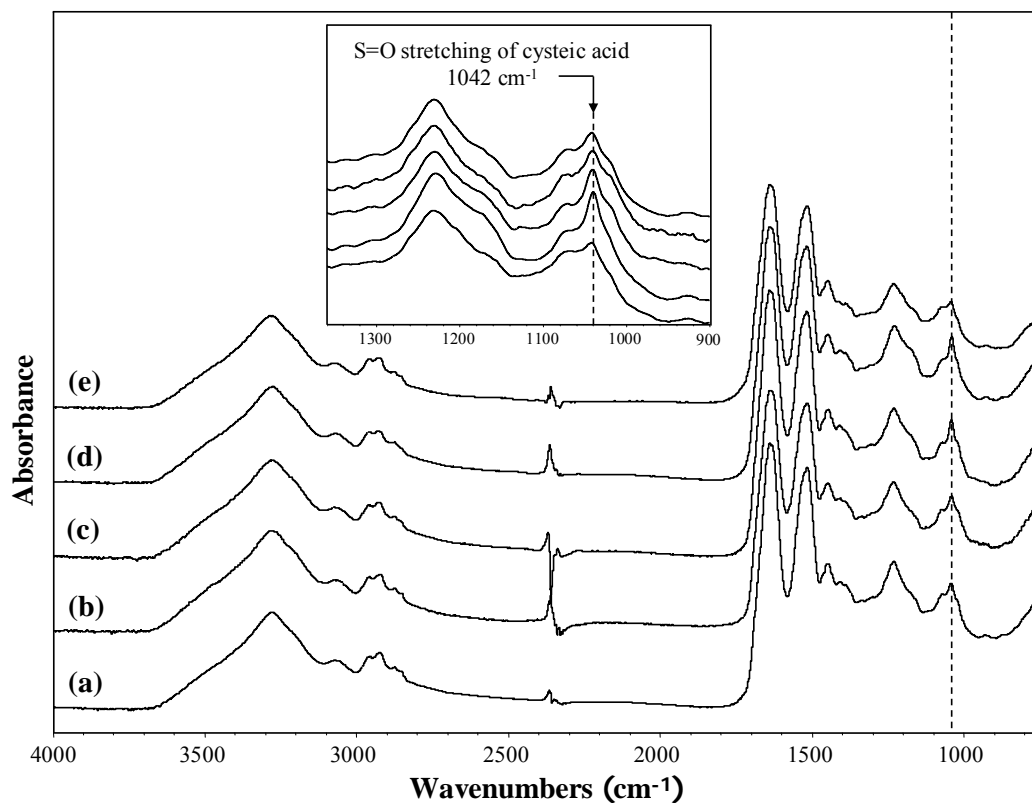


Figure 4-16 ATR-FTIR spectra of (a) virgin hair, (b) waved hair, (c) straightened hair, (d) dyed hair, and (e) UV-damaged hair.

The cysteic acid contents in all human hair types are compared. The normalization of ATR FT-IR spectra of keratin protein samples is carried out based on the amide I region at 1641 cm^{-1} , in which the peak area is large and not influenced by chemical treatment. The comparison of the peak area ratios of S=O stretching and amide I for virgin and treated-hairs is shown in Table 4-8. From the Table, the cysteic acid contents of treated-hairs are higher than that of the virgin hair. The cysteic acid contents of the dyed hair in cuticle region are increased remarkably. This result implicates that the $-\text{SS}-$ groups in hair decrease which in fact can affect the tensile strength of hair (see section 4.4.3).

Table 4-8 Cysteic acid contents in virgin and treated-hairs.

Type of hair	n	Peak area		Cysteic acid contents ^c	Average \pm SD
		amide I ^a	S=O ^b		
Virgin	1	14.170	0.340	0.0240	0.0227 \pm 0.0011
	2	13.102	0.289	0.0221	
	3	13.475	0.296	0.0220	
Waved	1	4.962	0.125	0.0252	0.0244 \pm 0.0015
	2	14.274	0.323	0.0226	
	3	13.892	0.351	0.0253	
Straightened	1	11.195	0.376	0.0336	0.0301 \pm 0.0030
	2	11.536	0.331	0.0287	
	3	11.718	0.330	0.0282	
Dyed	1	7.183	0.286	0.0398	0.0438 \pm 0.0038
	2	14.316	0.633	0.0442	
	3	14.397	0.682	0.0474	
UV damaged	1	6.086	0.144	0.0237	0.0276 \pm 0.0049
	2	11.992	0.311	0.0259	
	3	14.412	0.478	0.0331	

^apeak integration range is 1730-1580 cm⁻¹

^bpeak integration range is 1070-1020 cm⁻¹

^cpeak area ratios, S=O/amide I

Protein generally contains more than one secondary structures, which are correlated to the amide groups of protein. Secondary structures are associated with a characteristic pattern of hydrogen bonding between amide C=O and N-H groups. The secondary structures of protein can be classified as α -helix, β -sheet, β -turns, and random coil. The second derivative spectra were calculated to identify the positions of

the overlapping component bands in the amide I region (1730-1580 cm^{-1}) of which were used as initial parameters for curve fitting analysis.

The number and location of individual bands obtained from the second derivative of original (dotted line) spectrum were used in curve fitting as shown in Figure 4-17. The peak positions of secondary structure were calculated from deconvolved (solid line) spectrum. Absorption centers of curve fitting of virgin and treated-hairs, which can be referred from Table 4-9, were shown in Table 4-10. The secondary structure of virgin hair at 1650, 1615 and 1696, 1625, 1667 and 1684, and 1639 cm^{-1} are assigned to α -helix, antiparallel β -sheets, parallel β -sheets, β -turn, and random coil, respectively. These peaks are slightly shifted from those observed in treated-hairs, which might be due to the difference of hydrogen bonding of protein. The secondary structure of treated-hairs are represented by positive shift of individual bands in amide I bands as shown in Table 4-11. Although the curve fitting is the same for all type, the proportions of secondary structure depend on the type of treatment. When the virgin hair is treated chemically or by UVB irradiation, the structure was changed from α -helix to β -sheet or random coil. α -Helix structure (18.3%) is more favorable in virgin hair. Similarly, antiparallel β -sheets (27.5%) is highly populated in waved hair, and parallel β -sheets (28.1%) is highly populated in UV damaged hair. Straightened hair has more random coil structure (28.2%) than other type of hair. It should be noted that changing of secondary structure could be only analyzed in the cuticle region.

Table 4-9 Amide I band frequencies and assignments to secondary structure for protein.^{64,65}

Assignments	Wavenumbers (cm^{-1})	
	Literature 1 ⁶⁴	Literature 2 ⁶⁵
α -helix	1650-1657	1651
Antiparallel β -sheets	1612-1640, 1670-1690 (weak)	1611-1631
Parallel β -sheets	1626-1640	1622-1645
β -turn	1655-1675, 1680-1696	1668-1680, 1690-1692
Random coil	1640-1651	1668-1680

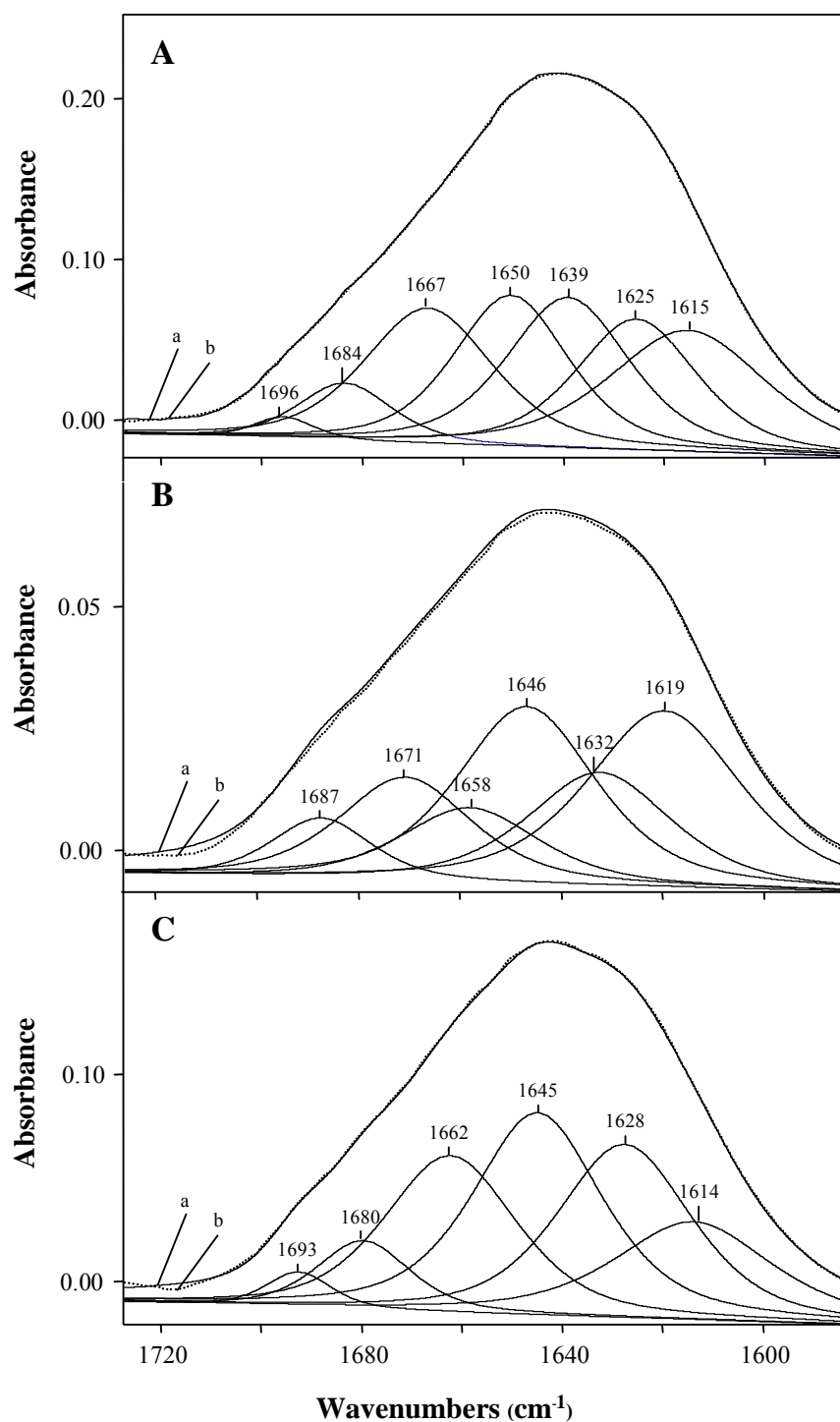


Figure 4-17 Curve fitting of the amide I region of the cuticle spectrum (depth of 1-2 μm from the hair surface) of (A) virgin hair, (B) waved hair, (C) straightened hair, (D) dyed hair, and (E) UV-damaged hair: (a) deconvoluted (solid line) spectrum and (b) original (dotted line) spectrum.

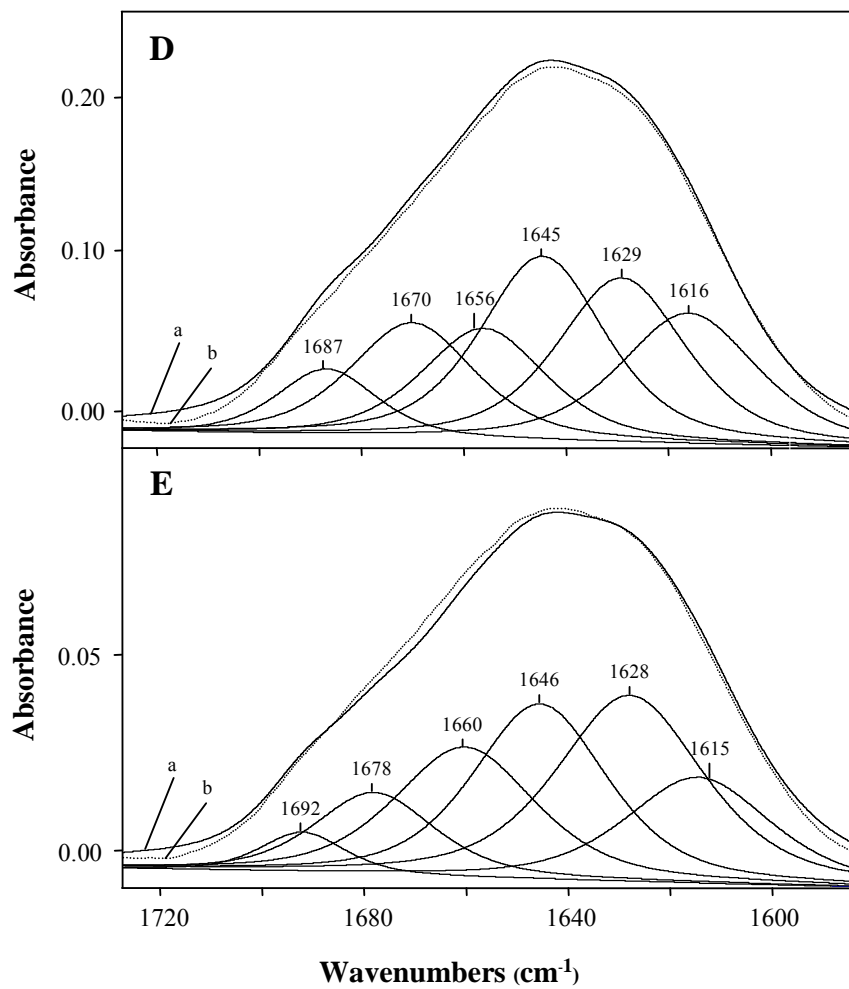


Figure 4-18 *continued*

Table 4-10 The number and location of individual bands obtained from second derivative of virgin and treated-hair.

Types of hair	Assignments (current work)									
	α -helix		Antiparallel β -sheets		Parallel β -sheets		β -turn		Random coil	
	Wavenumber (cm^{-1})	Area (%)	Wavenumber (cm^{-1})	Area (%)	Wavenumber (cm^{-1})	Area (%)	Wavenumber (cm^{-1})	Area (%)	Wavenumber (cm^{-1})	Area (%)
Virgin hair	1650	18.3	1615, 1696	21.6	1625	16.7	1667, 1684	23.9	1639	19.4
Waved hair	1658	10.6	1619	27.5	1632	16.6	1671, 1687	20.2	1646	25.1
Straightened hair	1662	21.4	1614, 1693	19.4	1628	24.3	1680	6.6	1645	28.2
Dyed hair	1656	14.3	1616	18.6	1629	21.7	1670, 1687	21.7	1645	23.7
UV-damaged hair	1660	18.7	1615, 1692	19.3	1628	28.1	1678	10.1	1646	23.8

Furthermore, the morphological surface of virgin and treated-hairs was investigated by SEM as shown in Figure 4-18. The morphological surface of waved and straightened hairs in cuticle region was changed remarkably. The morphology of cuticle region of the dyed hair was not changed significantly, possibly due to the fact that the hair surface was coated by the pigment color. The UV-damaged hair also seemed to be unaffected. These results suggest that only some treatment methods can cause physical damage on the hair surface. Nonetheless, all treatment affected the chemical structure at molecular level of hair, as previously confirmed by ATR FT-IR technique.

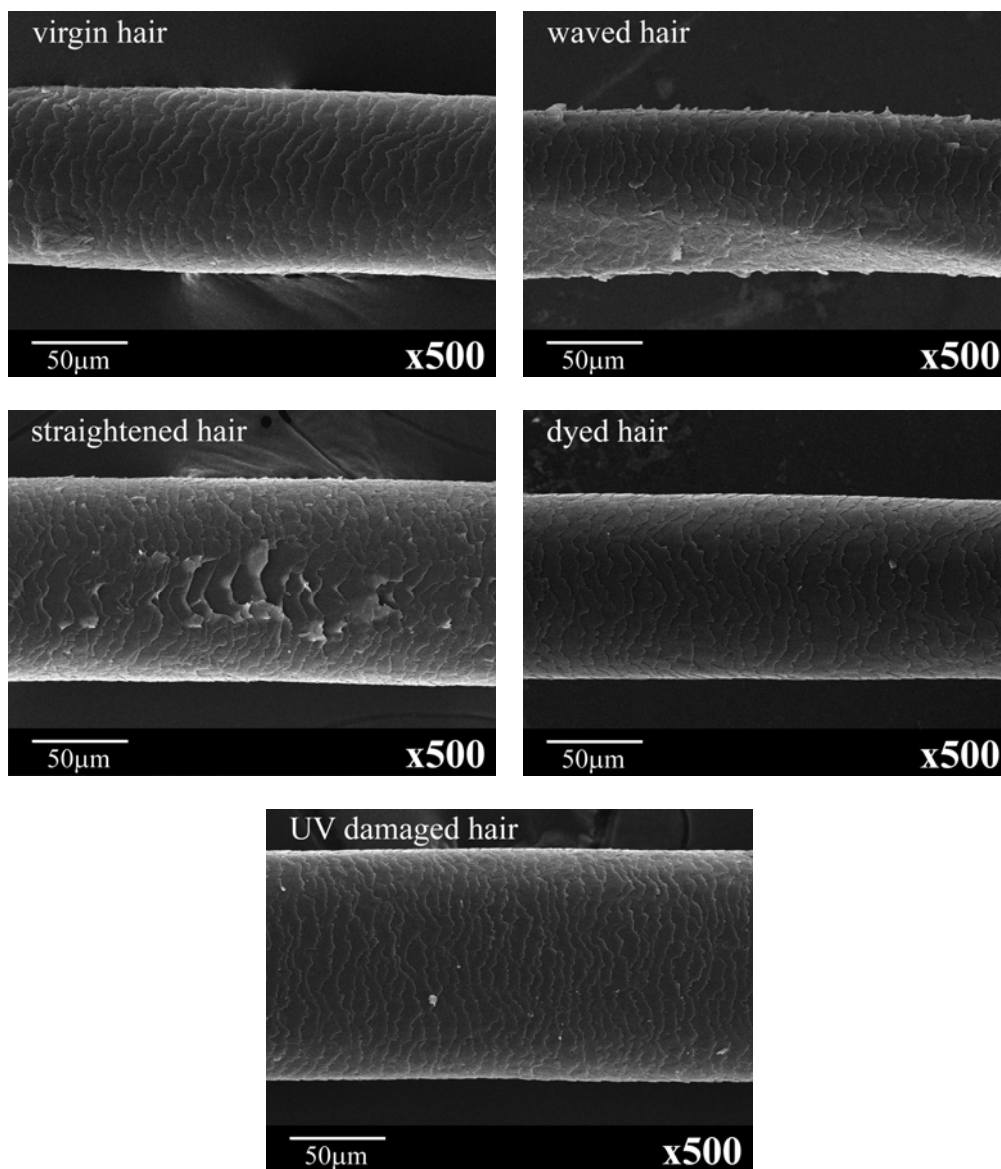


Figure 4-18 SEM images of virgin, waved, straightened, dyed, and UV-damaged hairs.

4.4 Physical and Mechanical Properties of Conditioner-Coated Hairs.

This part was divided into five parts. The two parts cover the ATR FT-IR and SEM analysis of coated hairs with five conditioner formula. The remained three parts are dedicated to the evaluation of the conditioner-coated hairs in term of tensile properties, hair texture, and resistant to wet combing.

4.4.1 ATR-FTIR spectra of conditioner-coated hairs

The ATR-FTIR spectra of the conditioner-coated hairs are shown in Figure 4-19. By comparison, the observed spectra of all coated hairs with various leave-on conditioners show different spectral feature at 2851-2957 cm^{-1} and 1000-1100 cm^{-1} from the virgin hair did. The peak intensity at 2851-2957 cm^{-1} increased because of the increasing $-\text{CH}_2-$ groups from the long chain alcohols and ester in the leave-on conditioners. Moreover, the intensities of C–O stretching signals of the alcohol at 1040 and 1080 cm^{-1} of almost all ingredients, such as glycerine, cetyl alcohol, stearyl alcohol, euxyl K300 (i.e. phenoxyethanol, methylparaben, ethylparaben, propylparaben, butylparaben, and *iso*-butylparaben) [see Figure 4-19(b)-(f)], are obviously higher than found in the untreated virgin hair. Besides, the peak intensity at 1000-1100 cm^{-1} also increases due to the $-\text{Si}-\text{O}-$ in cyclomethicone in the conditioners [Figure 4-19(b)-(f)]. Furthermore, the peak intensity of O–H stretching at 3283 cm^{-1} increases due to glycerine and positively charged polymer, the highest content in the leave-on conditioners (see Figure 4-19).

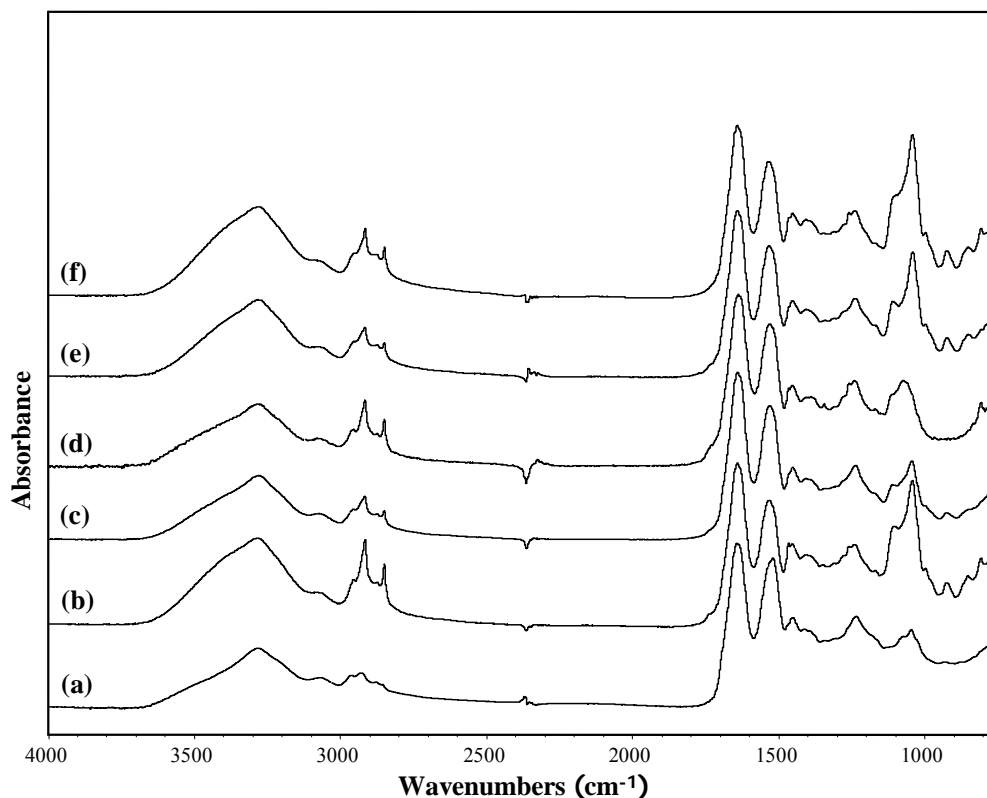


Figure 4-19 ATR-FTIR spectra of (a) virgin hair and the virgin hairs that were coated (b) LO, (c) LO+1%quat, (d) LO+1%chitosan, (e) LO+1%TMC, and (f) LO+1%HTACC.

4.4.2 Surface morphology of conditioner-coated hairs

The SEM images of virgin hairs that were coated by different leave-on conditioners were taken at 3-4 different positions along the hair strand. From Figures 4-20 to 4-24, patches of the conditioners are seen covering some or the whole areas of the hair strands. It is anticipated that the positively charged components in the conditioner should be attracted to the negative charged hair surface and therefore should somewhat affect the coating effectiveness of the conditioner. Apparently from SEM images in Figure 4-20, the leave-on conditioner without positively charged polymer (LO) cannot completely cover the hair fibers. On the other hand, the leave-on conditioners with cationic polymers (LO+1%quat, LO+1%chitosan, LO+1%TMC, or LO+1%HTACC) fully cover the hair surface (Figures 4-21 to 4-24). However, in case of the LO+1%chitosan-coated hair (Figure 4-22), the surface seems to be rougher than the others. This is probably because of the limited solubility of chitosan in the leave-on conditioner at the pH of conditioner (4.5-5.5) which is very close to the pKa (~6.5) of chitosan.

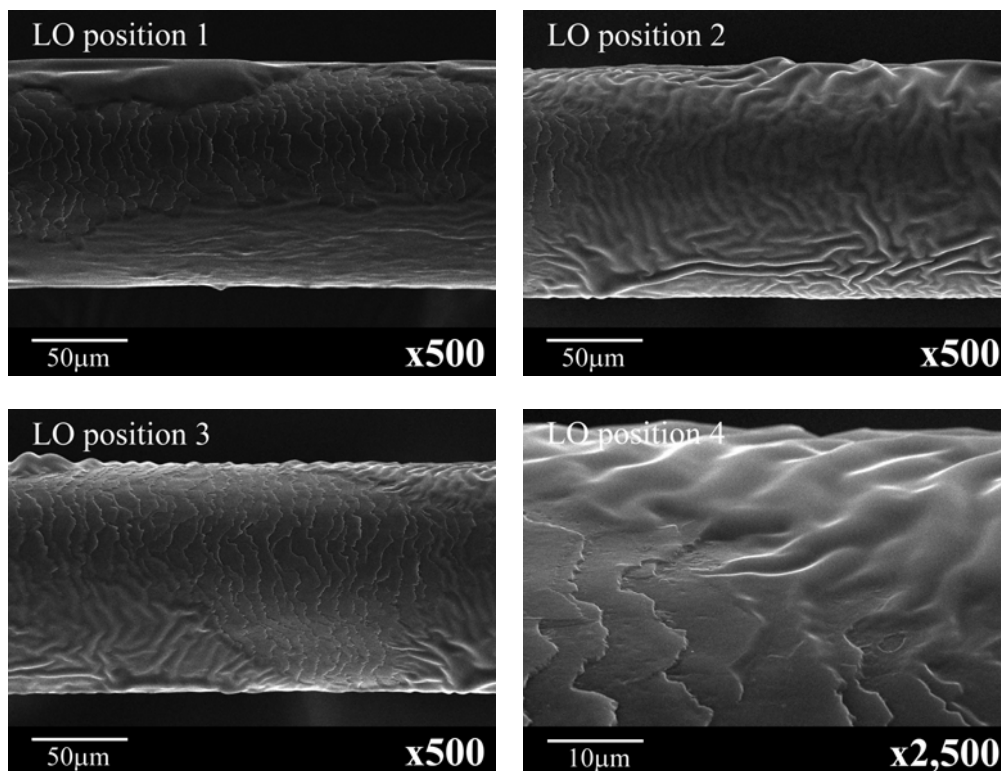


Figure 4-20 SEM images of virgin hair after the treatment with the leave-on conditioner without positively charged polymer.

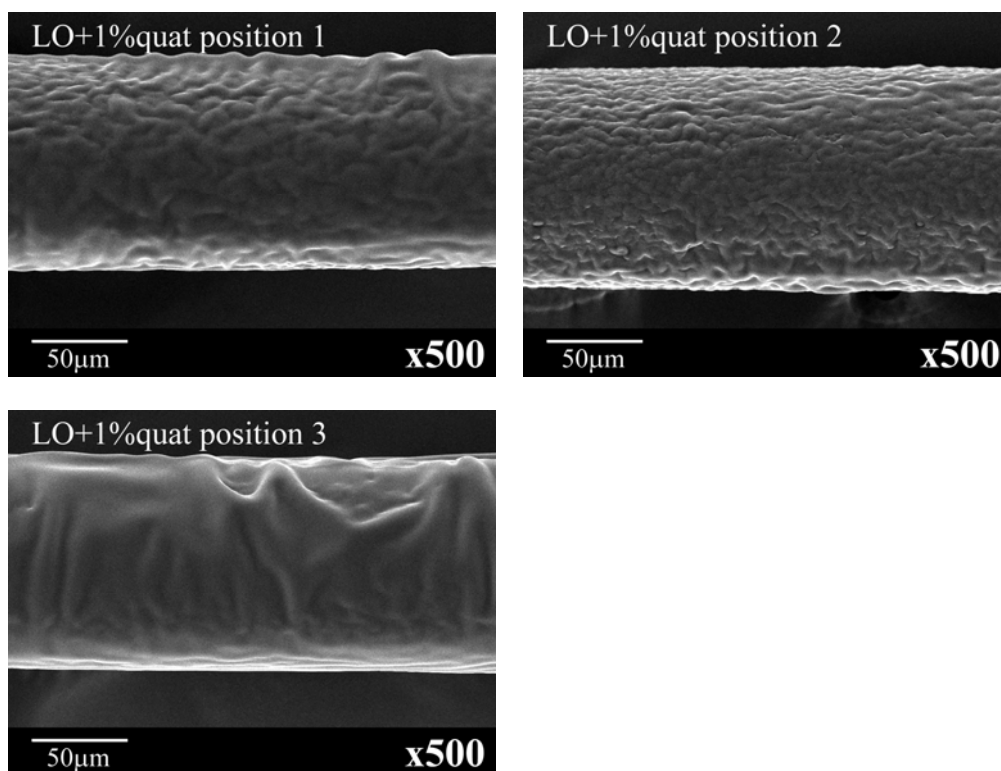


Figure 4-21 SEM images of virgin hair after the treatment with the leave-on conditioner containing 1%w/w polyquaternium-10.

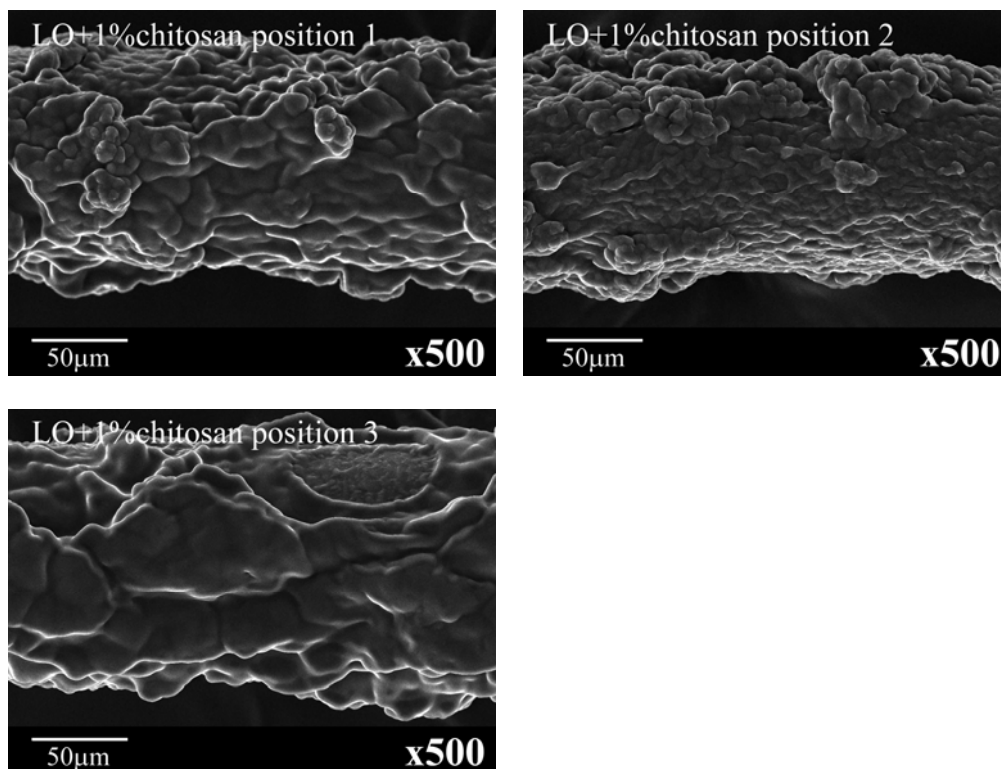


Figure 4-22 SEM images of virgin hair after the treatment with the leave-on conditioner containing 1%w/w chitosan.

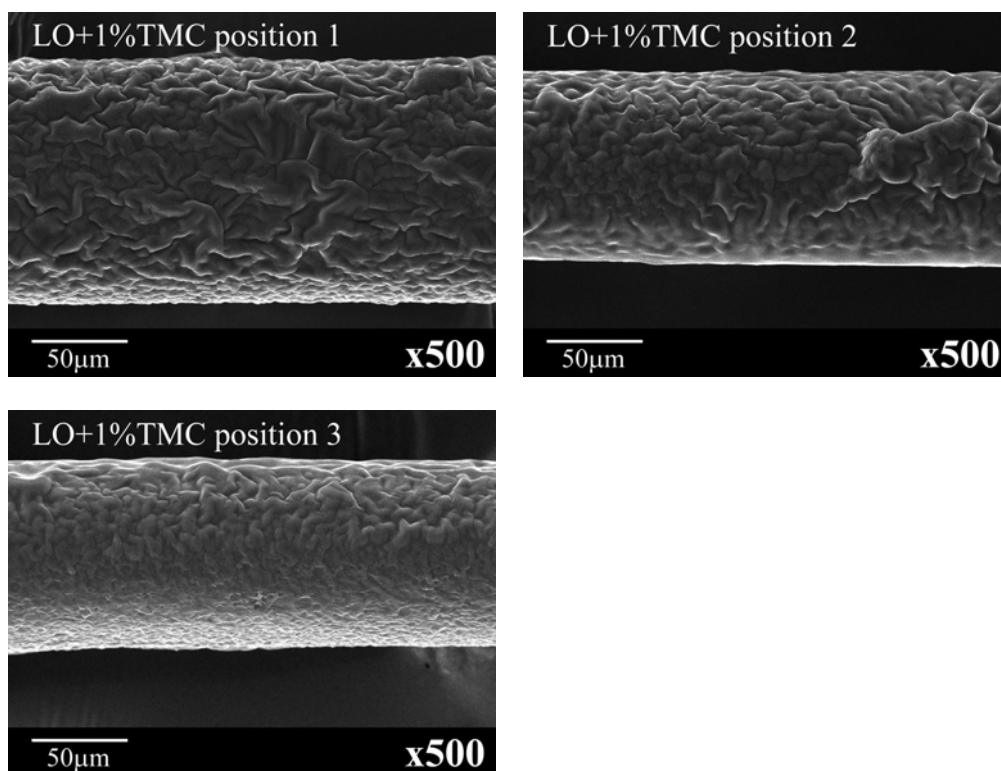


Figure 4-23 SEM images of virgin hair after the treatment with the leave-on conditioner containing 1%w/w TMC.

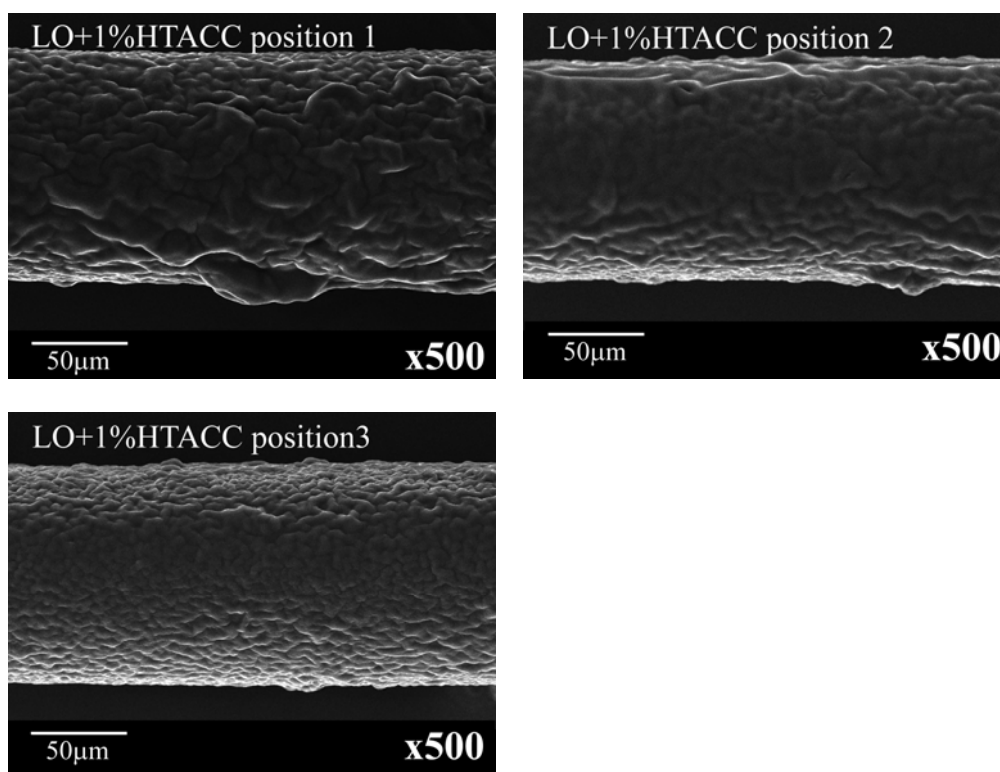


Figure 4-24 SEM images of virgin hair after the treatment with the leave-on conditioner containing 1%w/w HTACC.

4.4.3 Tensile properties of hair samples

This technique is used for measuring the tensile properties of keratin fiber that is related to the hair strength. The usual procedure for evaluating the tensile properties of keratin fiber is via load-elongation (stress/strain) method. The tensile test was performed at a fixed rate (20 mm/min), a fixed relative humidity (approximately 50%RH), and temperature (22°C). Figure 4-25 presents stress-strain curves for five hair types. The stress-strain curve of human hair is similar to that of wool and other keratinous fibers. When a keratin fiber is extended, the load elongation curve shows three distinct regions as marked in Figure 4-25. In the pre-yield region, also referred to as the Hookean region, the stress (load) is approximately linear to the strain (elongation). The ratio of stress to strain in this region is an elastic modulus. In this region, the resistance is provided by hydrogen bonds that are present between turns and stabilize the α -helix of keratin fiber. The yield region represents transition of keratin from α -form to β -form.⁶⁶ The chains unfold without any resistance, and hence the stress does not vary with strain. Typically, yield begins around 5% and post-yield begins at

around 25% strain. Then, the β -configuration again resists extension. Therefore, in the post-yield region, the stress again increases with strain until the keratin fiber breaks.

Table 4-11 presents the results from the tensile test of uncoated and coated hair by five leave-on conditioner formula. The parameters such as elastic modulus (N/m^2 ; Pa), plateau load ($\text{gmf/sq.}\mu\text{m}$), break extension (%strain), and break load ($\text{gmf/sq.}\mu\text{m}$) are reported. From the tensile tests of the uncoated virgin and damaged hairs, the elastic modulus and plateau loads are not significantly different from one another. The break load of the uncoated waved and straightened hairs are significantly different when compared with the virgin hair as shown in Figure 4-26. However, it is most likely that the chemical/UV treatment only affected the cuticle scales (as discussed in section 4.3), not the inner cortex part. In fact, the cortex contributes significantly to the tensile properties of hair.

Detailed comparison of virgin, waved, and straightened hairs reveals that the break load of the virgin hair is not affected by the presence of conditioner types. On the other hand, the break loads of the waved and straightened hairs increase significantly when the conditioners are applied (Figure 4-27). It is possible that the more uniform deposition and better covering of the leave-on conditioner layer on the hair strand than the virgin hair results in the increase of hair strength.

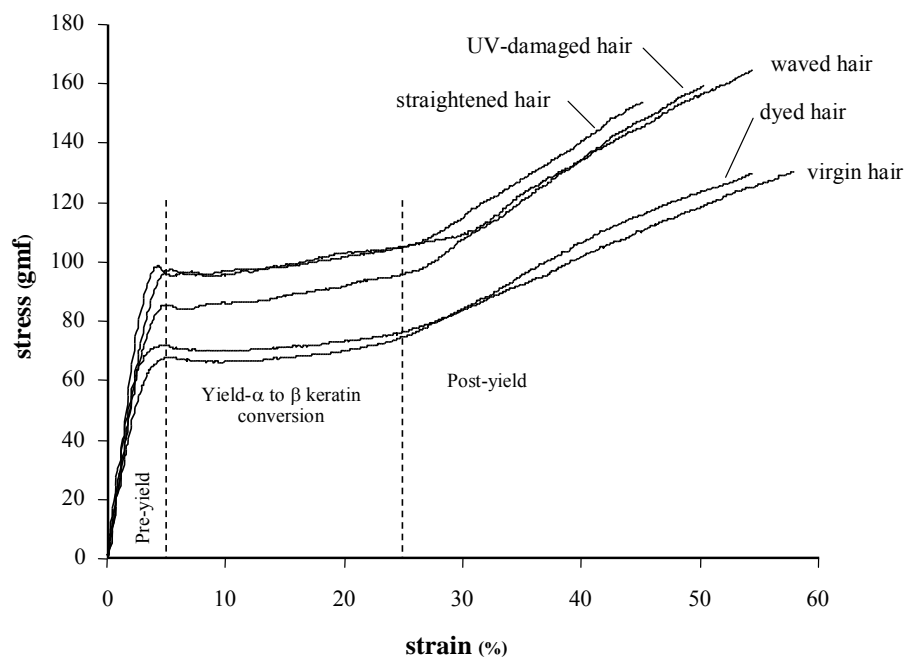


Figure 4-25 Stress-strain curves for five types of hair (virgin, waved, straightened hair, dyed hair, and UV-damaged hair).

Table 4-11 Tensile properties of uncoated and coated hair by five leave-on conditioner formula.

Hair types	Cross-sectional area (sq.µm)	Elastic modulus ($\times 10^9$ N/m ² ; Pa)	Plateau load ($\times 10^{-2}$ gmf/sq.µm)	Break extension (%)	Break load ($\times 10^{-2}$ gmf/sq.µm)
Virgin hair	7124.7 \pm 1221.4	2.76 \pm 0.28	1.32 \pm 0.03	57.19 \pm 4.66	2.16 \pm 0.06
LO-coated virgin hair	6094.4 \pm 1356.3	2.61 \pm 0.21	1.18 \pm 1.25	49.91 \pm 2.23	2.08 \pm 0.08
LO+1%quat-coated virgin hair	4917.8 \pm 1395.3	2.77 \pm 0.22	1.20 \pm 0.07	49.33 \pm 3.81	2.14 \pm 0.17
LO+1%chitosan-coated virgin hair	5749.5 \pm 808.3	2.89 \pm 0.33	1.23 \pm 0.05	50.95 \pm 4.02	2.12 \pm 0.96
LO+1%TMC-coated virgin hair	6107.5 \pm 1390.4	3.13 \pm 0.97	1.22 \pm 0.05	51.16 \pm 5.96	2.17 \pm 0.16
LO+1%HTACC-coated virgin hair	5954.5 \pm 1367.9	3.03 \pm 0.40	1.23 \pm 0.04	51.05 \pm 2.27	2.24 \pm 0.13
Waved hair	6870.8 \pm 1197.6	2.87 \pm 0.33	1.21 \pm 0.10	51.45 \pm 7.4	1.88 \pm 0.25
LO-coated waved hair	5697.9 \pm 1078.9	2.96 \pm 0.25	1.23 \pm 0.05	49.91 \pm 3.85	2.20 \pm 0.12
LO+1%quat-coated waved hair	6168.6 \pm 1085.3	2.85 \pm 0.26	1.21 \pm 0.06	49.18 \pm 3.11	2.15 \pm 0.17
LO+1%chitosan-coated waved hair	5760.8 \pm 939.7	3.01 \pm 0.29	1.25 \pm 0.03	49.50 \pm 4.80	2.21 \pm 0.20

The values presented here are based on 10 measurements.

Table 4-11 *continued*

Hair types	Cross-sectional area (sq.µm)	Elastic modulus ($\times 10^9$ N/m ² ; Pa)	Plateau load ($\times 10^{-2}$ gmf/sq.µm)	Break extension (%)	Break load ($\times 10^{-2}$ gmf/sq.µm)
LO+1%TMC-coated waved hair	6241.6 ± 1680.1	3.05 ± 0.35	1.23 ± 0.06	49.69 ± 3.98	2.22 ± 0.17
LO+1%HTACC-coated waved hair	5767.6 ± 1584.4	3.12 ± 0.26	1.25 ± 0.04	49.10 ± 2.90	2.26 ± 0.12
Straightened hair	7506.9 ± 1391.5	3.08 ± 0.39	1.18 ± 0.08	51.62 ± 8.0	1.83 ± 0.23
LO-coated straightened hair	6423.1 ± 878.9	3.00 ± 0.71	1.29 ± 0.23	46.97 ± 4.38	2.20 ± 0.28
LO+1%quat-coated straightened hair	7440.5 ± 1180.6	2.93 ± 0.27	1.19 ± 0.05	49.83 ± 6.17	2.11 ± 0.17
LO+1%chitosan-coated straightened hair	7167.4 ± 1486.6	2.95 ± 0.28	1.20 ± 0.06	49.16 ± 4.32	2.14 ± 0.17
LO+1%TMC-coated straightened hair	7221.9 ± 1220.0	3.05 ± 0.33	1.22 ± 0.07	48.82 ± 2.23	2.18 ± 0.17
LO+1%HTACC-coated straightened hair	4677.0 ± 706.8	3.09 ± 0.32	1.26 ± 0.03	45.68 ± 2.76	2.25 ± 0.07
Dyed hair	7438.4 ± 1025.8	3.12 ± 0.41	1.35 ± 0.04	49.92 ± 6.0	2.08 ± 0.17
UV-damaged hair	7303.1 ± 1506.3	3.07 ± 0.43	1.28 ± 0.05	50.23 ± 6.7	2.06 ± 0.25

The values presented here are based on 10 measurements.

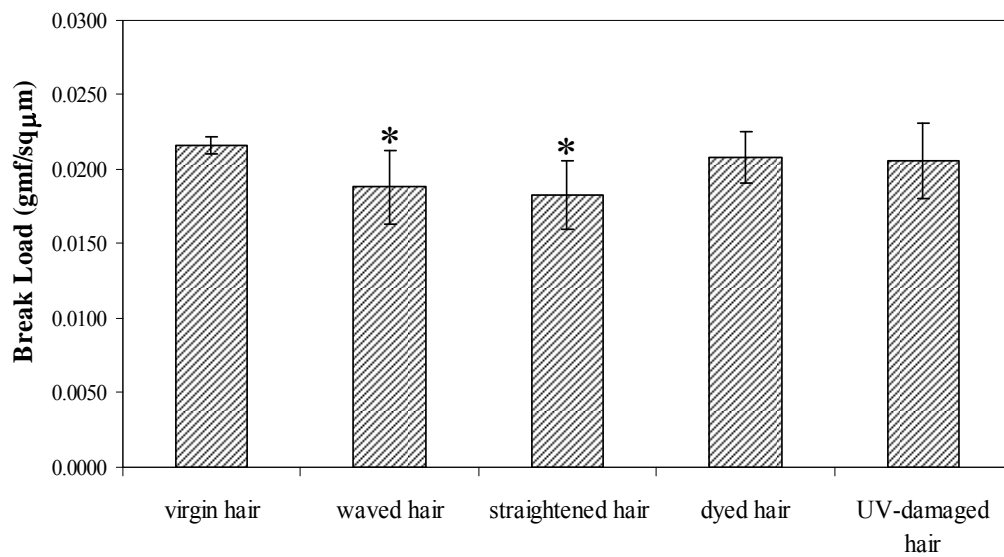


Figure 4-26 Break load of virgin, waved, straightened, dyed and UV-damaged hairs.

* $p < 0.05$ (compared to virgin hair).

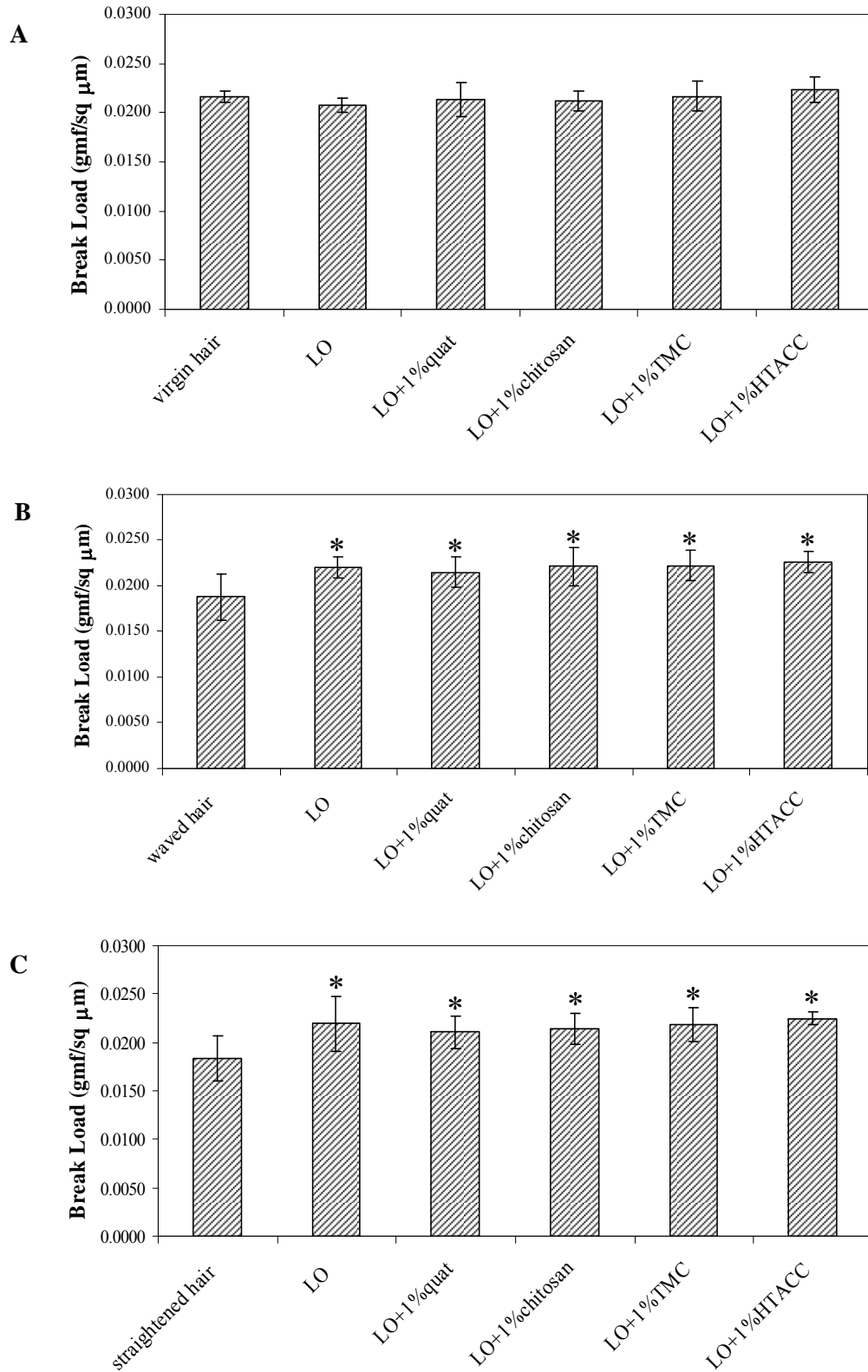


Figure 4-27 Comparison of break load of (A) virgin, (B) waved, and (C) straightened hairs with and without treatment by five leave-on conditioners. * $p < 0.05$ (compared to non-treated hair). The values presented here were averaged from 10 measurements.

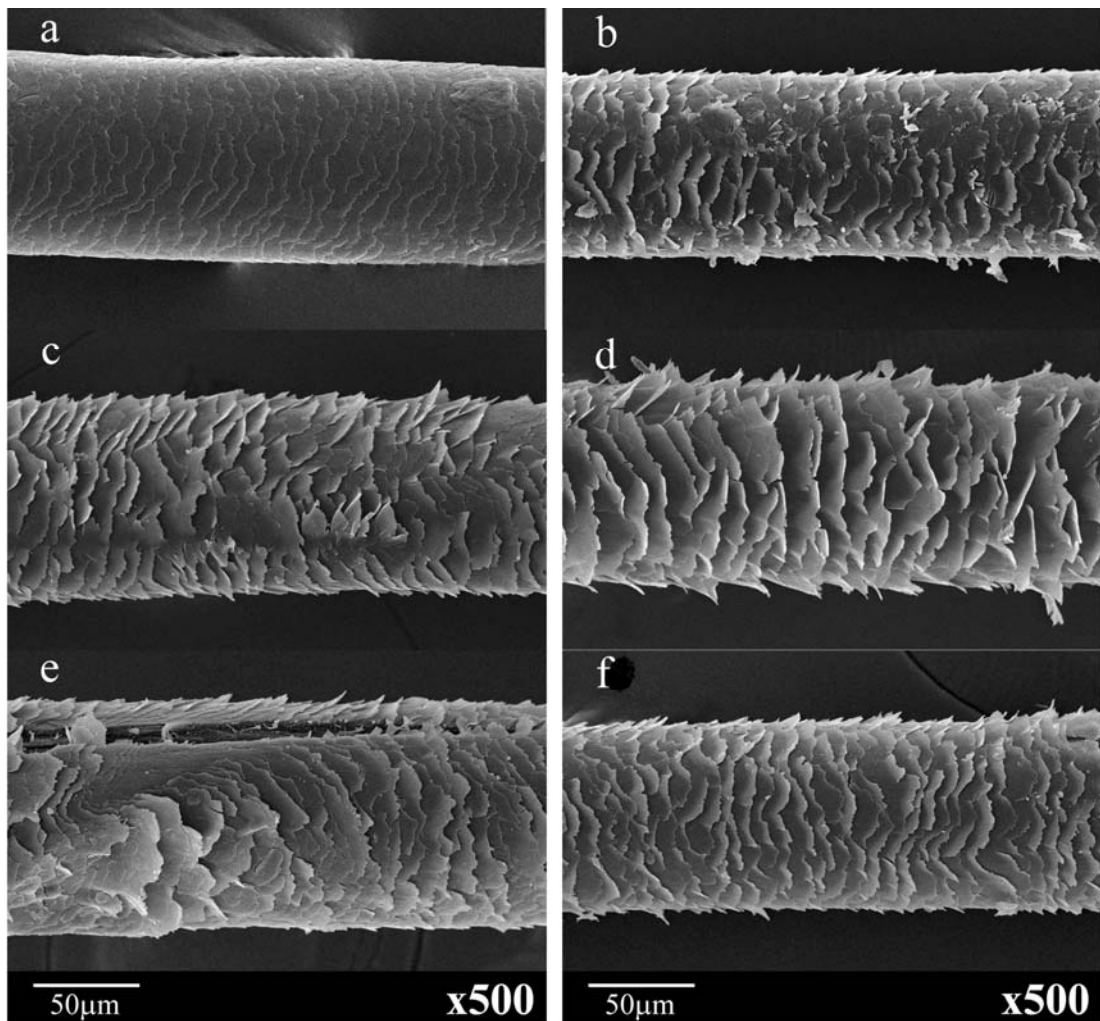


Figure 4-28 SEM images of fractured cuticle scales of virgin hair caused by hair extension at 50% relative humidity: (a) original virgin hair, tensile tested samples: (b) virgin, (c) waved, (d) straightened (e) dyed, and (f) UV-damaged hairs.

Figure 4-28 displays the SEM images of fractured in the cuticle scales. The cuticle scales of all broken hairs are lifted. Upon closely inspection, the cuticle scales of all chemically treated hairs are lifted quite extensively as shown in Figure 4-28(c)-(e). It is however noted here that lifting of cuticle scales cannot be correlated directly with the obtained tensile test results.

Additionally, fibrillation, smooth, splitting, and step is usually the four most common fracture patterns for human hair. The fracture pattern generally depends on the extent of hair damage, the relative humidity, and whether the fiber is twisted or contains flaws. If the hair and its cuticle are in good condition (e.g., near the root end), a smooth break tends to occur.¹ As a result, the fracture pattern of the five hair types are random pattern (i.e. smooth, splitting, and step) as shown in Appendix C.

4.4.4 Hair texture analysis

This technique was used for measuring the friction force (g.mm) of hair surface that is directly related to the smooth or slippery feel on hair. In the procedure, a probe was passed through hair tresses surface at speed of 10 mm/sec and the friction force was measured as a function of distance. The friction forces are shown in Figure 4-29.

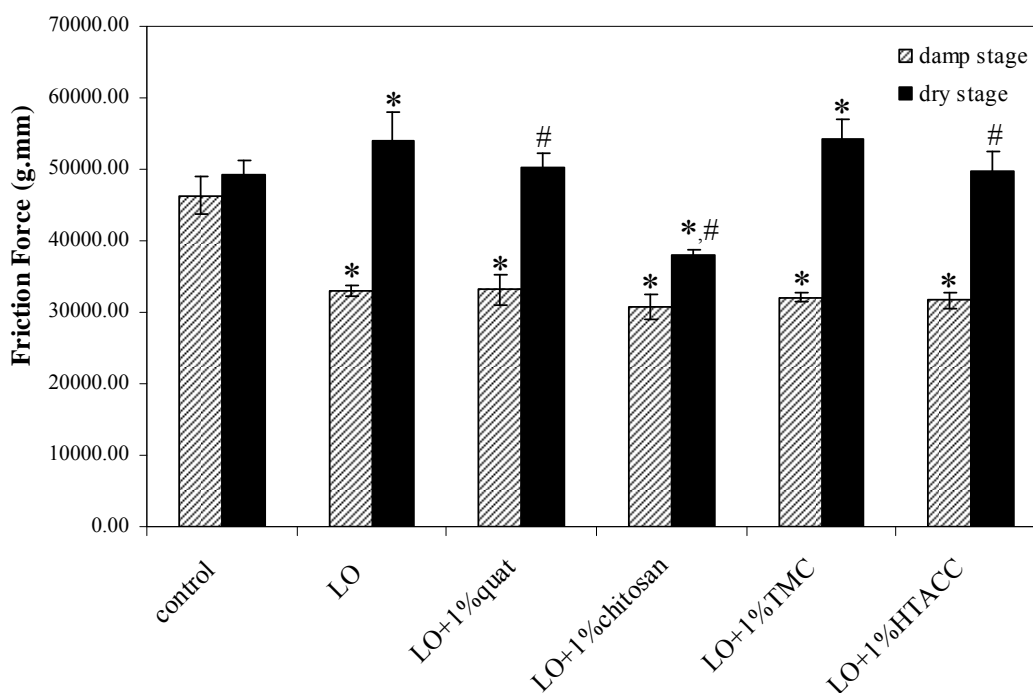


Figure 4-29 Comparison of the friction force of hair surface, subjected to treatment by five leave-on conditioner formula and DI water (control). * $p < 0.05$ (compared to control) and # $p < 0.05$ (compared to LO). The values presented were averaged from 5 measurements.

The leave-on conditioner usually provides easier combing and detangling in both damp and dry conditions. Consequently, this study was carried out with hairs in both damp and dry stages. The results in Figure 4-29 are reported in terms of the friction force that is directly correlated to the smooth feel. The friction force in damp stage is always lower than in the dry stage. In the damp stage, the friction force is not significantly different when compared between each conditioners formula. However, in the dry stage, the friction force of hair coated with LO+1%chitosan is the lowest.

4.4.5 Wet combing test

This technique is used for measuring the friction force (gmf) generated upon combing conditioner-coated hair tresses with a metal comb to determine ease of combing and hair detangling. In the usual procedure, hair tresses are passed through a comb at a speed of 40 inch/min and the friction force is measured as a function of distance.

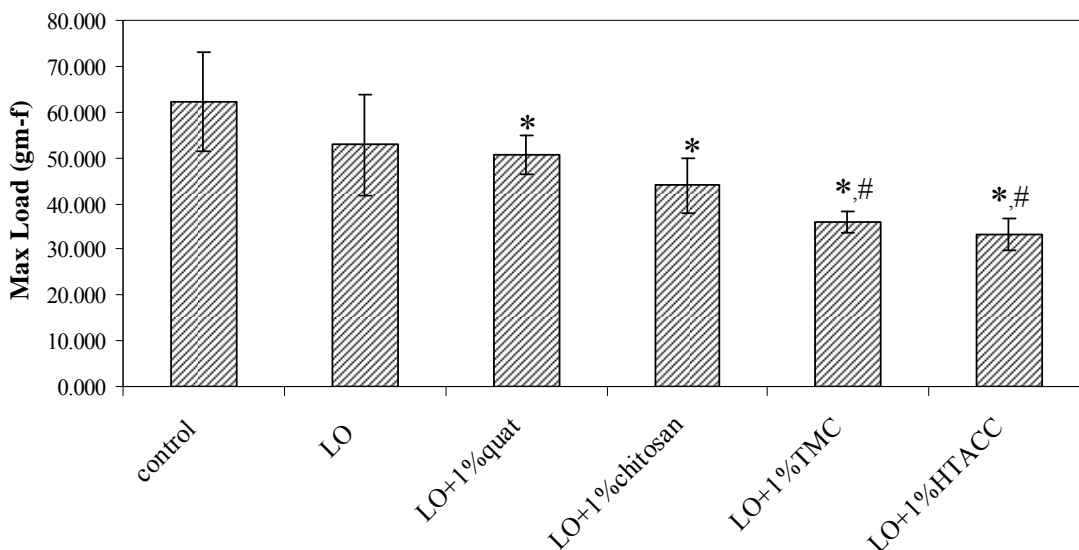


Figure 4-30 Comparison of max loads of hairs tresses subjected to treatment by five leave-on conditioner formulas and DI water (control). * $p < 0.05$ (compared to control) and # $p < 0.05$ (compared to LO). The values presented were averaged from 5 measurements.

From Figure 4-30, all leave-on conditioners containing chitosan and its derivatives result in lower max loads than does the leave-on conditioner containing polyquaternium-10 (product in market). Thus, chitosan and its derivatives potentially reduce the friction during wet combing quite effectively.

CHAPTER V

CONCLUSION

5.1 Conclusions

Two positively charged derivatives of chitosan, *N,N,N*-trimethylammonium chitosan chloride (TMC) and *N*-[(2-hydroxyl-3-trimethylammonium)propyl]chitosan chloride (HTACC), were prepared from chitosan with MW of 45,000 g/mol. TMC with 17-22%*DQ* and HTACC with 24-139%*DQ* were obtained. The %*DQ* of HTACC could be varied by varying GTMAC mole equivalent in the synthesis reaction. For TMC, varying the methylating agent amount did not affect the %*DQ* of TMC. Instead, when replacing the solvent used for the reaction from NMP by DMF-H₂O (1:1), the %*DQ* was increased by upto 15%. TMC was able to dissolve in aqueous solution with pH<6.5, while HTACC dissolved in the pH of 1 to 14. %*DQ*-dependent cytotoxicity against human keratinocyte cells was observed for both TMC and HTACC.

A homemade ATR accessory with a slide-on miniature Ge μ IRE equipped in an FTIR microspectrometer was used to analyze the chemical functional groups on hair surfaces. All prepared conditioners was successfully coated on the hair, as evidenced from the ATR-FTIR and SEM analyses. The leave-on conditioner could flatten the lifted cuticle scales of damaged hairs. It is thus believed that the leave-on conditioner provides a protective coating to the hair surfaces for prevention of future damage. In the tensile test, all prepared and commercially-available conditioners were able to significantly increase the breaking load of conditioner-coated waved and straightened hairs. In wet combing test, chitosan and its derivatives potentially reduced the friction during wet combing more effectively than the commercial-grade conditioner did.

5.2 Future Direction

The future plan should cover the study of antibacterial activity of the prepared leave-on conditioner. This is because chitosan and its derivatives possess antibacterial activity which should find extensive application in hair-care products. Moreover, the use of chitosan-filled conditioners should be tested for skin allergy, which is a method for medical diagnosis of allergies with human before being used commercially. These studies should help broaden applications of chitosan and its derivatives, especially in cosmetic products.

REFERENCES

1. Robbins, C. R. Chemical and physical behavior of human hair. 4thed. New York: Springer-Verlag, 2002.
2. Sieval, A. B.; Thanou, M.; Kotze, A. F.; Verhoef, J. C.; Brussee, J.; Junginger, H. E. Preparation and NMR characterization of highly substituted *N*-trimethyl chitosan chloride. *Carbohydrate Polymers* 36(2-3) (1998): 157-165.
3. Seong, H. S.; Whang, H. S.; Ko, S. W. Synthesis of a quaternary ammonium derivative of chito-oligosaccharide as antimicrobial agent for cellulosic fibers. *Journal of Applied Polymer Science* 76(14) (2000): 2009-2015.
4. Robbins, C. R.; Kelly, C. H. Amino acid composition of human hair. *Textile Research Journal* 40(10) (1970): 891-896.
5. Ward, W. H.; Lundgren, H. P. In advances in protein chemistry. vol. 9. New York: Academic Press, 1955.
6. Clay, R. C.; Cook, K.; Routh, J. I. Studies in the composition of human hair. *Journal of the American Chemical Society* 62(10) (1940): 2709-2710.
7. Bradbury, J. H.; Chapman, G. V.; Hambly, A. N.; King, N. L. R. Separation of chemically unmodified histological components of keratin fibres and analyses of cuticles. *Nature* 210(5043) (1966): 1333-1334.
8. Pauling, L.; Corey, R. B. Two hydrogen-bonded spiral configurations of the polypeptide chain. *Journal of the American Chemical Society* 72(11) (1950): 5349-5349.
9. Pauling, L.; Corey, R. B. The structure of hair, muscle, and related proteins. *Proceedings of the National Academy of Sciences of the United States of America* 37(5) (1951): 261-271.
10. Hoting, E.; Zimmermann, M. Sunlight-induced modifications in bleached, permed, or dyed human hair. *Journal of the Society of Cosmetic Chemists* 48 (1997): 79-91.

11. Dean, R. T.; Fu, S.; Stocker, R.; Davies, M. J. Biochemistry and pathology of radical-mediated protein oxidation. *Biochemical Journal* 324(1) (1997): 1-18.
12. Maron, S. H.; Prutton, C. F. Principles of physical chemistry. New York: Macmillan, 1958.
13. Gilreath, E. S. Fundamental concepts of inorganic chemistry. New York: McGraw-Hill, 1958.
14. Lang, G.; Wendel, H.; Konrad, E. Cosmetic composition based upon chitosan derivatives, new chitosan derivatives as well as processes for the production thereof. *U.S. Patent Application 4,528,283*, 1985.
15. Maresch, G.; Titze, H. J.; Lang, G. Sulphopropyl derivatives of chitin and chitosan, process for their preparation, and their use. *D.E. Patent Application 3,432,227*, 1986.
16. Omura, H.; Uehara, K.; Okisaka, K.; Tanaka, Y.; Naito, Y. Hair cosmetic. *J.P. Patent Application 2,134,312*, 1990.
17. Satou, H.; Go, N. Hair setting agent. *J.P. Patent Application 8,026,948.*, 1996.
18. Nishimoto, H.; Toda, T. Hair-treating agent composition. *J.P. Patent Application 2001019624*, 2001.
19. Yamamoto, H.; Taniuchi, S. Hair dyeing agents. *W.O. Patent Application 03/051321 A1*, 2003.
20. Shimogaki, H.; Nishito, M.; Yamada, H.; Kurita, H. Gray hair-preventing/improving agent. *J.P. Patent Application 2004315442*, 2004.
21. Krause, T.; Baumeister, J.; Weber, D.; Lang, G.; Beyer, A.; Florig, E.; Gaenger, K.; Schiemann, H. Hair treatment compositions containing N-hydroxy-alkyl-O-benzyl chitosans and methods of using same. *U.S. Patent Application 2005/0226838 A1*, 2005.
22. Liu, Z. X. New type wash articles. *C.N. Patent Application 1916145*, 2007.
23. Gaillard, Y.; Pepin, G. Screening and identification of drugs in human hair by high-performance liquid chromatography-photodiode-array UV detection and gas chromatography-mass spectrometry after solid-phase extraction a powerful tool in forensic medicine. *Journal of Chromatography A* 762(1-2) (1997): 251-267.

24. Phinney, K.; Sander, L. Liquid chromatographic method for the determination of enantiomeric composition of amphetamine and methamphetamine in hair samples. *Analytical and Bioanalytical Chemistry* 378(1) (2004): 144-149.
25. Mercolini, L.; Mandrioli, R.; Saladini, B.; Conti, M.; Baccini, C.; Raggi, M. A. Quantitative analysis of cocaine in human hair by HPLC with fluorescence detection. *Journal of Pharmaceutical and Biomedical Analysis* 48(2) (2008): 456-461.
26. Berankova, K.; Habrdova, V.; Balikova, M.; Strejc, P. Methamphetamine in hair and interpretation of forensic findings in a fatal case. *Forensic Science International* 153(1) (2005): 93-97.
27. Felli, M.; Martello, S.; Marsili, R.; Chiarotti, M. Disappearance of cocaine from human hair after abstinence. *Forensic Science International* 154(2-3) (2005): 96-98.
28. Lachenmeier, K.; Musshoff, F.; Madea, B. Determination of opiates and cocaine in hair using automated enzyme immunoassay screening methodologies followed by gas chromatographic-mass spectrometric (GC-MS) confirmation. *Forensic Science International* 159(2-3) (2006): 189-199.
29. Nishida, M.; Yashiki, M.; Namera, A.; Kimura, K. Single hair analysis of methamphetamine and amphetamine by solid phase microextraction coupled with in matrix derivatization. *Journal of Chromatography B* 842(2) (2006): 106-110.
30. Tadeo, J. L.; Sanchez-Brunete, C.; Miguel, E. Determination of polybrominated diphenyl ethers in human hair by gas chromatography-mass spectrometry. *Talanta* 78(1) (2009): 138-143.
31. Kempson, I. M.; Skinner, W. M. ToF-SIMS analysis of elemental distributions in human hair. *Science of The Total Environment* 338(3) (2005): 213-227.
32. Chen, B. J.; Lee, P. L.; Chen, W. Y.; Mai, F. D.; Ling, Y. C. Hair dye distribution in human hair by ToF-SIMS. *Applied Surface Science* 252(19) (2006): 6786-6788.

33. Kuzuhara, A.; Hori, T. Reduction mechanism of thioglycolic acid on keratin fibers using microspectrophotometry and FT-Raman spectroscopy. *Polymer* 44(26) (2003): 7963-7970.
34. Kuzuhara, A. Analysis of structural change in keratin fibers resulting from chemical treatments using Raman spectroscopy. *Biopolymers* 77(6) (2005): 335-344.
35. Kuzuhara, A. Analysis of structural changes in bleached keratin fibers (black and white human hair) using Raman spectroscopy. *Biopolymers* 81(6) (2006): 506-514.
36. Kuzuhara, A. Analysis of structural changes in permanent waved human hair using Raman spectroscopy. *Biopolymers* 85(3) (2007): 274-283.
37. Wang, Q.; Boles, R. G. Individual human hair mitochondrial DNA control region heteroplasmy proportions in mothers and children. *Mitochondrion* 6(1) (2006): 37-42.
38. Panayiotou, H.; Kokot, S. Matching and discrimination of single human-scalp hairs by FT-IR micro-spectroscopy and chemometrics. *Analytica Chimica Acta* 392(2-3) (1999): 223-235.
39. Bilinska, B. On the structure of human hair melanins from an infrared spectroscopy analysis of their interactions with Cu^{2+} ions. *Spectrochimica Acta Part A: Molecular and Biomolecular Spectroscopy* 57(12) (2001): 2525-2533.
40. Feughelman, M.; Lyman, D. J.; Willis, B. K. The parallel helices of the intermediate filaments of α -keratin. *International Journal of Biological Macromolecules* 30(2) (2002): 95-96.
41. Urban, M. W. Attenuated total reflectance spectroscopy of polymers: Theory and Practice. Washington, DC: American Chemical Society, 1996.
42. Ekgasit, S.; Ishida, H. Optical depth profiling by attenuated total reflection fourier transform infrared spectroscopy using an incident beam with arbitrary degree of polarization. *Vibrational Spectroscopy* 13(1) (1996): 1-9.
43. Brugnerotto, J.; Lizardi, J.; Goycoolea, F. M.; Arguelles-Monal, W.; Desbrieres, J.; Rinaudo, M. An infrared investigation in relation with chitin and chitosan characterization. *Polymer* 42(8) (2001): 3569-3580.

44. Kasaai, M. R. A review of several reported procedures to determine the degree of *N*-acetylation for chitin and chitosan using infrared spectroscopy. *Carbohydrate Polymers* 71 (2008): 497-508.
45. Lavertu, M.; Xia, Z.; Serreqi, A. N.; Berrada, M.; Rodrigues, A.; Wang, D.; Buschmann, M. D.; Gupta, A. A validated ¹H NMR method for the determination of the degree of deacetylation of chitosan. *Journal of Pharmaceutical and Biomedical Analysis* 32(6) (2003): 1149-1158.
46. Takahashi, T.; Imai, M.; Suzuki, I. High-potential molecular properties of chitosan and reaction conditions for removing *p*-quinone from the aqueous phase. *Biochemical Engineering Journal* 25 (2005): 7-13.
47. Pedroni, V. I.; Gschaidner, M. E.; Schulz, P. C. UV Spectrophotometry: Improvements in the study of the degree of acetylation of chitosan. *Macromolecular Bioscience* 3 (2003): 531-534.
48. Jiang, X.; Chen, L.; Zhong, W. A new linear potentiometric titration method for the determination of deacetylation degree of chitosan. *Carbohydrate Polymers* 54(4) (2003): 457-463.
49. Varum, K. M.; Ottoy, M. H.; Smidsrod, O. Water-solubility of partially *N*-acetylated chitosans as a function of pH: effect of chemical composition and depolymerisation. *Carbohydrate Polymers* 25(2) (1994): 65-70.
50. Rinaudo, M.; Pavlov, G.; Desbrières, J. Influence of acetic acid concentration on the solubilization of chitosan. *Polymer* 40(25) (1999): 7029-7032.
51. Sorlier, P.; Denuziere, A.; Viton, C.; Domard, A. Relation between the degree of acetylation and the electrostatic properties of chitin and chitosan. *Biomacromolecules* 2(3) (2001): 765-772.
52. de Britto, D.; Forato, L. A.; Assis, O. B. G. Determination of the average degree of quaternization of *N,N,N*-trimethylchitosan by solid state ¹³C NMR. *Carbohydrate Polymers* 74(1) (2008): 86-91.
53. Runarsson, O. V.; Holappa, J.; Jonsdottir, S.; Steinsson, H.; Masson, M. *N*-selective 'one pot' synthesis of highly *N*-substituted trimethyl chitosan (TMC). *Carbohydrate Polymers* 74(3) (2008): 740-744.
54. Sajomsang, W.; Tantayanon, S.; Tangpasuthadol, V.; Daly, W. H. Synthesis of methylated chitosan containing aromatic moieties: chemoselectivity

- and effect on molecular weight. *Carbohydrate Polymers* 72(4) (2008): 740-750.
55. Cho, J.; Grant, J.; Piquette-Miller, M.; Allen, C. Synthesis and physicochemical and dynamic mechanical properties of a water-soluble chitosan derivative as a biomaterial. *Biomacromolecules* 7(10) (2006): 2845-2855.
 56. Lim, S. H.; Hudson, S. M. Synthesis and antimicrobial activity of a water-soluble chitosan derivative with a fiber-reactive group. *Carbohydrate Research* 339(2) (2004): 313-319.
 57. Mosmann, T. Rapid colorimetric assay for cellular growth and survival: application to proliferation and cytotoxicity assays. *Journal of Immunological Methods* 65(1-2) (1983): 55-63.
 58. Sashiwa, H.; Shigemasa, Y. Chemical modification of chitin and chitosan 2: preparation and water soluble property of *N*-acylated or *N*-alkylated partially deacetylated chitins. *Carbohydrate Polymers* 39(2) (1999): 127-138.
 59. Thanou, M. M.; Kotze, A. F.; Scharringhausen, T.; Lueben, H. L.; de Boer, A. G.; Verhoef, J. C.; Junginger, H. E. Effect of degree of quaternization of *N*-trimethyl chitosan chloride for enhanced transport of hydrophilic compounds across intestinal Caco-2 cell monolayers. *Journal of Controlled Release* 64(1-3) (2000): 15-25.
 60. Howling, G. I.; Dettmar, P. W.; Goddard, P. A.; Hampson, F. C.; Dornish, M.; Wood, E. J. The effect of chitin and chitosan on the proliferation of human skin fibroblasts and keratinocytes in vitro. *Biomaterials* 22(22) (2001): 2959-2966.
 61. Ng, L. T.; Swami, S. IPNs based on chitosan with NVP and NVP/HEMA synthesised through photoinitiator-free photopolymerisation technique for biomedical applications. *Carbohydrate Polymers* 60(4) (2005): 523-528.
 62. Wiegand, C.; Hipler, U. C. Evaluation of biocompatibility and cytotoxicity using keratinocyte and fibroblast cultures. *Skin Pharmacology and Physiology* 22(2) (2009): 74-82.
 63. Signori, V.; Lewis, D. M. FTIR investigation of the damage produced on human hair by weathering and bleaching processes: Implementation of

- different sampling techniques and data processing. *International Journal of Cosmetic Science* 19(1) (1997): 1-13.
64. Pelton, J. T.; Mclean, L. R. Spectroscopic methods for analysis of protein secondary structure. *Analytical Biochemistry* 277 (2000): 167-176.
65. Tonin, C.; Aluigi, A.; Songia, M. B.; D'Arrigo, C.; Mormino, M.; Vineis, C. Thermoanalytical characterisation of modified keratin fibres. *Journal of Thermal Analysis and Calorimetry* 77 (2004): 987-996.
66. Seshadri, I. P.; Bhushan, B. In situ tensile deformation characterization of human hair with atomic force microscopy. *Acta Materialia* 56(4) (2008): 774-781.

APPENDICES

APPENDIX A

Determination of %DQ of *N,N,N*-trimethylammonium chitosan chloride (TMC)

The %DQ of TMCs were determined from the relative ratios between the signal at 3.10 ppm can be assigned to three methyl groups of quaternary ammonium group and the signal of H-1 (δ 4.38-5.34 ppm), H-2 (δ 2.95 ppm), H-2',3,4,5,6,6' (δ 3.25-4.30 ppm), H-2,2',3,4,5,6,6' (δ 2.95 ppm and 3.25-4.30 ppm), or $-NHCOCH_3$ (δ 1.84 ppm) of chitosan analyzed by 1H NMR. The position of those signals in the TMC spectra is shown in Figure A-1. %DQ, %DS_{N(CH₃)₂}, %DS_{NHCH₃}, and %DS (total) are quaternization, *N,N*-dimethylation, *N*-methylation, and a total degree of *N*-methylation of chitosan were determined from 1H NMR as shown in Tables A-1 to A-5.

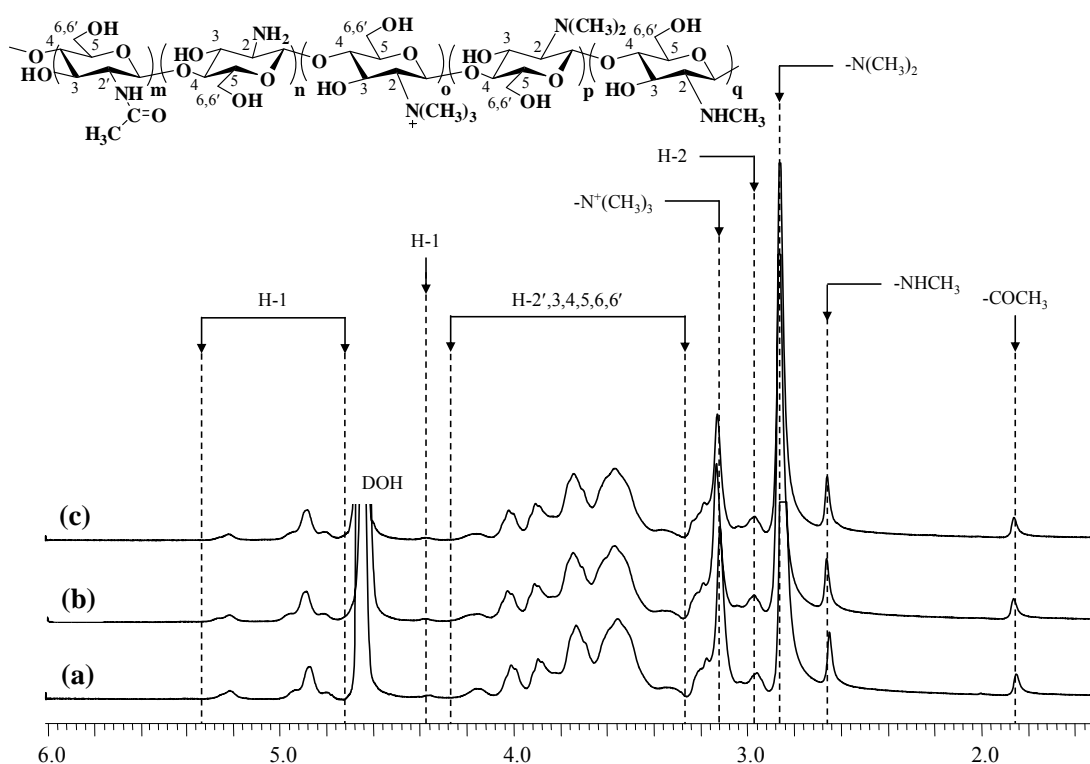


Figure A-1 1H NMR spectra of synthesized TMCs using (a) 4, (b) 5, and (c) 6 equivalents of CH_3I in comparison with the number of NH_2 in chitosan (solvent: $D_2O/TFA, 25^\circ C$).

Table A-1 Degree of quaternization (%DQ^a) was determined from the relative ratio between $-N^+(CH_3)_3$ and H-1.

Sample	n	Integration				%DQ ^a (1)	average ± SD	%DS _{N(CH₃)₂} (2)	average ± SD	%DS _{NHCH₃} (3)	average ± SD	%DS (total) (1)+(2)+(3)	average ± SD
		N ⁺ (CH ₃) ₃	N(CH ₃) ₂	NHCH ₃	H-1								
	1	100	220.94	44.82	36.30	30.6		101.4		13.7		145.8	
TMC _{CH₃14eq}	2	100	215.98	42.04	60.39	18.4	22.6 ± 6.9	59.6	73.0 ± 24.7	7.7	9.5 ± 3.6	85.7	105.1 ± 35.2
	3	100	205.65	38.3	59.25	18.8		57.8		7.2		83.8	
	1	100	228.75	50.12	49.42	22.5		77.1		11.3		110.9	
TMC _{CH₃15eq}	2	100	245.20	51.72	33.29	33.4	28.3 ± 5.5	122.8	100.5 ± 22.8	17.3	16.4 ± 4.7	173.4	145.1 ± 31.7
	3	100	233.79	70.90	38.36	29.0		101.6		20.5		151.1	
	1	100	253.62	7.38	77.74	14.3		54.4		1.1		69.7	
TMC _{CH₃16eq}	2	100	265.82	19.50	66.85	16.6	24.6 ± 15.8	66.3	107.9 ± 82.6	3.2	11.6 ± 16.3	86.1	144.0 ± 114.7
	3	100	316.40	71.07	25.98	42.8		203.0		30.4		276.1	

$$^a \text{Degree of quaternization} = \%DQ = \left[\frac{\int N^+(CH_3)_3 / 9}{(\int H-1) \times DD} \right] \times 100$$

Table A-2 Degree of quaternization (%DQ^a) was determined from the relative ratio between $-N^+(CH_3)_3$ and H-2.

Sample	n	Integration				%DQ ^a (1)	average ± SD	%DS _{N(CH₃)₂} (2)	average ± SD	%DS _{NHCH₃} (3)	average ± SD	%DS (total) (1)+(2)+(3)	average ± SD
		N ⁺ (CH ₃) ₃	N(CH ₃) ₂	NHCH ₃	H-2								
	1	100	220.94	44.82	21.59	51.5		170.6		69.2		291.2	
TMC _{CH₃14eq}	2	100	215.98	42.04	26.33	42.2	46.3 ± 4.7	136.7	148.8 ± 18.9	53.2	58.1 ± 9.7	232.1	253.1 ± 33.1
	3	100	205.65	38.3	24.64	45.1		139.1		51.8		236.0	
	1	100	228.75	50.12	29.02	38.3		131.4		57.6		227.2	
TMC _{CH₃15eq}	2	100	245.20	51.72	29.43	37.8	40.9 ± 5.1	138.9	144.8 ± 17.2	58.6	71.9 ± 24.0	235.2	257.6 ± 45.9
	3	100	233.79	70.90	23.74	46.8		164.1		99.6		310.5	
	1	100	253.62	7.38	32.91	33.8		128.4		7.5		169.7	
TMC _{CH₃16eq}	2	100	265.82	19.50	30.71	36.2	34.3 ± 1.7	144.3	142.8 ± 13.7	21.2	32.9 ± 32.8	201.6	209.9 ± 45.0
	3	100	316.40	71.07	33.86	32.8		155.7		70.0		258.5	

$$^a \text{Degree of quaternization} = \%DQ = \left[\frac{\int N^+(CH_3)_3 / 9}{\left(\int H-2 \right) \times DD} \right] \times 100$$

Table A-3 Degree of quaternization (%DQ^a) was determined from the relative ratio between $-N^+(CH_3)_3$ and H-2',3,4,5,6,6'.

Sample	n	Integration				%DQ ^a (1)	average ± SD	%DS _{N(CH₃)₂} (2)	average ± SD	%DS _{NHCH₃} (3)	average ± SD	%DS (total) (1)+(2)+(3)	average ± SD
		N ⁺ (CH ₃) ₃	N(CH ₃) ₂	NHCH ₃	H-2',3,4,5,6,6'								
	1	100	240.15	21.65	360.98	21.7		78.3		14.1		114.1	
TMC _{CH₃14eq}	2	100	212.24	13.25	364.34	21.5	21.7 ± 0.1	68.5	71.6 ± 5.7	8.6	10.2 ± 3.4	98.6	103.5 ± 9.2
	3	100	208.83	12.00	360.69	21.7		68.1		7.8		97.7	
	1	100	229.78	36.43	365.82	21.4		73.9		23.4		118.8	
TMC _{CH₃15eq}	2	100	218.17	38.11	371.18	21.1	21.1 ± 0.4	69.1	70.3 ± 3.1	24.2	24.6 ± 1.4	114.4	116.0 ± 2.4
	3	100	218.53	42.09	378.28	20.7		68.0		26.2		114.9	
	1	100	264.66	12.72	442.90	17.7		70.3		6.8		94.8	
TMC _{CH₃16eq}	2	100	261.50	21.66	439.56	17.8	17.8 ± 0.1	70.0	70.1 ± 0.2	11.6	14.0 ± 8.7	99.4	101.9 ± 8.6
	3	100	260.75	43.92	438.09	17.9		70.0		23.6		111.5	

$$^a \text{Degree of quaternization} = \%DQ = \left[\frac{\int N^+(CH_3)_3 / 9}{\left(\int H-2',3,4,5,6,6' / 6 \right) \times DD} \right] \times 100$$

Table A-4 Degree of quaternization (%DQ^a) was determined from the relative ratio between $-N^+(CH_3)_3$ and H-2,2',3,4,5,6,6'.

Sample	n	Integration				%DQ ^a (1)	average ± SD	%DS _{N(CH₃)₂} (2)	average ± SD	%DS _{NHCH₃} (3)	average ± SD	%DS (total) (1)+(2)+(3)	average ± SD
		N ⁺ (CH ₃) ₃	N(CH ₃) ₂	NHCH ₃	H-2,2',3,4,5,6,6'								
	1	100	220.94	44.82	360.22	25.4		56.1		11.4		92.9	
TMC _{CH₃14eq}	2	100	215.98	42.04	398.4	23.0	24.1 ± 1.2	49.6	51.7 ± 3.9	9.7	10.1 ± 1.2	82.2	85.8 ± 6.1
	3	100	205.65	38.3	381.98	24.0		49.3		9.2		82.4	
	1	100	228.75	50.12	385.53	23.7		54.3		11.9		89.9	
TMC _{CH₃15eq}	2	100	245.20	51.72	412.69	22.2	23.3 ± 0.9	54.4	54.8 ± 0.9	11.5	13.4 ± 3.0	88.0	91.5 ± 4.6
	3	100	233.79	70.90	383.02	23.9		55.9		16.9		96.7	
	1	100	253.62	7.38	464.39	19.7		50.0		1.5		71.1	
TMC _{CH₃16eq}	2	100	265.82	19.50	478.10	19.1	19.0 ± 0.8	50.9	52.8 ± 4.1	3.7	6.0 ± 6.1	73.7	77.8 ± 9.4
	3	100	316.40	71.07	503.89	18.2		57.5		12.9		88.5	

$$^a \text{Degree of quaternization} = \%DQ = \left[\frac{\int N^+(CH_3)_3 / 9}{(\int H-2,2',3,4,5,6,6' / 6) \times DD} \right] \times 100$$

Table A-5 Degree of quaternization (%DQ^a) was determined from the relative ratio between $-N^+(CH_3)_3$ and $-NHCOCH_3$.

Sample	n	Integration				%DQ ^a (1)	average ± SD	%DS _{N(CH₃)₂} (2)	average ± SD	%DS _{NHCH₃} (3)	average ± SD	%DS (total) (1)+(2)+(3)	average ± SD
		N ⁺ (CH ₃) ₃	N(CH ₃) ₂	NHCH ₃	-NHCOCH ₃								
	1	100	220.94	44.82	29.73	19.8						112.0	
TMC _{CH₃14eq}	2	100	215.98	42.04	1.87	314.6	216.9 ± 170.7	1019.1	686.7 ± 538.4	396.7	262.2 ± 204.7	1730.4	1165.9 ± 913.5
	3	100	205.65	38.3	1.86	316.3						1655.2	
	1	100	228.75	50.12	18.79	31.3						185.8	
TMC _{CH₃15eq}	2	100	245.20	51.72	18.74	31.4	27.9 ± 5.9	115.4	98.9 ± 22.1	48.7	46.9 ± 2.0	195.5	173.7 ± 29.8
	3	100	233.79	70.90	27.94	21.1						139.7	
	1	100	253.62	7.38	1.82	323.2						1624.3	
TMC _{CH₃16eq}	2	100	265.82	19.50	4.67	126.0	155.5 ± 155.0	502.2	604.8 ± 580.3	73.7	60.8 ± 20.5	701.9	821.1 ± 750.7
	3	100	316.40	71.07	33.78	17.4						137.2	

$$^a \text{Degree of quaternization} = \%DQ = \left[\frac{\int N^+(CH_3)_3 / 9}{\left(\int NHCOCH_3 / 3 \right) \times DD} \right] \times 100$$

APPENDIX B

Determination of IC₅₀ of *In vitro* cytotoxicity on HaCaT cells line

The IC₅₀ values were calculated from a logarithmic regression ($y = a \cdot \log(x) + b$ in Table B-1) which obtained from the graph of the concentration (x axis) and the cell viability (y axis) as shown in Figure B-1.

Table B-1 The IC₅₀ values (*in vitro* cytotoxicity) of chitosan MW 45000, TMCs, and HTACCs on HaCaT cells line as determined by the MTT assay at pH 6.0.

Sample	$y = a \cdot \log(x) + b$			$y = 50\%$	
	a	b	r ²	log (x)	x = IC ₅₀
Chitosan 85% <i>DD</i>	3.6454	91.712	0.2057	-	>5000 ^a
TMC 22% <i>DQ</i>	-13.370	93.279	0.6161	3.237	1725.9
TMC 21% <i>DQ</i>	-28.129	94.633	0.8147	1.587	38.6
TMC 18% <i>DQ</i>	-25.034	78.806	0.9003	1.151	14.1
HTACC 24% <i>DQ</i>	4.8118	91.227	0.4580	-	>1000 ^a
HTACC 84% <i>DQ</i>	-25.316	107.21	0.8141	2.260	181.9
HTACC 139% <i>DQ</i>	-29.271	115.60	0.6599	2.241	174.2

^aThe IC₅₀ value could not certainly calculated due to the log (x) value is negative.

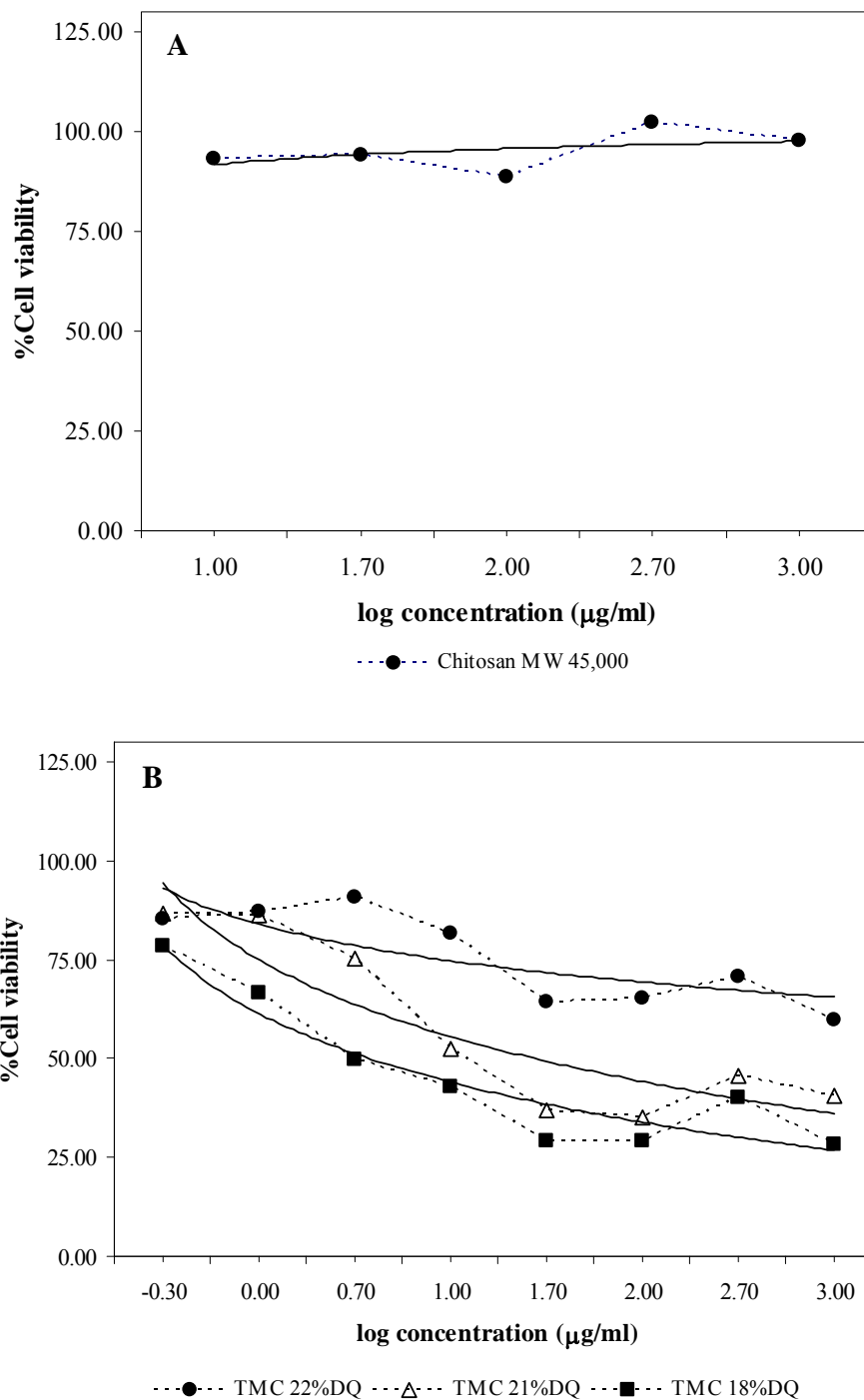


Figure B-1 Relationship between the log concentration ($\mu\text{g/ml}$) and the cell viability (%): (A) chitosan MW 45,000, (B) TMCs, and (C) HTACCs. Logarithmic trendline (solid line) and original trendline (dotted line).

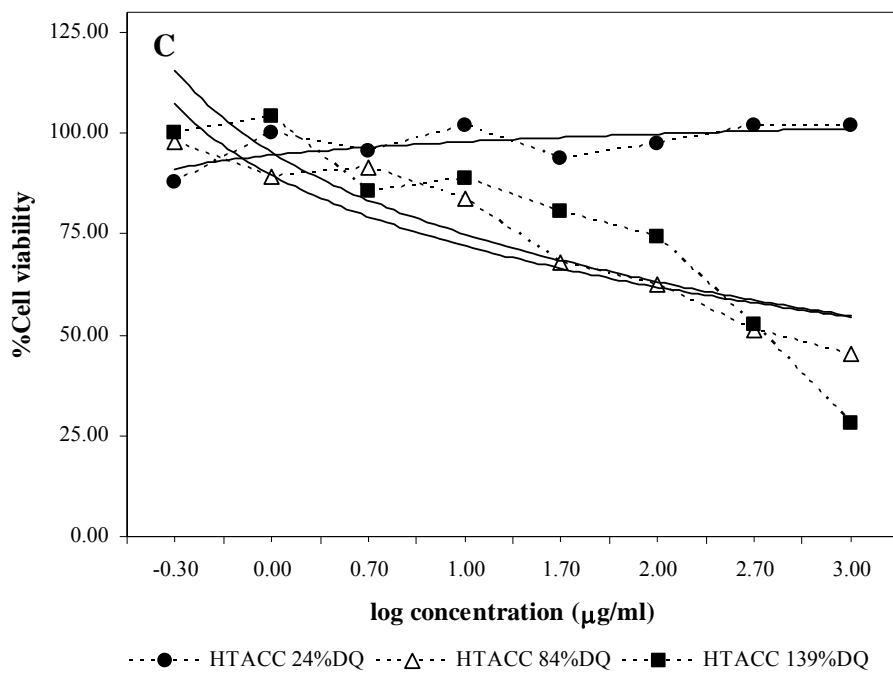


Figure B-1 *continued*

APPENDIX C

The fracture patterns for five types of hair

As a result, virgin, straightened and UV-damaged hairs are observed with the step pattern as shown in Figure C-1. Waved and dyed hairs are observed with the smooth and splitting pattern, respectively. Additionally, if the hair and its cuticle are near the root end, a smooth break tends to occur. As the fiber becomes dryer, below 90%RH, step fractures are the most commonly observed fracture pattern. Fibrillation and splitting describe a distinct cortical fracturing pattern and tend to occur more with twisted or kinky fibers or when the relative humidity is low.

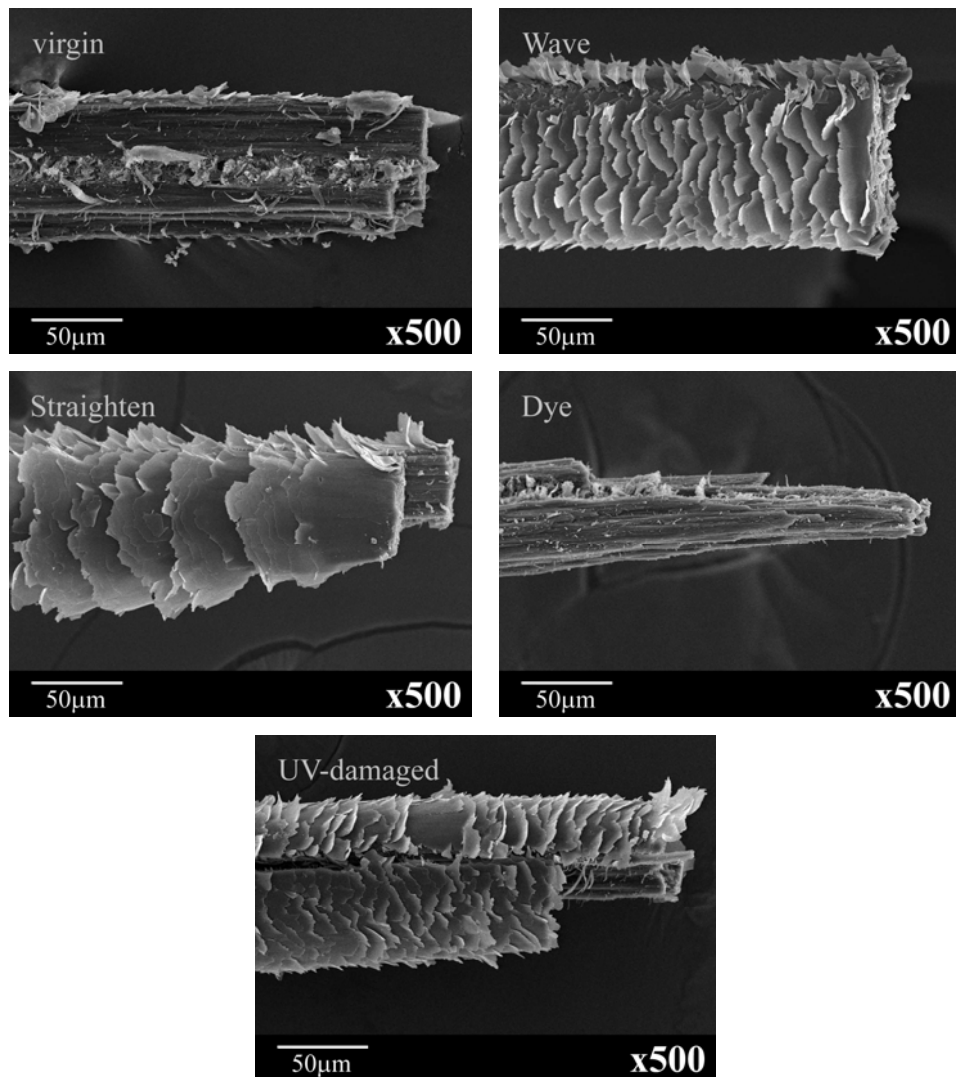


Figure C-1 The fracture patterns for five types of hair.

VITAE

Teerachai Kerdcholpetch was born in Bangkok, Thailand, on October 16th, 1983. He received a Bachelor Degree of Chemistry from the Faculty of Science, Chulalongkorn University, Bangkok, Thailand in 2006. In the same year, he studied in Master Degree program in Petrochemistry and Polymer Science, Faculty of Science, Chulalongkorn University and completed the degree in May 2009.

Presentation in Conference:

- | | |
|----------------|--|
| March 2008 | The 16 th Science Forum, Faculty of Science, Chulalongkorn University, Bangkok, Thailand. |
| July 2008 | The 5 th National Chitin-Chitosan Conference, Center for Chitin-Chitosan Biomaterials (CCB), Metallurgy and Materials Science Research Institute (MMRI), Chulalongkorn University, Bangkok, Thailand. |
| September 2008 | The 5 th Thailand Materials Science and Technology Conference, Miracle Grand Convention Hotel, Bangkok, Thailand. <u>Best Poster Award for Student in Polymer Session</u> |
| December 2008 | The 4 th Mathematics and Physical Science Graduate Conference, Faculty of Science, National University of Singapore, Singapore. |
| January 2009 | Pure and Applied Chemistry International Conference 2009, Faculty of Science, Naresuan University, Phitsanulok, Thailand. <u>The Outstanding Poster Presentation Award</u> |

Publication: “Sustained Release of Amoxicillin from Chitosan Tablets”
Archives of Pharmacal Research 30(4) (2007): 526-531.